Fabrication of Polymeric Materials as Thermo-Responsive Gels for Drug Delivery System

Onpreeya Boonrat

Thesis Submitted in Partial Fulfillment of the Requirements for the Degree of Doctor of Philosophy in Pharmaceutical Sciences
Prince of Songkla University
2022

Fabrication of Polymeric Materials as Thermo-Responsive Gels for Drug Delivery System

Onpreeya Boonrat

Thesis Submitted in Partial Fulfillment of the Requirements for the Degree of Doctor of Philosophy in Pharmaceutical Sciences
Prince of Songkla University
2022

Thesis Title	Fabrication of polymeric materials as thermo-responsive gels for drug delivery system
Author	Miss Onpreeya Boonrat
Major Program	Pharmaceutical Sciences

Major Advisor	**Examining Committee:**
……..……	……..…….....…..…Chairperson
(Prof. Dr. Vimon Tantishaiyakul)	(Assoc. Prof. Dr. Satit Puttipipatkhachorn)
	……..…….....…..……Committee
	(Prof. Dr. Vimon Tantishaiyakul)
Co-advisor	
……..…….	……..…….....……Committee
(Assoc. Prof. Dr. Namon Hirun)	(Prof. Dr. Damrongsak Faroongsang)
	……..…….....…….Committee
	(Prof. Dr. Ruedeekorn Wiwattanapatapee)

The Graduate School, Prince of Songkla University, has approved this thesis as partial fulfilment of the requirements for the Doctor of Philosophy Degree in Pharmaceutical Sciences.

……..……..

(Prof. Dr. Damrongsak Faroongsang)

Dean of Graduate School

This is to certify that the work here submitted is the result of the candidate's own investigations. Due acknowledgement has been made of any assistance received.

……...……..…….....Signature
(Prof. Dr. Vimon Tantishaiyakul)
Major Advisor

...…….....…..…....Signature
(Assoc. Prof. Dr. Namon Hirun)
Co-advisor

……..…..…….....Signature
(Miss Onpreeya Boonrat)
Candidate

I hereby certify that this work has not been accepted in substance for any degree, and is not being currently submitted in candidature for any degree.

……...…...……..Signature

(Miss Onpreeya Boonrat)

Candidate

ชื่อวิทยานิพนธ์ การพัฒนาวัสดุพอลิเมอร์แบบเจลที่ตอบสนองต่ออุณหภูมิสำหรับระบบนำส่งยา
ผู้เขียน นางสาว อรปรียา บุญรัตน์
สาขาวิชา เภสัชศาสตร์
ปีการศึกษา 2565

บทคัดย่อ

ไฮโดรเจลที่ตอบสนองต่ออุณหภูมิรูปแบบใหม่ซึ่งประกอบด้วยเมทิลเซลลูโลส (MC) ที่ความเข้มข้น 4% โดยน้ำหนัก และพลูโรนิค F127 (PF) ที่ความเข้มข้นต่างๆกัน (12, 14, 16, 18 และ 20% โดยน้ำหนัก) ได้ถูกพัฒนาและตรวจสอบคุณลักษณะได้สำเร็จ สิ่งที่น่าสนใจเกี่ยวกับงานนี้คือสารละลายเดี่ยวของ 12PF และ 14PF ไม่เป็นเจลที่อุณหภูมิร่างกาย แต่การผสมกับเมทิลเซลลูโลสสามารถเกิดเป็นเจลได้ ลักษณะภายนอกที่มองเห็นได้ของส่วนผสมพลูโรนิค127/เมทิลเซลลูโลส (12PF/MC, 14PF/MC, 16PF/MC, 18PF/MC และ 20PF/MC) มีลักษณะเป็นสารละลายใสที่อุณหภูมิแวดล้อมและมีลักษณะเจลแข็งขุ่นที่อุณหภูมิร่างกาย ความขุ่นของส่วนผสมเหล่านี้ระหว่างการให้ความร้อนอาจเป็นผลมาจากเมทิลเซลลูโลสกระทบต่อพลูโรนิคในระบบ ความเข้มข้นที่เกิดไมเซลและปริมาณความร้อนของกระบวนการการรวมตัวเป็นไมเซลลดลงโดยการรวมเมทิลเซลลูโลสเข้ากันกับพลูโรนิค อุณหภูมิที่สารละลายเปลี่ยนเป็นเจลสามารถปรับและลดลงได้โดยการเพิ่มความเข้มข้นของ PF นอกจากนี้ เอทิโดรเนต โซเดียม (EDS) ยาที่ใช้ในการรักษาโรคกระดูกพรุนและโรคแคลเซียมในเลือดสูง ที่ความเข้มข้น $4x10^{-3}$M ถูกเติมเข้าไปในไฮโดรเจลและทำการตรวจสอบพฤติกรรมของเจล พบว่า EDS ที่ความเข้มข้น $4x10^{-3}$M ไม่ได้เปลี่ยนแปลงการไวต่อความร้อนการเป็นเจลและพฤติกรรมวัฏภาคของส่วนผสมข้างต้น ดังนั้นการศึกษานี้จึงบ่งชี้ได้ว่าการผสม MC กับ PF เป็นวิธีการที่มีศักยภาพในการปรับปรุงคุณลักษณะทางความร้อนของระบบนำส่งยาที่ก่อตัวเป็นเจลในร่างกายได้

ในบรรดาส่วนผสมต่างๆ ส่วนผสมของ 12PF/MC และ 14PF/MC ถูกเลือกเพื่อทำการศึกษาเพิ่มเติมเนื่องจากมีคุณลักษณะที่เป็นสถานะสารละลายใกล้กับอุณหภูมิแวดล้อม (24 °C) และก่อตัวเป็นเจลภายในอุณหภูมิร่างกาย (37 °C) ส่วนผสมเหล่านี้มีความเหมาะสมเพื่อเป็นตัวนำส่งแบบฉีดได้ 12PF/MC และ 14PF/MC แสดงคุณสมบัติยึดเกาะเยื่อเมือกได้ดีกว่า 12PF และ 14PF เดี่ยว อย่างมีนัยสำคัญ ตามลำดับ นอกจากนี้ ความเข้ากันได้ทางชีวภาพของสารผสมเหล่านี้แสดงผลที่ดีต่อเซลล์ไฟโบรบลาสต์ การศึกษาลำดับถัดมาคือ เติม ด็อกซีไซคลิน ไฮเครท (DX) ที่ความเข้มข้น 0.25 และ 0.5% โดยน้ำหนัก เข้ากับส่วนผสม 12PF/MC และ 14PF/MC และทำการประเมินประสิทธิผลสำหรับการใช้เป็นระบบนำส่งยาเกี่ยวกับปริทันต์ แม้ว่าอุณหภูมิการเกิดเจลและความหนืด

ของส่วนผสมที่บรรจุด้วย DX จะเปลี่ยนแปลงที่ช่วงอุณหภูมิสูง อย่างไรก็ตาม ส่วนผสมทั้งหมดยังคงมีลักษณะเหมือนเจลได้ซึ่งครอบคลุมอุณหภูมิแวดล้อมและอุณหภูมิของร่างกาย นอกจากนี้ การผสม DX เข้ากันกับส่วนผสม 12PF/MC และ 14PF/MC ยังแสดงฤทธิ์ต้านแบคทีเรียได้เช่นเดียวกับสารละลายยาบริสุทธิ์ สิ่งนี้บ่งชี้ว่าตัวนำส่งแบบ PF/MC ทั้งสองไม่ได้ขัดขวางการออกฤทธิ์ต้านแบคทีเรียของยา 12PF/MC และ 14PF/MC ยังแสดงรูปแบบการปลดปล่อยยา DX ที่ช้าอีกด้วย ดังนั้น ในการศึกษานี้แสดงให้เห็นว่าตัวนำส่งของส่วนผสมที่เหมาะสมของ PF/MC ที่ตอบสนองต่ออุณหภูมิมีแนวโน้มที่จะพัฒนาเป็นระบบนำส่งยาปริทันต์ที่มีประสิทธิภาพได้

การกระเจิงของรังสีเอกซ์มุมเล็ก (SAXS) ได้ถูกนำมาใช้เพื่อศึกษาพฤติกรรมทางความร้อนของส่วนผสม PF/MC ที่สัมพันธ์กับการเปลี่ยนวัฏภาคและคุณลักษณะทางรีโอโลยี ส่วนผสมของ PF/MC ในการศึกษาครั้งนี้ ได้แก่ 11PF, 17PF, 11PF/MC, และ 17PF/MC จากผลการทดลองด้วยวิธีการเอียงหลอดและการวิเคราะห์ทางรีโอโลยี พบว่า 11PF ไม่เป็นเจล แต่การรวมกับกับเมทิลเซลลูโลส (MC) (4% โดยน้ำหนักของเมทิลเซลลูโลส) ทำให้ระบบสามารถสร้างเจลได้เมื่ออุณหภูมิเพิ่มขึ้น นอกจากนี้พบว่าการเพิ่ม MC ลงใน 17 PF (17PF/MC) สามารถลดอุณหภูมิการเกิดเจลของ 17PF ได้ โครงสร้างของเจล มีการจัดเรียงตัวเป็นระเบียบมีลักษณะรูปทรงสี่เหลี่ยมลูกบาศก์แบบกลางหน้าในที่อุณหภูมิปานกลางเหนืออุณหภูมิการเกิดเจล ที่อุณหภูมิสูงขึ้น (55–70 °C) สังเกตพบว่าเส้นโค้งของการกระเจิงแสงมุมเล็ก (SAXS) ยกตัวสูงขึ้นด้วย เหตุการณ์นี้เป็นผลจาก MC ช่วยให้เกิดการเชื่อมต่อกันเป็นโครงร่างตาข่ายกับไมเซลที่อุณหภูมิสูงได้ การเกิดเจลนี้อาจสัมพันธ์กับการที่ MC ช่วยเชื่อมโครงสร้างไมเซลของ PF ที่เหมือนกับการเกิดโครงร่างตาข่ายเจลของ MC นอกจากนี้ EDS ได้ถูกเติมเข้าไปในส่วนผสมต่างๆ และทำการศึกษา พบว่ายาไม่ส่งผลกระทบต่อการเกิดเจลและการจัดเรียงโครงสร้างของโพลีเมอร์อย่างมีนัยสำคัญ มากไปกว่านั้น ส่วนผสมของ 11PF/MC เป็นของเหลวที่อุณหภูมิ 25 °C และกลายเป็นเจลที่อุณหภูมิร่างกาย 37 °C ดังนั้น จากการศึกษาครั้งนี้พบว่าการผสม PF กับ MC มีศักยภาพที่สำคัญในการปรับอุณหภูมิของเจลให้เหมาะสมเพื่อเป็นระบบนำส่งยาเข้าสู่ภายในร่างกาย

คำสำคัญ: พลูโรนิค F127, เมทิลเซลลูโลส, ไฮโดรเจล, ระบบนำส่งยา, โรคปริทันต์อักเสบ

Thesis Title Fabrication of polymeric materials as thermo-responsive gels for drug delivery system

Author Miss Onpreeya Boonrat

Major Program Pharmaceutical Sciences

Academic Year 2022

ABSTRACT

Novel thermo-responsive hydrogels comprising 4% w/w Methylcellulose (MC) and various Pluronic F127 (PF) concentrations (12, 14, 16, 18, and 20% w/w) were successfully developed and characterized. The interesting thing in this work was neat 12PF and 14PF solutions did not form gel but blending with MC could form gel. Visual appearance of the PF/MC blends (12PF/MC, 14PF/MC, 16PF/MC, 18PF/MC, and 20PF/MC) were clear solutions at ambient temperature and exhibited turbid hard gel at physiological temperature. The turbidity during heating of these blends may be caused by the effect of MC on the PF system. The critical micelle concentration (CMT) and the enthalpy of micellization were reduced by including MC into PF. The sol-to-gel transition temperature can be modulated and decreased by increasing PF concentrations. Besides, $4x10^{-3}$ M Etidronate sodium (EDS); used to treat hypercalcemia and osteoporosis was added into hydrogels and investigated their gels behavior. EDS at a centration of $4x10^{-3}$ M, did not alter the thermosensitive gelation and the phase behavior of the blends. Thus, this study indicates that blending of PF with MC is a potential method to improve the thermal characteristics of *in situ* gel-forming drug delivery systems.

Among of the blends, 12PF/MC and 14PF/MC blends were selected for further study. Since their characteristics were in solution state near ambient temperature (24 °C) and formed *in situ* gels at body temperature (37 °C). These mixtures were found to be suitable as injectable implant matrices. 12PF/MC and 14PF/MC showed substantially better mucoadhesive properties than neat 12PF and 14PF, respectively. Furthermore, the biocompatibility of these mixtures was well shown on fibroblasts. The next study was addition the Doxycycline hyclate (DX) at concentrations of 0.25 and 0.5% w/w into 12PF/MC and 14PF/MC blends and evaluated its effectiveness for using as a periodontal drug delivery system. Although, the gelation temperature and viscosity of the DX-loaded blends were changed at high temperatures range. However, all blends still exhibited gel-like characteristics covering the ambient and body temperature. Moreover, DX-incorporated 12PF/MC and 14PF/MC blends presented the same antibacterial activity as the pure drug solution. This indicated that both PF/MC matrices did not prohibit the antibacterial activity of the drug. The 12PF/MC and 14PF/MC also exhibited slow-release profile of DX. Therefore, in the present study demonstrated that

the appropriate mixtures of thermo-responsive of PF/MC are promising matrices for the development of an efficient periodontal drug delivery system.

The small-angle X-ray scattering (SAXS) was applied for study the behavior of PF/MC blends which related to the temperature-dependent phase transition and rheological characteristic. The blending of PF/MC in this study were 11PF, 17PF, 11PF/MC, and 17PF/MC. As results of test tube tilting method and rheological analysis, 11PF cannot form gel. But blending 11PF with 4% w/w methylcellulose (MC) (11PF/MC) enabled the system to form gel upon heating. In addition, adding MC into 17 PF (17PF/MC) could reduce the gelation temperature of 17PF. The ordered structure of these gels exhibited a face-centered cubic (FCC) phase at intermediate temperature above the gelation temperature; the steep upturn of the SAXS curves was observed in the small scattering vector range at high temperatures (55–70 °C). This occurrence was a result of MC-assisted interconnected network of micelles at high temperatures. This gelation may be related to that MC assisted intermicellar organization the PF micelle structure, similar to the gelation network of MC. In addition, EDS was incorporated into the matrices. The results found that the drug did not significantly affect the thermosensitive gelation and the ordered structure of the polymeric systems. Moreover, the blend of 11PF/MC was solution at 25 °C and became gel at body temperature of 37 °C. Therefore, this study revealed that blending PF with MC is a potential strategy for modulating the thermosensitive characteristics of the *in situ* gel forming drug delivery.

Keywords: Pluronic F127, Methylcellulose, Hydrogel, Drug delivery system, Periodontitis

ACKNOWLEDGEMENTS

I would like to express my sincerest gratitude to my wonderful advisor, **Professor Dr. Vimon Tantishaiyakul**, for her smart insight, helpful advice, high generosity, and valuable support throughout my thesis. I would like to thank my co-advisor, **Associate Professor Dr. Namon Hirun**, Faculty of Pharmacy, Thammasat University, Pathumthani, for his continual help, kind discussion and excellent suggestion.

I would like to thank **Professor Dr. Teerapol Srichana**, Department of Pharmaceutical Technology, for allowing me to use microorganism pathogens for my research. I would like to acknowledge the Synchrotron Light Research Institute, Nakhonratchasima, for all small angle X-ray scattering (SAXS) facilities, and **Dr. Siriwat Soontaranon** as well as staff of BL 2.2 for their assistance in SAXS experiment. I also would like to acknowledge the Scientific and Technological Equipment, Walailak University, Nakhonsithammarat for use of rheometer and DSC. In addition, I special thanks to Department of Pharmaceutical Chemistry and Department of Pharmaceutical Technology for providing me in scientific equipment with the facility to conduct my lab work.

I am appreciative of all financial support from Graduate School [PSU-Ph.D. Scholarship (Grant No. PSU/020/2557)], Graduate research funding at Faculty of Pharmaceutical Sciences, and Drug Delivery System Excellence Center (DDSEC), Faculty of Pharmaceutical Sciences, Prince of Songkla University.

I am very much thankful for my friends, scientists, colleagues and staff in Faculty of Pharmaceutical Sciences for their kindness and support. Besides, I am especially grateful to **Mrs. Titpawan Nakpeng, Mr. Panithi Raknam, Miss Jirayu Buatong, Miss Uthaiwan Thammapokin**, and **Miss Mingkhwan Julwanna** for their beautiful friendship and encouragement during my long-term study. Moreover, I am also thankful to my aunt and **Khunthong family**, who provided me with comfortable accommodation and well assist during my education.

Most importantly, I would like to express my immense gratitude and appreciation to my beloved family. My Ph.D. study could not be successful without the love and understanding of **my parents**, who were always my strength, warm big hug and support in every situation. Their love makes me feel appreciated myself and purposeful to move forward with my graduation and daily life.

Onpreeya Boonrat

CONTENTS

LIST OF TABLES

LIST OF FIGURES

LIST OF FIGURES (Continued)

LIST OF FIGURES (Continued)

LIST OF FIGURES (Continued)

LIST OF ABBREVIATIONS AND SYMBOLS

%	Percentage
ΔH	Enthalpy change
®	Registered trademark
A. actinomycetemcomitans	*Aggregatibacter actinomycetemcomitans*
ATCC	American Type Culture Collection
BL	Beamline
C2C12	Mouse myoblast cell line.
CMT	Critical micelle temperature
DSC	Differential scanning calorimetry
DX	Doxycycline hyclate
ECM	Extracellular matrix
EDS	Etidronate sodium
EPA	Environmental Protection Agency
FCC	Face center cubic
g	Gram
G′	Storage modulus
G″	Loss modulus
ISO	International Organization for Standardization
keV	Kilo electron volt
L929	Mouse fibroblast cell line
LCST	Lower critical solution temperature
LT_{gel}	Lower temperature gel
M	Molar
MC	Methylcellulose
MC3T3-E1	Mouse pre-osteoblastic cell line
mg	Milligram
Mill-Q	Water is simply water purified using a Millipore
min	Minute

LIST OF ABBREVIATIONS AND SYMBOLS (Continued)

ml	Milliliter
mm	Millimeter
nm	Nanometer
^{o}	Degree
^{o}C	Degree Celsius
P. gingivalis	*Porphyromonas gingivalis*
P. intermedia	*Prevotella intermedia*
Pa	Pascal
Pa.s	Pascal-second
PEO	Poly (ethylene oxide)
PF	Pluronic F127
POO	Poly (propylene oxide)
rad/s	Radian per second
RNA	Ribonucleic acid
s.d.	Standard deviation
SAXS	Small Angle X-ray Scattering
SEM	Scanning Electron Microscopy
sol	Solution
Temp	Temperature
TTM	Test tube inversion method or Tube tilling method
USFDA	The United States Food and Drug Administration
UT_{gel}	Upper temperature gel
UV-Vis	UV Visible Spectrophotometer
w/w	Weight by weight
α	Alpha
β	Beta
$\Delta G'_{relative}$	Rheological synergy

LIST OF PAPERS AND PROCEEDINGS

These are list of papers and proceedings that involving in this thesis work.

List of Publications

1. **Boonrat, O**., Tantishaiyakul, V., and Hirun, N. 2022. Micellization and gelation characteristics of different blends of pluronic F127/methylcellulose and their use as mucoadhesive in situ gel for periodontitis. Polymer Bulletin (79): 4515-4534. https://doi.org/10.1007/s00289-021-03722-w.
2. **Boonrat, O**., Tantishaiyakul, V., and Hirun, N. 2021. Structural characterization using SAXS and rheological behaviors of pluronic F127 and methylcellulose blends. Polymer Bulletin (78): 1175–1187. https://doi.org/10.1007/s00289-020-03154-y.

List of Proceedings

1. **Boonrat, O**. and Tantishaiyakul, V. Effect of methylcellulose and xyloglucan on gelation temperature and cytotoxic enhancement of Pluronic-127 injectable hydrogel for drug delivery system. The 11th IMT-GT UNINET Conference 2018 – *Bioscience for A Sustainable Future*, Hotel Jen, Penang, Malaysia, December 11-12, 2018. 142-148.
2. **Boonrat, O**. and Tantishaiyakul, V. A Novel method to simulate organogel implantation using UV spectroscopy. The joint international conferences of the 5th Current Drug Development 2018 (CDD 2018) and the 3rd Herbal and Traditional Medicine 2018 (HTM2018). The 60th Anniversary of His Majesty the King's Accession to the Throne International Convention Center (PSU Conference Hall), Prince of Songkla University, Hat Yai, Songkhla, Thailand. May 23-25, 2018. 115-116.

REPRINTS WERE MADE WITH PERMISSION FROM THE PUBLISHERS

Reprints with permission of Polymer Bulletin Journal (Paper 1)

no-reply@copyright.com <no-reply@copyright.com>
ศ. 20/5/2022 16:58
ถึง: mai_658@hotmail.com <mai_658@hotmail.com>

SPRINGER NATURE

Thank you for your order!

Dear Ms. Onpreeya Boonrat,

Thank you for placing your order through Copyright Clearance Center's RightsLink® service.

Order Summary

Licensee:	Prince of Songkla University
Order Date:	May 20, 2022
Order Number:	5312991387961
Publication:	Polymer Bulletin
Title:	Structural characterization using SAXS and rheological behaviors of pluronic F127 and methylcellulose blends
Type of Use:	Thesis/Dissertation
Order Total:	0.00 USD

View or print complete details of your order and the publisher's terms and conditions.

Sincerely,

Copyright Clearance Center

Tel: +1-855-239-3415 / +1-978-646-2777
customercare@copyright.com
https://myaccount.copyright.com

CCC RightsLink®

Reprints were made with permission from the publishers (Continued)

Reprints with permission of Polymer Bulletin Journal (Paper 2)

no-reply@copyright.com <no-reply@copyright.com>
ส่ง: 20/5/2022 17:13
ถึง: mai_658@hotmail.com <mai_658@hotmail.com>

SPRINGER NATURE

Thank you for your order!

Dear Ms. Onpreeya Boonrat,

Thank you for placing your order through Copyright Clearance Center's RightsLink® service.

Order Summary

Licensee:	Prince of Songkla University
Order Date:	May 20, 2022
Order Number:	5313000807212
Publication:	Polymer Bulletin
Title:	Micellization and gelation characteristics of different blends of pluronic F127/methylcellulose and their use as mucoadhesive in situ gel for periodontitis
Type of Use:	Thesis/Dissertation
Order Total:	0.00 USD

View or print complete details of your order and the publisher's terms and conditions.

Sincerely,

Copyright Clearance Center

Tel: +1-855-239-3415 / +1-978-646-2777
customercare@copyright.com
https://myaccount.copyright.com

CCC RightsLink®

CHAPTER 1

INTRODUCTION

1.1 Literature review

1.1.1 Hydrogels

Hydrogels are three-dimensional, hydrophilic, polymeric networks that can maintain their structure in a large amount of water or biological fluid (1). The network structure of hydrogels is capable to absorb water from 10–20% (an arbitrary lower limit) up to thousands of times for their dry weight (2). The existence of water in the hydrogel plays an important role in the overall penetration of the active ingredient into and out of the gel and can be associated with any hydrogel structure (3). The water molecules in hydrogels can be divided into bound water and bulk water. When the first water molecules enter the dry hydrogel, the hydrophilic part of the matrix will hydrate the most polar which is called *primary bound water*, and the networks swell. While the water molecules contacting the hydrophobic part of the network are called *secondary bound water*. After the high polar and low polar groups have interacted with bound water molecules, the network will imbibe additional water until reaching an equilibrium swelling level. The additional swelling water that is imbibed after the ionic, polar, and groups become saturated with bound water is called *free water* or *bulk water*, and is filled in the space within the network (2).

Currently, hydrogels are very popular and the number of patents and commercial products exist. The main areas of hydrogel applications are manufacturing contact lenses, biosensors, foods, cosmetics, wastewater adsorbents, hygiene products, wound dressings, tissue engineering scaffolds, and drug delivery systems (4, 5). For medicinal and pharmaceutical applications, hydrogels display various advantages and properties that make attractively and widely utilized (1-3, 6). The high-water content of hydrogel structure is similar to the native extracellular matrix (ECM) in the body, resulting in biocompatible hydrogels. In addition, the porosity of hydrogels deserves for loading bioactive molecules or drugs and subsequent drug release at a rate dependent on the diffusion coefficient of the small molecule or macromolecule through the gel network. Due to the soft behavior of hydrogels, it is easy to deformable to various shapes of the applied surface. Furthermore, the mucoadhesive or bioadhesive properties of the polymer used in some hydrogels can interact with the mucosa lining in the gastrointestinal (GI) tract, colon, vagina, nose, and other parts of the body leading to their ability to prolong their residence time at the delivery location. Besides, the

viscoelastic property of fully swollen or hydrated hydrogels minimizes irritation to the surrounding tissues after implantation. Moreover, the thermodynamic compatibility with water of hydrogels allows them to swell in aqueous media. However, their limitations also are low mechanical strength, hard to handle, difficult to load drugs and cells before cross-linking in vitro as a prefabricated matrix, rapid drug release, and difficult to sterilize (2, 6). For all that, these hydrogel limitations are challenging for further development.

Hydrogels can be classified according to various characteristics: their origins (natural, synthetic, or a combination of both), their properties (mechanical or physical), the natures of their polymer side groups (ionic or non-ionic), the types of cross-link (chemical or physical), and their responses to various chemical and physical stimuli (7). The hydrogel systems transform in response to infinitesimal changes of environmental stimuli include physical (temperature, electric fields, light, pressure, sound, magnetic fields), chemical (pH, ions), or biological ones, also called *intelligent* or *smart hydrogels* (8, 9). These smart hydrogels providing such 'sensor' properties can undergo reversible volume phase transitions or sol-gel phase transitions upon changes in the environmental condition by triggering the polymer chain in the matrix (8).

Commonly, the 3D network of hydrogel is made up by a porous structure of cross-linked polymers, in which the morphology, averaged porous size (ξ), porous-size distribution, including the molar mass between two neighbor crosslinks are based on several factors such as fabrication method, the concentration of monomer and/or polymer solution, and the crosslinking agent (10). As mentioned, the monomer or polymer chains in a hydrogel network can be connected by chemically and physically crosslinked (Fig. 1.1).

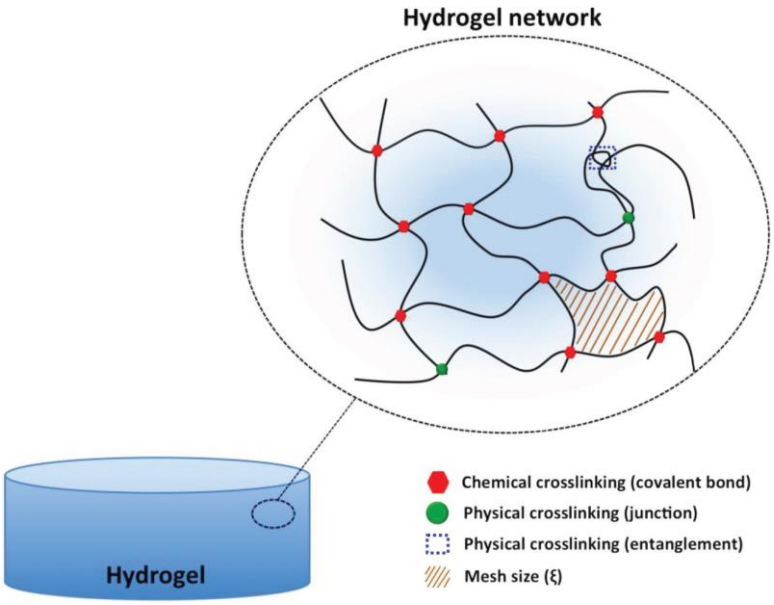

Fig. 1.1 Schematic of various crosslinks in hydrogel networks (10).

In the chemically crosslinked (or chemical hydrogels) the polymer chains are crosslinked by covalent bonds and once destroyed by chemically or enzymatically reaction and produce permanent hydrogel. The cross-linking process occurred with the addition of small molecule cross-linking, polymer-polymer conjugation, photosensitive agents, or by the enzyme-catalyzed reaction. These hydrogels allow absorption of water and/or bioactive compounds without dissolution and permit drug release by diffusion (10). Although the permanent networks lead to high mechanical strength, their biomedical applications are found some limitations: (i) since the most small cross-linker molecules are toxic (6), and (ii) prolonged photosensitivity and irradiation lead to a local increase in temperature, thereby damaging adjacent cells and tissues (3).

In the physically crosslinked (or physical hydrogel's) the polymer chains are linked together by non-covalent bonds (physical interactions) such as electrostatic interaction, dipole-dipole, H-bonds, and hydrophobic forces, and by entanglements and junctions (10). These physical hydrogel’s forms by without the need for chemical modification or the addition of cross-linking entities in vivo, and display reversible behavior and biodegradable. They are poor in mechanical strength and pore size of physical network, and gelation time (6). These limitations can be improving their gelation time, control drug release, and mechanical property by: (i) increasing the polymer solution concentration, (ii) adding some salts or small molecules, and (iii) using modified polymers into polymer matrices (3).

During the last two-decade, Smart hydrogel is the ideal candidate for the development of self-regulating drug delivery system with improved therapeutic efficiency. Temperature and pH are the most commonly used stimuli to activate the therapeutic activity of hydrogels as they are biologically and physiologically related. Between the different possible external and internal stimuli, changes in temperature have proved to be easy and weak adverse effects on the tissues compared to other stimuli.

1.1.2 Thermo-responsive hydrogels

Thermo-responsive hydrogels (or temperature-sensitive hydrogels) are able to swell or collapse as a result of temperature changes in surrounding fluid. They can be classified into negatively and positively thermo-responsive hydrogels. Negative thermo-responsive hydrogels are identified by their lower critical solution temperature (LCST). Below the LCST, the hydrogel swells in solution, and above this temperature the polymer shrinks. On the other hand, positive temperature-sensitive hydrogels are identified by their upper critical solution temperature (UCST). Below UCST, the polymer shrinks, and above UCST it swells. By adjusting the temperature of the critical

solution in a physiological range, these hydrangeas are reliable candidates for *in situ* administration of drugs and biologic products (9).

At room or ambient temperature, this thermo-responsive hydrogel can be applied together with a drug into the target tissue, afterwards the system may turn into a gel at physiological temperature (37 °C) (11). It is important that this may introduce the site-specific delivery of the drug and the release of the drug may be controllable. This hydrogel may be administered via various routes including as oral, rectal, ocular, parenteral, nasal, vaginal, dermal and transdermal deliveries (1, 8).

Decisive characteristics of thermo-responsive hydrogels can be investigated by various techniques which include spectrometry, differential scanning calorimetry, and rheology. The major characteristics for verifying thermo-responsive hydrogels such as gelation temperature (sol-gel phase transition), viscoelasticity, gelation mechanism, scattering of light, cloud point, thermal behavior. Moreover, biocompatibility, bioadhesivity, and drug release mechanism are intents to evaluate (12)

The thermo-responsive polymers play an important role in their hydrogel's characteristics. Generally, polymers used for thermo-responsive hydrogels are composed of moderately hydrophobic groups (methyl, ethyl, and propyl) or a mixture of hydrophilic and hydrophobic segments (9). They can be divided into two major classes based on their origin; naturally occurring polymers and synthetic materials. Natural polymers that extensively used to prepare thermo-responsive hydrogel are chitosan, dextran, collagen, alginate, gelatin, hyaluronic, xyloglucan, cellulose and its derivative (13, 14). Moreover, synthetic biodegradable polymers are also developed as thermo-responsive hydrogel such as poly (ethylene glycol) (PEG), poly (D,L-lactic acid-co-glycolic acid) (PLGA), and poly (N-isopropylacrylamide) (PNIPAAm) (13, 15). Thermo-responsive hydrogels based on natural and synthetic polymers have been investigated for both hydrophilic and hydrophobic drug deliveries. For example, xyloglucan hydrogel has been developed for sustained-release of paracetamol (16). Encapsulation metronidazole loaded chitosan/α, β-glycerophosphate (CS/α, β-GP) thermosensitive hydrogel have been investigated for sustained drug release for periodontal delivery (17). Thermo-reversible Pluronic® F-127-based hydrogel containing liposomes-paclitaxel has been developed for controlled release and improved antitumor drug delivery (18).

In addition, polymer blends are plenty utilized as thermo-responsive hydrogels for reducing limitations and enhancing their particular function in physico chemical properties, which are absent in a single polymer. Some of polymeric blends have been reported in various administration routes. For instance, poloxamer 407 and hydroxypropyl methylcellulose (HPMC) or sodium carboxymethylcellulose (NaCMC) have been developed in different ratio as thermo-responsive hydrogel to improve the rheological ($T_{sol/gel}$) and mechanical properties of the hydrogel and suitable formulations for topical or local application (19). A 3D thermo-responsive comprised of hyaluronic acid and poly (N-isopropolyacrylamide, PNIPAAm) has been demonstrated the chemical and mechanical properties to promote human pluripotent

stem cells (hPSC) expansion and differentiation as a potential for biomedical applications (20). Carboxylated single wall carbon nanotubes (COOH-SWCNTs) and natural polymers (chitosan and collagen) have been integrated to formulate the injectable thermo-responsive hydrogels. Their mechanical gel network and osteoblast proliferation have been improved and can be applied in bone tissue engineering and regenerative medicine (21). In addition to the above, a polymer and polymer blends as thermo-responsive hydrogels are summarized in Table 1.1.

Table 1.1 Polymers used for thermo-responsive hydrogels**.**

Polymers	Drugs/ Biomolecules	Administration routes/ Applications	Refs
Single polymer			
Xyloglucan	Rufinamide-loaded chitosan nanoparticle	Direct nose to brain	(22)
Chitosan	Progesterone (PGT)/ randomly methylated-β-cyclodextrin complexes	Vaginal	(23)
Pluronic F127	Gold nanoparticles	Transdermal	(24)
Functionalized PPCN♦	-	Bone regenerative engineering	(25)
PNIPAAm ♣	Corticosteroid-loaded PLGA microsphere	Paranasal sinuses	(26)
Polyisocyanopeptide (PIC)	Lipoxin A_4	Periodontal	(27)
pHPMAmDL-b-PEG♥	Paclitaxel (PTX)	Antitumor	(28)
Polymer blends			
HEC/ NaCMC	-	Ocular	(29)
Chitosang-*g*- PNIPAAm ♣	-	Bone, Cartilage tissue engineering	(30)
MC-*g*- PNIPAAm ♣	-	Cartilage tissue engineering	(31)
MC/ Collagen	hMSC	Stem cell delivery	(32)
MC/ Alginate	BMP-9/ VEGF	Bone tissue engineering	(33)
MC/ Xyloglucan	Metronidazole	Periodontal	(34)
Pluronic F127/ Chitosan	Tacrolimus	Ocular	(35)
Pluronic F127/ HPMC	Gold nanoparticles	Transdermal	(24)
Poloxamer/ Hyaluronic	Acyclovir	Ocular	(36)
Pluronic F127/ GZ♠	Protein (BSA)	Vaccine adjuvants	(37)
Pluronic F127/ MC	Etidronate	Bone formation	(38)
Pluronic F127/ MC	Docetaxel	Anticancer	(39)

♦ Poly(poly-ethyleneglycol citrate-co-N-isopropylacrylamide)

♣ Poly(N-isopropylacrylamide)

♥ Poly(N-(2-hydroxypropyl) methacrylamide lactate) and poly(ethylene glycol)

♠ GZ = poly (methyl vinyl ether-co-maleic anhydride)

1.1.3 Pluronic®

The most commonly used thermo-responsive hydrogels are poly (ethylene oxide)-b-poly (propylene oxide)-b-poly (ethylene oxide) triblock copolymer (PEO–PPO–PEO) which well known in the trade names of Pluronic®, Tetronic®, and Poloxamer®. The United States Food and Drug Administration (USFDA) and Environmental Protection Agency (EPA) are approving some of them for application in food additives, pharmaceutical ingredients, and agricultural products (40). Pluronic® is a class of surface-active, amphiphilic molecules. This triblock copolymer consists of a hydrophilic (PEO) and hydrophobic (PPO) units that can be modified and resulted in different structures such as Pluronic P-85, P-103, F-87, F-98, F-108, and F-127 (41). As increasing the temperature, PPO chains are dehydrated and become insoluble this may induce the formation of micellar structure and aggregation and gelation (42). The gelation of Pluronic® may depend on the concentrations of the polymer and also the certain temperature of each system. Upon cooling or lowering the systems, the polymer is hydrated and relatively soluble in water and the system turns into solution (43). As concentration of Pluronic® decreases, sol to gel transition temperature increases (44). The temperature that micelles are formed is referred to as the critical micelle temperature (CMT). The CMT of Pluronic® is generally range from 25 to 40 °C that covering the body temperature (37 °C) (41). The gelling process by multiple phase transition of Pluronic F127 in concentrated aqueous solution upon heating was investigated by Liu and Li and schematic diagram is shown in Fig. 1.2.

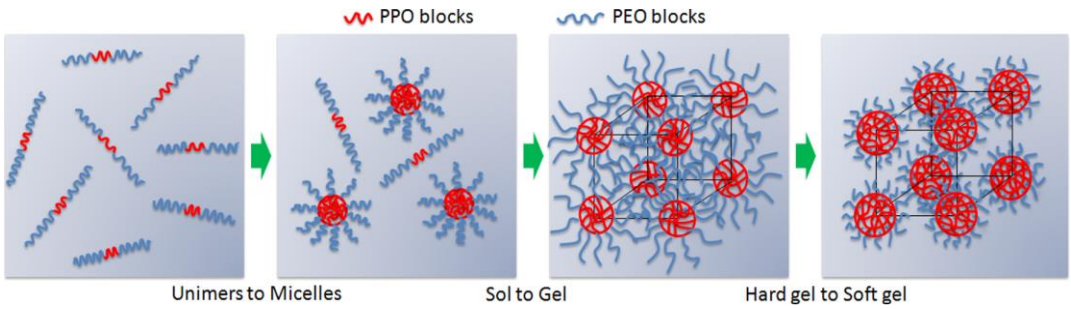

Fig. 1.2 Schematic diagram for multiple phase transitions in concentrated aqueous solutions of Pluronic F127 in a heating process (45).

Pluronic based hydrogel has been widely investigated due to their ability to increase bioavailability (drug solubility and drug absorption); to promote drug stability, to reduce toxicity and to control drug release (44). However, pluronic has some disadvantages including poor mechanical strength, short residence time, high

permeability and limitation of molecular weight (42). Pluronic F127 may be able to form gel at a concentration ≥ 15% w/w (46). Nevertheless, Pluronic F127 at high concentrations (20% wt) is toxic on pre-osteoblasts (MC3T3-E1) and myoblasts cell line (C2C12) (38). Our research group has recently developed thermo-responsive hydrogels by blending Pluronic F127 with methylcellulose and lead to reduce pluronic's toxicity (38). Besides our studies, Pluronic F127 has been blended with various polymers/biopolymers including HPMC (24), chitosan (35), poly (methyl vinyl ether-co-maleic anhydride) (37).

1.1.4 Methylcellulose

Cellulose is a linear macromolecule consisting of (1–4) linked β-D-glucopyranosyl monomers (47). Cellulose itself is insoluble in water due to the strong hydrogen bonds formed between cellulose chains (48). Methylcellulose (MC) is water soluble that is modified from cellulose substituting some hydroxyl groups of cellulose with methyl groups (49). The degree of methyl substitution is between 1.4 and 2.0 (50). MC is extensively utilized in various areas such as biotechnology, paints, pharmaceuticals, cosmetics and foods (51).

MC is a thermo-responsive gel that forms gel upon heating and returns to sol upon cooling (50). As increasing temperature hydrogen bonds become weaker and the "cage structure" is sufficiently disrupted at the gelation temperature to facilitate a phase separation. The hydrophobic segments subsequently aggregate together, forming a bicontinuous network (52). MC with an appropriate degree of substitution can form gel in a temperature range from 50°C to 75°C. Moreover, MC at high temperature range also shows turbidity effect (53). Gelation mechanism of MC upon heating has been reported by Li and colleagues (54) and schematic drawing is shown in Fig. 1.3. However, degree of substitution, molecular weight, and salts (salt-assisted and salt-suppressed) are factors affecting on thermal gelation and turbidity of MC (50).

MC has been considered as an appropriated hydrogel-based system for enhancing local drug concentration at target site, non-toxic, and reducing toxic effects in normal cells (39). A limitation of MC hydrogel is that its sol-to-gel transition at temperatures is higher than the body temperature (50-70°C). The gelation temperature of MC should be lowered below a body temperature for *in vivo/ in situ* applications (39). The gelation temperature of MC may be decreased by the addition of metal salts, citrate, sugars (sucrose, fructose, and sorbitol), and glycerol has been demonstrated (55). Besides, small molecules of gallic acid could reduce gelation temperature of MC (56). MC has been blended with various polymers including chitosan, agarose and pluronic. The blending of Pluronic F127 with MC has been found to optimize the gelation temperature of the system. The blends have been employed to delivery various drugs including insulin (subcutaneous delivery) (57), etidronate (bone osteogenesis)

(38), timolol maleate (ocular delivery) (46) and docetaxel (anti-cancer drug delivery) (39).

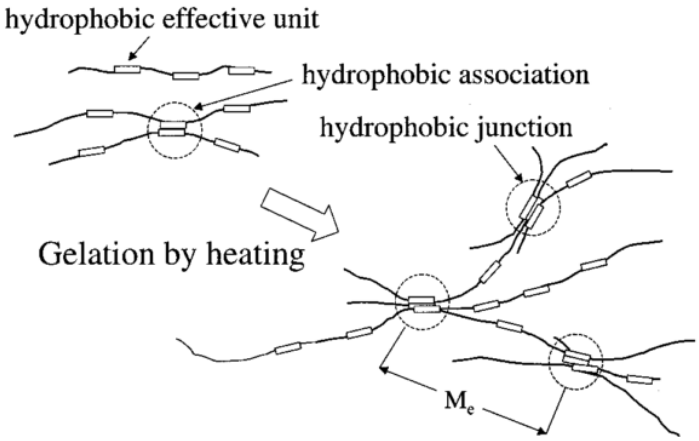

Fig. 1.3 Schematic drawing showing gelation though the hydrophobic effective units of methylcellulose chains upon heating (54).

1.1.5 Periodontitis

Periodontitis is an inflammatory disease of gums involving the periodontal ligaments degradation, periodontal pocket formation and alveolar bone resorption, resulting in the disruption of the supporting structure of the teeth (58). As reported by WHO, the global population suffers from severe periodontitis around 10-15% (59).

The growth and accumulation of gram-negative anaerobes in the pockets are the majors caused of the disease, such as *Aggregatibacter actinomycetemcomitans, Porphyromonas gingivalis, Fusobacterium nucleatum*, and *Prevotella intermedia*. Gram-negative anaerobes release toxins and enzymes that can stimulate body's immune response causing the destruction of alveolar bone and connective tissues (58, 60).

First signs of periodontal disease usually begin with gingivitis (reddened, swollen, and bleed), then the disease progressed by gum tissues begin to recede causing pocket formation which may cause tooth sensitivity to temperature and pressure change. As pocket formation progresses, supporting bone loss may be noted around the teeth. Abscess formation, the collection of pus pockets denoted by pain, swelling and discharge from the gum tissues is a later sign of disease, Finally, the destruction of alveolar bone and connective tissues are destroyed result in tooth loss (58, 60).

The goals of treatment are to eliminate infected tissues caused by bacterial plaque and to regenerate lost/damaged periodontal tissues. However, the complete eradication of the organisms from the infected sites was not achieved by surgical, mechanical treatments (scaling and root planning), and systemic drugs (58, 60).

1.1.6 Periodontitis local drug delivery

At the present time, controlled local drug delivery procedure is more favorable as compared to the systemic procedure owing to the fact that it essential focuses on enhancing the therapeutic outcomes by reaching factors like site-specific delivery, lower dose requirement, bypass of first pass metabolism, reduction in gastrointestinal side effects and decreasing in dosing frequency. Overall, controlled local drug delivery system for periodontitis provides a safe and effective approach of treatment that enhances patient compliance. Advance polymer-based delivery systems like fibers, gels, micro/nanoparticles, and chips/films made from a variety of natural and synthetic materials have been successfully tested for sustained drug release (Fig. 1.4). These systems are biocompatible, biodegradable, and mucoadhesive. They can fill the pockets, and have strong retention on the target site.

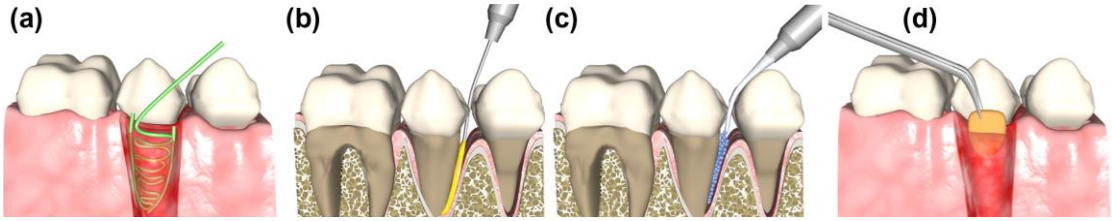

Fig. 1.4 Advance drug delivery system for periodontitis: (a) Fibers, (b) Gels, (c) Miro/nanoparticles, and (d) Chips/films (61).

As shown in Fig. 1.4a, fibers are threadlike and reservoir-type drug delivery systems. They are placed into the pockets circumferentially using an applicator and are sealed in place by applying cyanoacrylate adhesive. Therefore, the entrapped drug provides sustained release by diffusing out through the fiber system into the pocket (62). In 1979, Goodson and colleagues made up cellulose acetate hollow fibers filled with tetracycline hydrochloride. Results were less rapid the drug released and effected in reducing pathogenic subgingival microorganisms as compared to scaling and root planning (63). Then 1983, they developed monolithic fibers made of tetracycline-loaded ethylene vinyl acetate to retard the drug release, the drug could be maintained longer for a week in deep periodontal pockets (64). A few polymers such as poly(ε-caprolactone), polyurethane, polypropylene, cellulose acetic acid derivation propionate and ethyl vinyl acetic acid derivation have been examined as matrices for the delivery of drug to the periodontal pocket (65). The disadvantages of fibers are time-consuming during clinical treatment insertion process and it needs to remove on a weekly basis. Thus, the patients and the clinician were discomforted (58, 62).

Gels are semisolid systems that widely apply as antibiotics delivery for periodontitis treatment by injection into the intrapocket (Fig. 1.4b). Injectable hydrogels are popular as the intrapocket drug delivery for the treatment of periodontitis. Since these systems can be made *in situ* in nature by using specific polymers. This device is easy to use and short time for administration by small needle, low pain, low bleeding on probing, and proper fixation to the periodontal pocket. Moreover, they possess a higher biocompatibility and bioadhesivity, allowing adhesion to the mucosa in the dental pocket. Furthermore, they can be quickly eradicated by typical catabolic pathways, reducing the risk of host irritant or allergic reactions at the site of application (58, 62). Chitosan gel with or without 15% metronidazole demonstrated effectiveness in the clinical treatment of chronic periodontitis, applied adjunctive to scaling and root planing (SRP) in comparison to SRP alone (66). A thermo-responsive hydrogel composed of methylcellulose and xyloglucan loaded-metronidazole (1% w/w) has been developed as an *in situ* mucoadhesive and sustained release for the treatment of periodontitis (34). An injectable metronidazole delivery system for periodontal treatment based on chitosan/gelatin/β-glycerolphosphate thermo-responsive gel has been evaluated. Results showed sustained release of drugs that are effective for inhibition of anaerobic gram-positive over time and found as no cytotoxic effects on HEK 293 cells (67).

Micro/nanoparticles are solid spherical polymeric structures containing drug dispersed throughout the polymeric matrix (62). They are free-flowing powders, regarding as smart vehicles for drug delivery to the pocket area (Fig. 1.4c). Their advantages are frequently used to enhance the therapeutic value of a variety of water soluble/insoluble medicinal drugs and bioactive molecules by shielding of unstable drug before and after administration, improving solubility, enhanced bioavailability and decreased frequency and intensity of adverse effects (68). Local drug delivery of doxycycline hyclate in HPMC microspheres have been evaluated in patients. Clinical parameters result like probing pocket depth and *Porphyromonas gingivalis* amounts in the periodontal pocket significantly reduced (69). The silver nanoparticles in the size of 5 nm have been synthesized and exhibited aerobes and anaerobic activity of oral pathogens like *A. actinomycetemcomitans*, *F. nuceatum, S. mitis, S. mutans* and *S. sanguis* (70). Triclosan-loaded PLGA nanoparticles have been preliminary in vivo studies in dogs with induced periodontal defects. The results revealed that triclosan released quickly from nanoparticles and penetrate through the junctional epithelium (71).

Chips/Films are matrix drug delivery devices comprising of drugs distributed throughout the polymer. The drugs are released by diffusion and/or matrix dissolution or erosion. Chips/Films could be placed in the cavity over the lining of the cheeks or the surface of the gums, or be cut/punched in appropriate sizes for insertion into pockets (Fig. 1.4d). Chips/Films composed of water-insoluble nondegradable polymers release drugs by only diffusion, whereas those made of soluble or biodegradable polymers release by diffusion and matrix erosion or dissolution. Chips/Films are less discomfort to the patient as compared to fibers, they present an easy insertion and appropriate sizing for suiting the pockets (72). Several natural and

synthetic biodegradable polymers have been used for this device. The films consisted of water-soluble polymer Eudragit S1 and non-water-soluble polymer Eudragit L1 for the delivery of clindamycin have been prepared. An in vitro release study revealed that insoluble films release the drug by diffusion and soluble films release the drug by dissolution of the carrier (73). The single-layer films made from PLGA micromatrices loaded with Ipriflavone into a Chitosan film were compared with multilayer films composed of Chitosan/PLGA/Chitosan (three layers). In vitro experiments have shown that composited micromatrix films are an appropriate dosage form for extending the release of Ipriflavone for 20 days (74). The distinguishing films made of poly (vinyl alcohol) (PVA) and carboxymethyl-chitosan (CMCS) were mixed by blending/casting methods and loaded with ornidazole as a delivery system for periodontitis drugs. The blended films were exhibited pH-responsive swelling, presented biocompatibility, and found to be good retention at the application site and retained high drug concentration at least for five days (75).

Besides these 4 devices, liposome systems are designed to mimic the bio-membranes in terms of structure and bio-behavior, and consequently are explored are a plan for focus on periodontal biofilms. Another is the use of low-dose antibiotics. The low-dose of the drug does not act to kill bacteria, but rather to change the way of body responds on over production of collagenase enzyme, causing the destruction of gum tissue (62). Nowadays, some commercial products of local drug delivery devices for periodontitis treatment are available in the market (Table 1.2.).

Table 1.2 Marketed products for the treatment of periodontitis (58).

Market name	Dosage form	Drug	Manufacturer
Actinide	Nonbiodegradable fibers	Tetracycline	Alzacorn
Actisite	Nonbiodegradable fibers	Tetracycline hydrochloride	Alza Corporation
Atridox	Biodegradable mix of doxycycline gel and doxycycline hyclate powder in syringe	Doxycycline	Atrix labs
Dentamycine	Powder	Minocycline	Sunstar Corp
Dentomcin	Gel	Minocycline hydrochloride dihydrate	Henry Schein UK Holdings Ltd.
Elyzol	Gel	Minocycline	Dumex Pharma
Elyzol	Gel	Metronidazole	Colgate-Palmolive (UK) Ltd
Periochip	Chip	Chlorhexidine gluconate	Dexcel Pharma Technologies Ltd
Periochip	Chip	Chlorhexidine	Perioproducts Ltd
Gluconate	Insert	Metronidazole	Perioproducts Ltd

1.1.6 Doxycycline hyclate

Doxycycline is a broad-spectrum antibiotic drug in a group of tetracyclines and preferred to other tetracyclines in the treatment of specific infections because of its reliable absorption and its long half-life, which permits less frequent dosage (76). Doxycycline exists in three forms: hydrochloride, monohydrate, and hyclate. In this study, doxycycline hyclate is expected to use as a model drug. Doxycycline hyclate is the hemiethanolate hemihydrate of doxycycline hydrochloride (Fig. 1.5). It exists as a yellow hygroscopic crystalline powder which is freely soluble in water (50 mg/ml). The molecular weight is 1025.89 g/mol with pKa: 3.5, 7.7, 9.5 (at 20 °C). Unfortunately, it is a highly photosensitive drug (77). Doxycycline hyclate as a valuable agent in treating and managing many infectious diseases such as, skin, dental, respiratory, and urinary tract by inhibiting the bacterial protein synthesis due to the disruption of transfer RNA and messenger RNA at the ribosomal sites (78).

Various carriers have been reported as the delivery systems for doxycycline hyclate. PLGA (Lactic- co-glycolic acid) coated chitosan microspheres loaded with hydroxyapatite and doxycycline hyclate complex have been developed for periodontal drug delivery (79). Trimethylene carbonate/ϵ-caprolactone (TMC/CL) bioresorbable polymeric implants for controlled doxycycline hyclate release for periodontal treatment have been investigated (80). Doxycycline-loaded chitosan nanoparticles for improving drug delivery and efficacy in the treatment of bacterial uterine infections have been determined (81). A doxycycline-HP-β-CD inclusion complex in an *in situ* thermally sensitive poloxamer has been studied and it represents a potentially effective as ophthalmic delivery system (82).

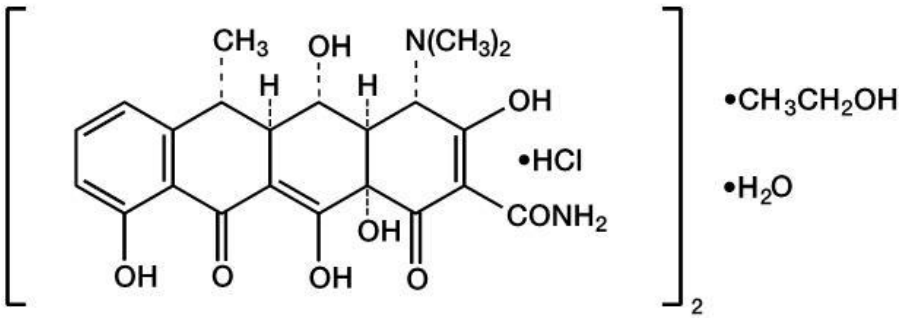

Fig. 1.5 Chemical structure of Doxycycline hyclate (Product information: Sigma Aldrich, D9891)

1.1.7 Etidronate

Bisphosphonates (BP) are a category of drugs used to treat various bone diseases, such as osteoporosis, Paget's disease, bone malignancy and other skeletal complications involving excessive bone loss (83). All BP drugs share a common P–C–P functional unit in their chemical structures, which is called the *'geminal bisphosphonate'* unit. (83). Etidronate is well known as one of bisphosphonates (BP) derivatives, which is normally used in a salt form of Sodium etidronate (Etidronate disodium). The chemical structure of Etidronate acid is shown in Fig. 1.6a. It has three active binding sites, which allow ionic coordination to occur between Ca^{2+} in the hydroxyapatite and any of the oxygen atoms bonded to the BP or the α-carbon moiety (84). While Disodium etidronate is an organic sodium salt produced by the substitution of two protons of Etidronate acid (Fig. 1.6b).

(a) (b)

Fig. 1.6 Chemical structures of (a) Etidronate acid, (b) Etidronate disodium (Product information: TCI chemical, D4159)

Etidronate is a first-generation non-nitrogen containing bisphosphonate that intracellularly metabolized into ATP analogues. These metabolites inhibit osteoclastic resorption (osteoclasts apoptosis) and decreases bone turnover process (83, 85). Etidronate is considered a weaker anti-resorptive agent than the other bisphosphonates (clodronate, alendronate and risedronate) (86). Generally, the bioavailability of bisphosphonates (intestinal absorption) is low (less than 1 to 10%) both in animals and in humans, probably because of low lipophilicity and high negative charge (84). The most common adverse effects associated with bisphosphonates are renal toxicity, acute-phase reactions, gastrointestinal (GI) toxicity, and osteonecrosis of the jaw (ONJ)(87). The incidence of these adverse events varies significantly between bisphosphonates. The oral formulations of etidronate produce remarkably few upper GI adverse and common diarrhea. Administration of etidronate by intravenous route for the treatment of malignant hypercalcaemia cause of renal toxicity were reported (85).

Therefore, local delivery of etidronate to the site of application could enhance their bioavailability and reduce adverse effects. Various approaches such as liposome, nanoparticle, and microparticles could be developed for etidronate local delivery system.

1.2 Background and rationale

As refer to literature review, application of hydrogels as drug delivery systems, especially for thermo-responsive hydrogels is attractive to use as injectable *in situ* drug delivery. The systems are solution at or below ambient temperature and then become gel at body temperature by *in vivo/ in situ* injection. The injectable thermosensitive hydrogel systems exhibit many advantages, such as enhanced solubility of hydrophobic drugs, enhanced safety (no organic solvents, no toxic initiators, and less systemic toxicity), simple drug formulation and administration, without surgery procedure, sustained release behavior, site-specificity, and delivery of various types of drugs (hydrophilic drugs, hydrophobic drugs, peptides, proteins, nucleic acid) (88). Therefore, in situ administration of drugs assisted by injectable thermo-responsive is an interesting route for local drug delivery.

Polymers are an important role on the characteristics and biological activities of thermo-responsive hydrogels. Pluronic F127 is a triblock copolymer demonstrating the thermo-responsive behavior. In aqueous solution Pluronic F127 at constant concentrations can form gels at reaching critical micelle temperature (or CMT) at above 25°C. While, it also forms to gel at concentration reaching to critical micelle concentration (or CMC) at concentrations above 15% w/w, depending on temperature (46). It provides an excellent drug delivery system for a number of routes of administration and is compatible with many different substances (41). On the other hand, Pluronic F127 has several drawbacks, such as poor gel durability, weak mechanical strength, and rapid drug release, toxic to the cells on (MC3T3-E1 and C2C12) high concentrations about 20% w/w (38, 88). Thus, Pluronic F127 based grafted polymers and blended with other polymers are the common approach to circumvent the above issues.

Blending Pluronic F127 with some polymers or biopolymers can reduce toxicity itself like a chitosan and carrageenan able to sustained release of drug (89, 90). Interestingly, there have found that combination of Pluronic F127 and methylcellulose, could not only sustained release but also reduced toxicity of drug as comparison with free drug (38, 39).

Methylcellulose is a thermo-responsive gel that form gel upon heating and return to sol upon cooling. Methylcellulose based hydrogel provide many advantages such as nontoxic, reduce toxicity in normal cells, and also enhance local drug concentration at target site but it from gel at high temperature at above 50°C. Therefore, gelation temperature of methylcellulose should close to body temperature.

In 2016, our research group investigated EDS-loaded thermo-responsive hydrogel composed of various concentrations of Pluronic F127 (12, 14, 16, 18, and 20 %w/w) and a constant concentration of methyl cellulose (4% w/w): 12PF/MC, 14PF/MC, 16PF/MC, 18PF/MC, and 20PF/MC. The results were found that the blends could reduce the toxicity of Pluronic F127 as compared to their corresponding dose. In

addition, these hydrogels could sustain drug delivery for osteogenesis applications. Nevertheless, hydrogel characteristics and gel formation mechanisms should be additionally studied.

Therefore, thermo-responsive hydrogels of Pluronic F127 and methylcellulose were investigated their sol-gel characteristics and gel formation mechanisms in this work. Moreover, thermo-responsive hydrogels were examined the efficient for periodontitis drug delivery system. Furthermore, structural characterization of Pluronic F127, Methylcellulose, and their blends were employed by Small-Angle X-ray Scattering (SAXS).

1.3 Objectives

The objectives of this study were:

1. To prepare the polymeric thermo-responsive hydrogels consisting of Pluronic F127 (PF) and Methylcellulose (MC) for drug delivery systems.
2. To investigate the thermo-responsive characteristics of prepared hydrogels.
3. To select the optimize hydrogels for investigation as *in situ* periodontitis drug delivery system.
4. To determine the structural characteristic of Pluronic F127, Methylcellulose and their blends by Small-Angle X-ray Scattering (SAXS).

CHAPTER 2

RESULTS AND DISCUSSION

FOR PLURONIC F127, METHYLCELLULOSE AND THEIR BLENDS

This chapter aims to discuss about preparation and characterizations of thermo-responsive hydrogels containing various concentrations of pluronic F127 (PF) and 4% w/w methylcellulose (MC).

2.1 Hydrogels preparation

Different concentration of PF solution ranging from 12, 14, 16, 18, and 20% w/w were prepared by dispersing the accurate amount of PF powder in cold water on ice bath under stirring condition for 30 min or until its powder completely dissolved and transparent solution was obtained. These solutions were referred as 12PF, 14PF, 16PF, 18PF, and 20PF, respectively. All were placed in refrigerator at least 24 hours for ensuring complete solubilization (38).

4% w/w MC solution (MC) was prepared by dispersing the required amount of MC powder in hot water (about 70°C) with vigorous stirring. After complete dispersion, the temperature of the mixture was reduced on ice bath with continuous stirring until clear solution appeared. Then it was kept in refrigerator at least 24 hours to ensure completely homogenous (11).

The blends were prepared by dispersing the precise quantity of PF powder (12, 14, 16, 18, and 20% w/w PF) in cold MC solution (which has been prepared at least 24 hours as mentioned above) on ice bath under stirring for 30 min or until clear mixture was observed. These blends were denoted as 12PF/MC, 14PF/MC, 16PF/MC, 18PF/MC, and 20PF/MC, respectively. All PF/MC blends were refrigerated until thoroughly dissolved least 24 hours.

The blends loaded drug were performed by dissolving the accurate quantity of EDS powder in each PF/MC blends, which was mixed sequentially as described above. All the blends were further stirred and then cooled until clear solutions were monitored. The final concentration of EDS in all blends was 4×10^{-3}M (38). Samples were mentioned as 12PF/MC/EDS, 14PF/MC/EDS, 16PF/MC/EDS, 18PF/MC/EDS, and 20PF/MC/EDS, respectively.

Before testing, all sample were cooled and maintained in solution state. MC solution were clear faint yellow. Each PF solution was transparent watery. PF/MC

blends were clear faint yellow. Each PF/MC/EDS was also presented clear faint yellow fluid. These showed that the appearance of PF/MC systems was not disturbed by EDS.

2.2 Gelation temperature analysis

Test tube inversion method (TTM) was conducted for finding estimate the gelation temperature and qualitative analysis of the transition from clear gel to turbid gel. Samples were heated at temperature ranging from 16 °C to 70 °C and allowed to equilibrate for 20 min after each increment. Effect of heating on gelation of various PF concentrations are shown in Fig. 2.1. Based on TTM investigations, all concentrations of PF maintained clear solution state at 4 °C. As period of heating time, 12PF and 14PF were not formed gel at every time points. After heating at a rate 1°C/ min, 16PF, 18PF and 20PF formed clear hard gel about 30, 26, and 22 °C, respectively. There were observed that 16PF, 18PF and 20PF sustained clear hard gel at temperature during 30-70 °C, including at body temperature (37 °C). After equilibrated for 20 min, 16PF was turned to soft clear gel at temperature about 60 °C. Then, clear soft gel of 16PF was changed to viscous solution at 70 °C. This transition from gel to sol were not observed in 18PF and 20PF. This transformation was predicted that 18PF and 20PF were stronger gel than 16PF at high temperature. This result has been agreed with previous report that PF able to form gel at concentration greater than or equal to 15% w/w (46) and PF gels were transparent above 100 °C (91).

During heating at a rate 1°C/ min, MC changed behavior from clear solution (16-41 °C) to turbid soft gel (42-49 °C) and became turbid hard gel at high temperature (50-70 °C). Gelation temperature of MC was found about 50 °C. As shown in Fig. 2.2, MC were clear solution at 25 °C and 37 °C. Turbid hard gel was seen at 50, 60, 70 °C, respectively. This result is normally phenomenon in aqueous solution of MC that is soluble at lower critical solution temperature (LCST) and becomes gel at high temperature. Gelation process of MC are two steps, the first step is pre-gel (clear loose gel/ soft gel) occurring by hydrophobic interaction between highly methylated glucose zones, and the second step, is a phase separation appearing at temperatures 60 °C with formation of a turbid strong gel (53). Turbidity of MC and their blends were examined in next subtopic.

At low concentrations of PF (12PF and 14PF) did not form gel, but blending with MC, the blended (12PF/MC and 14PF/MC) were able to form gel. Gelation temperature of 12PF/MC, 14PF/MC, 16PF/MC, 18PF/MC, and 20PF/MC were about 26, 23, 21, 20, and 18 °C, respectively. As shown in Fig. 2.2, after samples were equilibrated at 25°C for 20 min, 12PF/MC was high viscous liquid. 14PF/MC, 16PF/MC, 18PF/MC, and 20PF/MC were slightly turbid gel depending on increasing

of PF concentrations. At body temperature (37 °C), MC did not produce gel, nevertheless, their blends (12PF/MC, 14PF/MC, 16PF/MC, 18PF/MC, and 20PF/MC) became turbid hard gel. At the temperature reaching to 50 °C, MC and their blends were turbid hard gel, especially for MC which was cloudiness than others. These blended gels were undeformed although temperature rising to 70 °C.

Gelation temperature of 12PF/MC/EDS, 14PF/MC/EDS, 16PF/MC/EDS, 18PF/MC/EDS, and 20PF/MC/EDS were about 26, 23, 21, 20, and 18 °C, respectively, that are similar to those corresponding systems without EDS. Effect of heating on gelation of PF/MC/EDS blends are shown in Fig. 2.3.

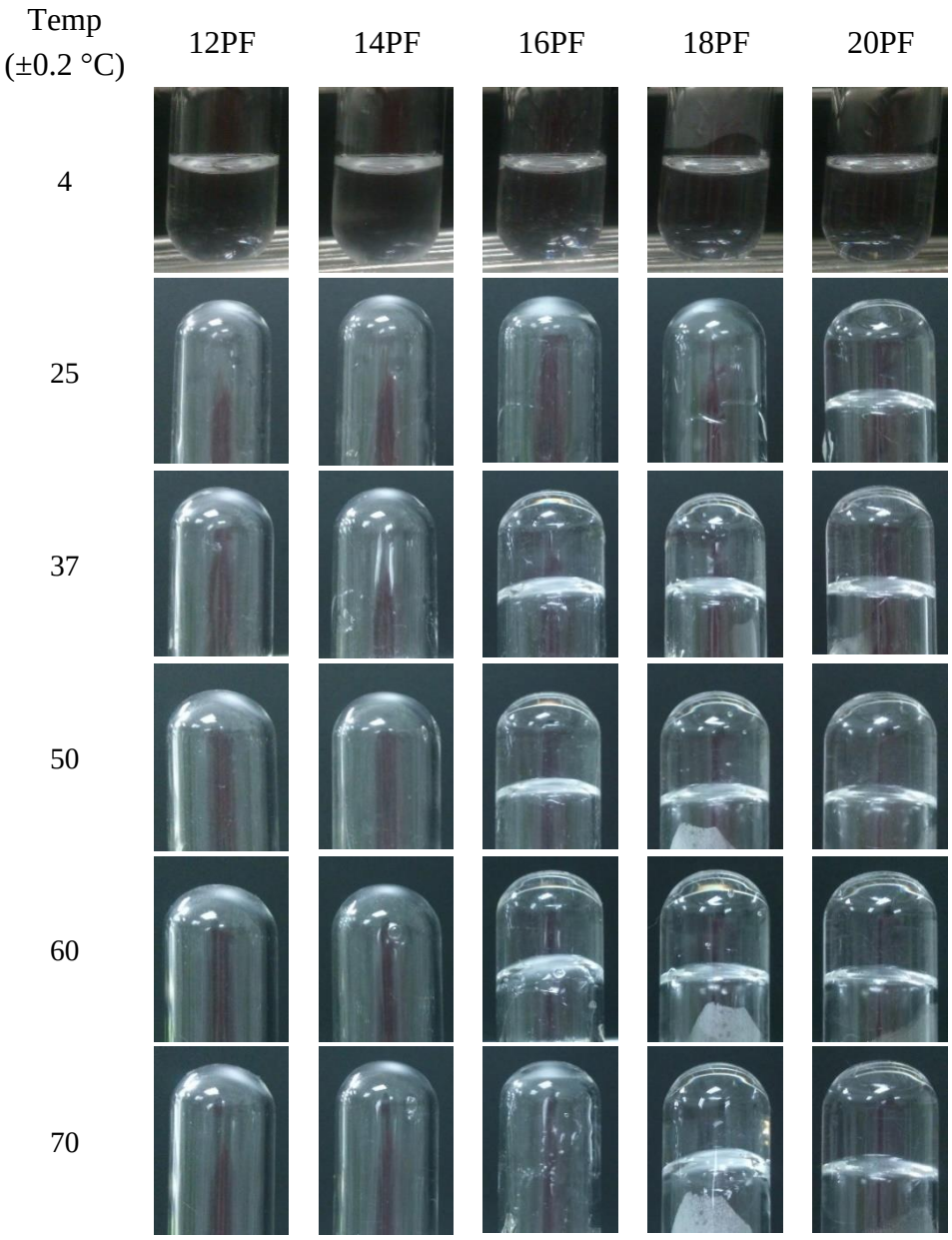

Fig. 2.1 Effects of heating on gelling and visible turbidity of various PF concentrations after heating over different time points.

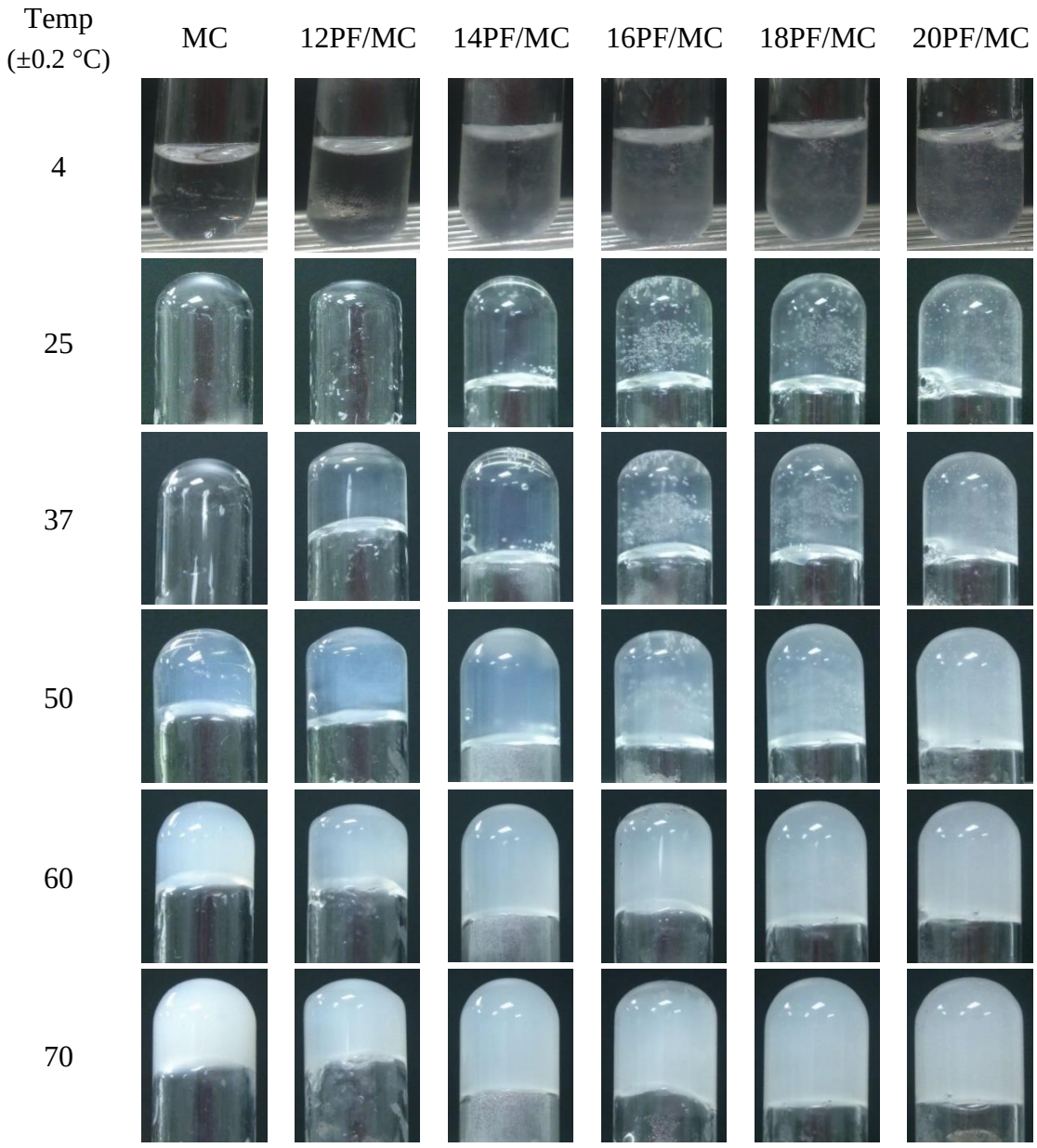

Fig. 2.2 Effects of heating on gelling and visible turbidity of PF/MC at various PF concentrations after heating over different time points.

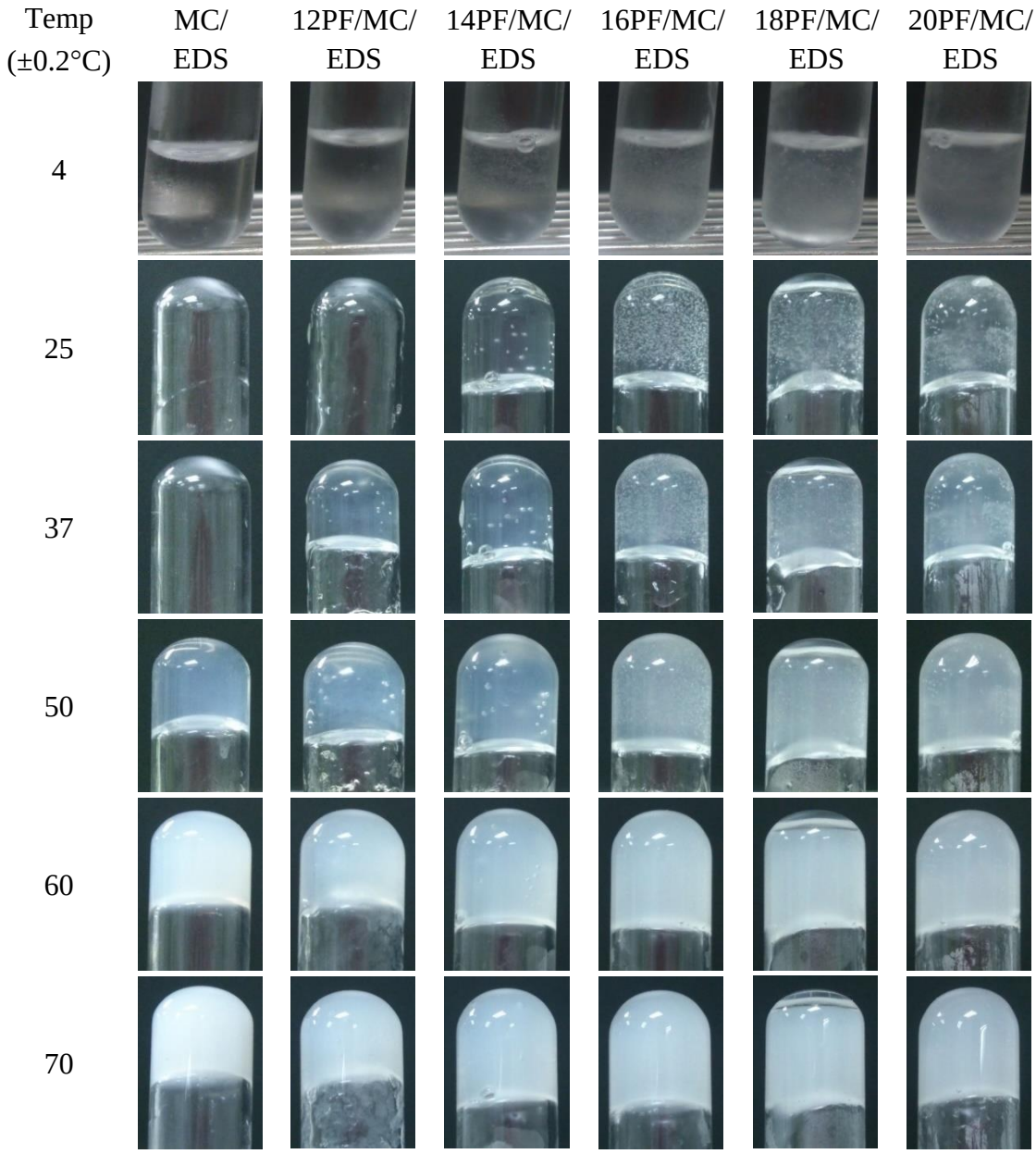

Fig. 2.3 Effects of heating on gelling and visible turbidity of PF/MC/EDS at various PF concentrations after heating over different time points.

2.3 Turbidity measurement

The turbidity appearance or cloud point of thermo-responsive polymer in aqueous can be monitored by visual observation. However, slight changing may not be detected by visual observation with the naked eye. UV-Vis spectroscopic approach was used in this study for viewing the different turbidity in each sample. The absorbance of MC was measured at 500 nm that has been previously reported (92).

Fig. 2.4a shows UV-Vis absorbance at 500 nm of MC and PF/MC blends system during heating from 20-70 °C at a rate of 1°C/min. During heating, MC gradually became turbid at temperature 45-55 °C. Then, absorbance was climbing to the highest turbidity at 70 °C.

The clear solutions of PF/MC slowly became turbid with the increasing temperature and turbidity was increased with PF dependance concentrations. 12PF/MC and 14PF/MC turned turbid about 40 °C. The 16PF/MC, 18PF/MC, and 20PF/MC blends were found turbid about 30, 26, and 20 °C, respectively. At high temperature, these turbid temperatures of PF/MC blends are lower than that of MC alone (Fig.2.4a)

The turbidness of MC/EDS and PF/MC/EDS blends were found to be in the same direction as MC and PF/MC blends (Fig. 2.4b). These revealed that EDS did not disturbed turbidity mechanism of MC and PF/MC co-solutions.

These absorbance at 500nm were found that turbidity decreased accordingly as the PF concentrations decreased. Effect of additives on the cloud points of aqueous solutions of PF has been previously investigated (93). Commonly, additives that increase hydrophilicity may increase the temperature of clouding, while additives that increase hydrophobicity of the system decrease the cloud point (93, 94). Consequently, the turbidity may be caused by the effect of MC on the PF system. For PF/MC mixtures, the clouding phenomenon may be mentioned to the capable dehydration of PEO moiety or hydrophilic moieties of micelles by MC. Micelles structure of PF attract or link each other and form inter-micellar bridges or micellar cluster with the approach of the cloud point as previously described (95). As shown in heating process (Fig. 2.4), clouding temperatures of PF/MC decreased as the concentration of PF increased. This may result from the higher attractive interaction of micelles with high amounts of PF.

(a)

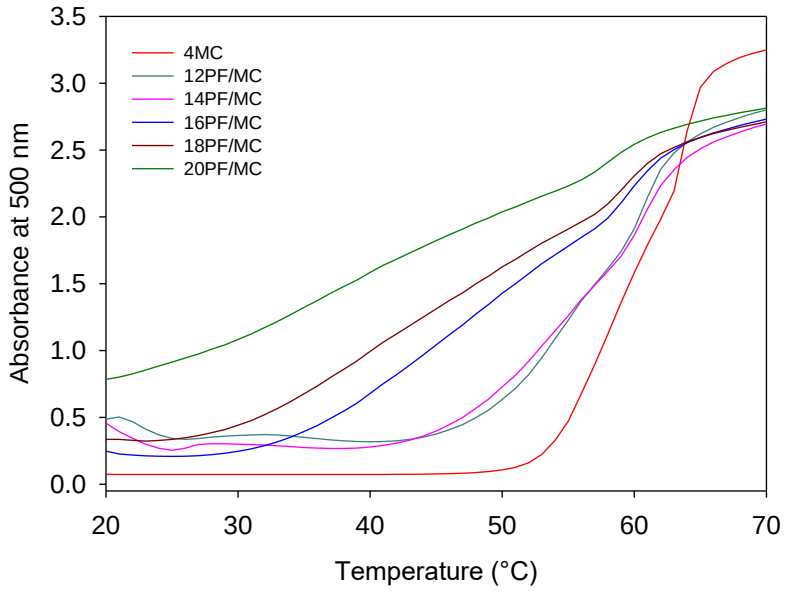

(b)

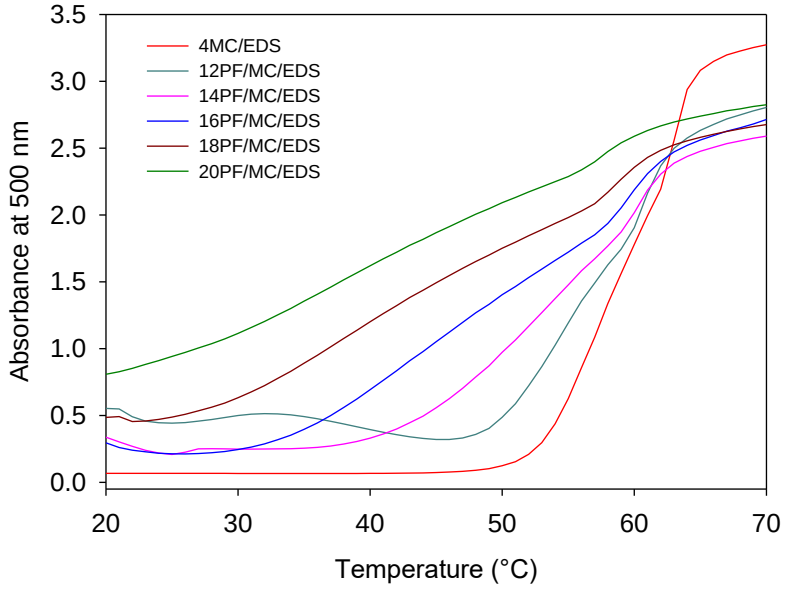

Fig. 2.4 UV-vis absorbance at 500 nm versus temperature of (a) MC and PF/MC at various concentrations of PF, (b) MC/EDS and PF/MC/EDS at various concentrations of PF during heating from 20-70 °C at a rate of 1 °C/min.

2.4 Micellization and gelation analysis

DSC was employed to investigate CMT and heat of micellization (ΔH) of PF solutions and PF/MC co-solutions during heating. The endothermic peak is considered as an indicator for the existence of micellization, with the peak onset and offset temperatures corresponding to the start and end of the process. Increasing either temperature or concentration of PF increased micellization (96).

Thermograms of various concentrations of PF, MC, and PF/MC are shown in Fig. 2.5. The solutions of 12PF, 14PF, 16PF, 18PF and 20PF showed endothermic peaks that were consistent for micellization at 19.8, 17.8, 17.4, 15.9 and 15.0 °C, respectively, during heating (Fig. 2.5a). The endothermic peaks shifted to lower temperatures in the presence of MC (Fig. 2.5b): the endothermic peaks for 12PF/MC, 14PF/MC, 16PF/MC, 18PF/MC and 20PF/MC were detected at 17.2, 16.5, 15.3, 13.0 and 11.5 °C, respectively. In addition, the endothermic peaks were not significantly changed in PF/MC co-solutions with EDS (Fig. 2.5c): the endothermic peaks for 12PF/MC/EDS, 14PF/MC/EDS, 16PF/MC/EDS, 18PF/MC/EDS and 20PF/MC/EDS were detected at 17.2, 17.0, 15.3, 13.6 and 11.6 °C, respectively. At this micellization temperature range, no peak was detected for EDS, MC solution and MC/EDS solution since the gelation mechanism of EDS and MC does not involve micellization. These indicated that micellization process of MC and PF/MC co-solutions were not interfere by EDS.

The endothermic peak is defined to the dehydration of PPO blocks which consecutively lead to micelle formation. The area under the endothermic peak (ΔH) is proportional to the amount of formed micelle (96). The enthalpy of micellization (ΔH) increased with the increase in PF concentrations (Figs. 2.5a and 2.6). These results are in accordance with previous findings which asserted that ΔH was proportional to the concentration of PF (96, 97). However, ΔH of the mixtures of PF/MC was lower than that of the corresponding PF concentration without MC (Figs. 2.5b-c and 2.6). This can be regarded as an indication of the involvement of MC on self-assembly and micellization of PF. The decrease in ΔH is suggestive of a reduction in the energy consumed for PPO dehydration (98). MC may enhance the dehydration of PPO and consequently lower the micellization temperature and ΔH of the PF/MC blends, which is not the case for their pure PF counterparts. In general, the appearance of endothermic peak may indicate the formation of micelles but cannot predict whether the system will be able to form gel. For the neat PF, the sol-to-gel transition was considered to occur when the micelle density attained a definite value, resulting in close packing of the micelles into an ordered structure with the PPO cores connected by PEO strands of the copolymer (96). When MC is present, its interaction with PF and the reduction of the intermolecular hydrogen bonding between the PEO moiety of PF and water may increase the connection between micelles. This may result in the sol-to-gel

transition and gel formation of the system even at the low concentrations of PF (12PF and 14PF), which would typically not form gel.

MC, various concentrations of PF and their blends including the blends present EDS were investigated by TTM, UV-Vis spectroscopy, and DSC. These three methods showed clearly that EDS (4×10^{-3}M) did not disturb their characteristics. Therefore, the blends present EDS were not mentioned for next studies in this chapter.

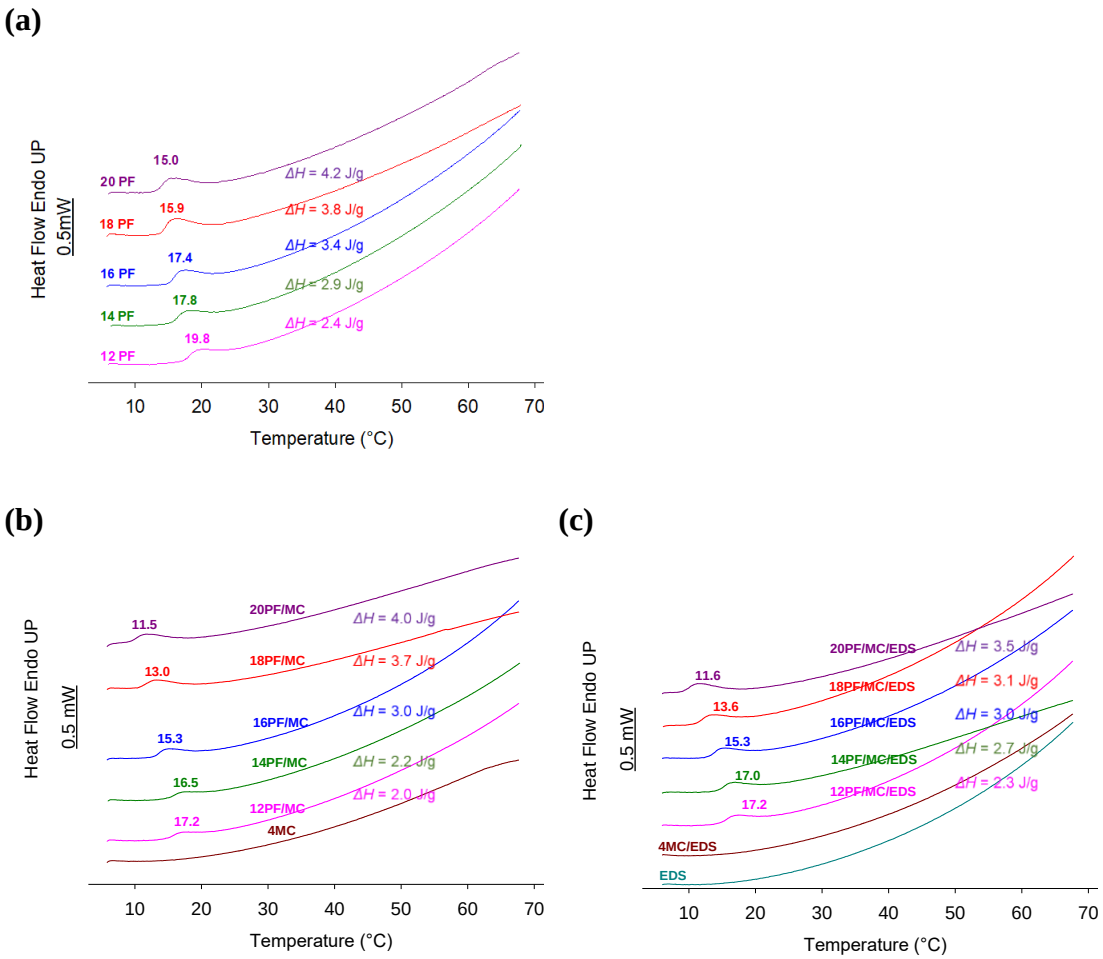

Fig. 2.5 DSC thermograms of (a) various concentrations of PF, (b) MC and PF/MC, and (c) EDS, MC/EDS, and PF/MC/EDS during heating at a rate of 1 °C/min.

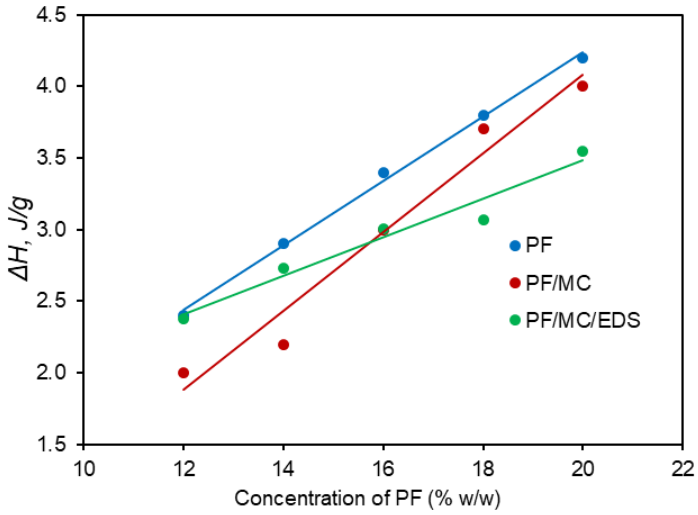

Fig. 2.6 Enthalpy of PF solution and the blends of MC and different concentrations of PF during heating ramps.

2.5 Rheological measurement

The sol-to-gel transition of PF and PF/MC was further investigated by comparing their viscoelasticities as a function of temperature. Viscoelastic moduli, storage modulus (G′) and loss modulus (G″) of the aqueous solutions of MC, 12PF, 14PF, 16PF, 18PF and 20PF upon heating are shown in Fig. 2.7.

Rheogram of MC solution (4% w/w) shows in Fig. 2.7a. MC with G"> G' was initially observed at low temperature lower than 46 °C, remained as liquid-like state. Then, G′ and G″ increased abruptly with crossover at 46.4 °C, which demonstrated that MC was change from liquid-like state (solution) to a solid-like state (gel). The cross over point (G″=G′) was demonstrated as sol-to-gel transition temperature of sample. Lastly, G″<G′ was observed at high temperature above than 46 °C. MC at low temperature has liquid-like state due to hydrophobic effective unit association. During heating, hydrophobic association progressively occurs, the gel is formed (54). This study found two-step gelation mechanism dependent on heating of MC which was similar to previous reported (54).

For the aqueous solutions of 12PF and 14PF (Fig. 2.7b-c), G″ was higher than G′ at all temperature range of this study (5–70 °C), indicating that 12PF and 14PF were in a liquid state. The effect of temperature on G′ and G″ for the 16PF, 18PF and 20PF aqueous solutions in early step are the same as described for 12PF and 14PF: G′ remained constant, the gradual increase of G″ with increase in temperature may be caused by the molecular motions occurring in the systems from micelle formation (99). These PF remained as liquid (G″>G′). Subsequently, G′ and G″ increased sharply with crossover at 29.5, 25.1 and 21.2 °C, respectively, for 16PF, 18PF and 20PF (Fig. 2.7d-f).

This sharp increase of both moduli corresponds to the sol-to-gel transition as micelles start to contact each other to form an ordered structure and inter-micellar entanglements as previously described (95). The crossover point is generally considered as the gel point, and it decreased with increase in PF concentrations. After crossover point, G′ was larger than G″ and both moduli reached their individual plateaus. Thus, these systems are in a solid-like state.

For 12PF/MC, 14PF/MC, 16PF/MC, 18PF/MC and 20PF/MC, both G′ and G″ increased together before reaching the crossover points as shown in Fig. 2.8a-e. At first step, G′ was smaller than G″. Next, increase of both G′ and G″ was observed due to range of micelle formation (based on DSC measurements). The increase of both G′ and G″ at this temperature range may be caused by the formation of the free PF micelles in coexistence with the PF micelles with attached MC as well as an increase in the number of micelles. This phenomenon was also observed in the mixture systems of PF and poly (acrylic acid) (100). MC can promote network formation or increase interface bonding during micelle formation as previously described (99, 101). Nevertheless, the PF/MC systems at this temperature range exist as solutions as G″>G′. However, all systems can turn to gel as G′ is larger than G″ with increase in temperature. The sol-to-gel temperatures for 12PF/MC, 14PF/MC, 16PF/MC, 18PF/MC and 20PF/MC were observed at 30.8, 24.6, 22.2, 20.3 and 18.2 °C, respectively.

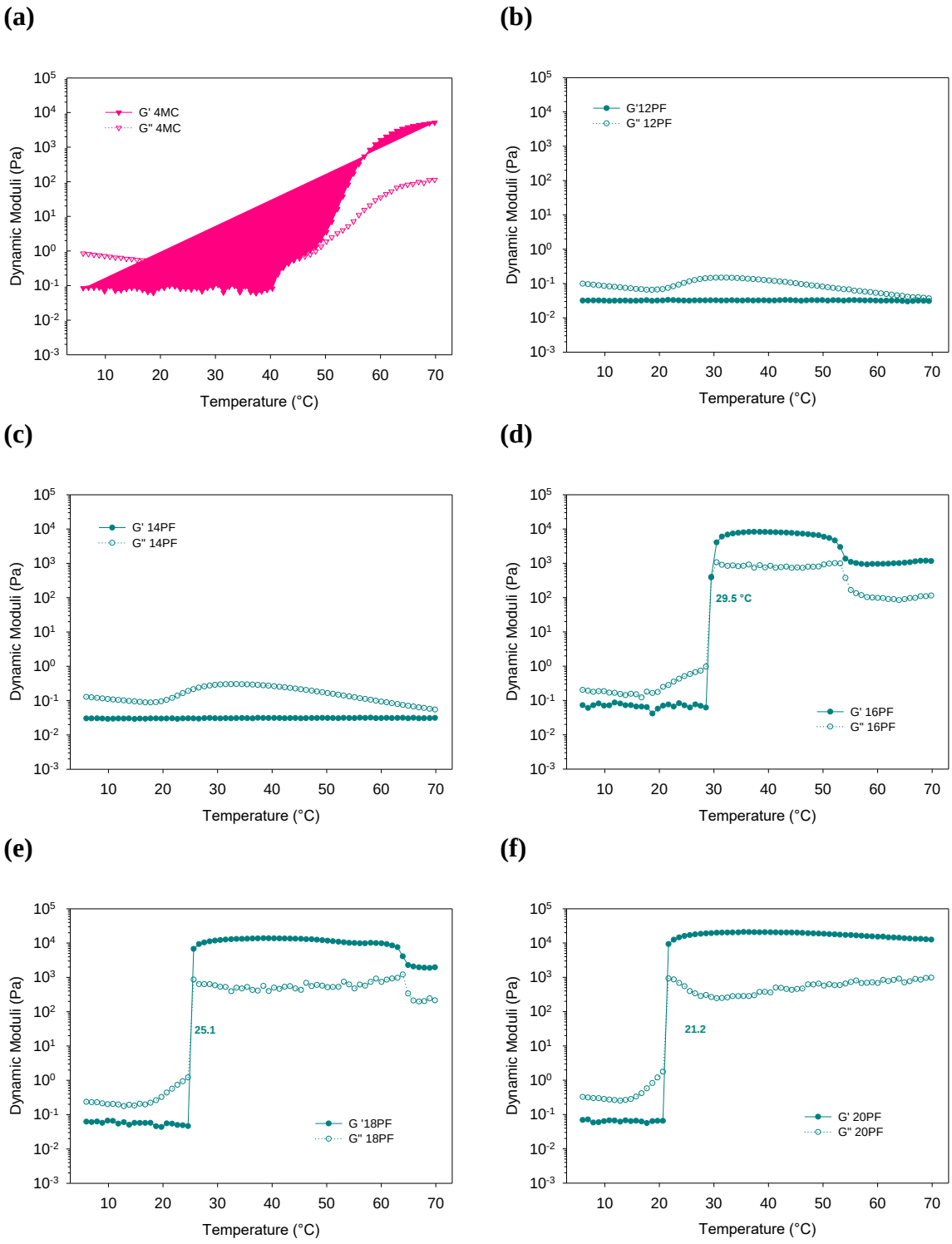

Fig. 2.7 Storage modulus G′ (closed symbols), loss modulus G″ (open symbols) as a function of temperature of MC (a), and PF at various concentration: (b) 12PF, (c) 14PF, (d) 16PF, (e) 18PF, and (f) 20PF. Samples were heated at a rate of 1 °C/min.

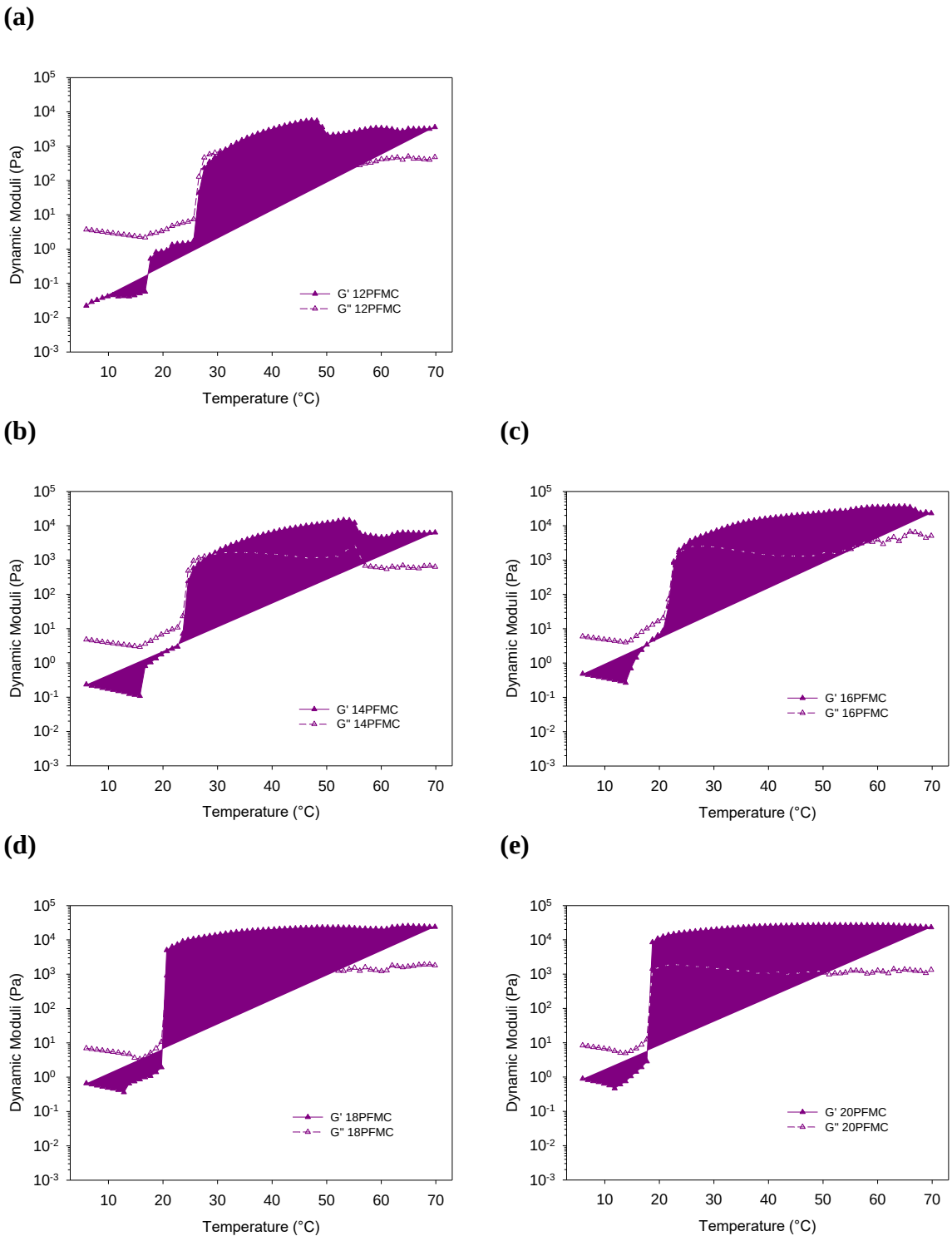

Fig. 2.8 Storage modulus G′ (closed symbols), loss modulus G″ (open symbols) as a function of temperature of (a) 12PF/MC, (b) 14PF/MC, (c) 16PF/MC, (d) 18PF/MC, and (e) 20PF/MC. Samples were heated at a rate of 1 °C/min.

2.6 Viscosity measurement

Viscosity measurement is a method to verify gelation strength of thermo-sensitive hydrogels. The gelation behavior of PF and PF/MC was also examined by measuring viscosity as a function of temperature.

The effect of temperature on the viscosity of the samples is shown in Fig. 2.9. Viscosity of MC at low temperature was higher than that of 16PF, 18PF and 20PF solutions. In addition, the viscosities of PF/MC co-solutions were much higher than those of their corresponding concentration of pure PF solutions. Also, the viscosity of PF/MC gels was slightly higher than those of their corresponding concentration of pure PF. Furthermore, the sharp increase in the viscosity of PF/MC appeared at much lower temperature than that of the corresponding concentration of the pure PF and was consistent with the sol-to-gel transition temperatures from viscoelastic investigations in this study.

The solution viscosity of all samples decreased slightly at low temperature (5-12 °C) due to shrinkage of coil size or dehydration of the unimers (the dominant species), especially PPO blocks as previously described (102-104). Further increase in temperature resulted in micelle formation as the PPO blocks tended to be even more hydrophobic. The sharp increase in viscosity around the sol-to-gel transition temperature of PF was previously described as lower T_{gel} (LT_{gel}) by Li and Hyun (105) and was also observed in this study. When the temperature was further increased, the viscosity plateaued and then declined. The temperature at this point is referred to as the upper T_{gel} (UT_{gel}) (105). In this study, the sol-to-gel transition was determined by the crossover point ($G'=G''$) which is relatively close to LT_{gel} for the neat PF solutions (Fig. 2.10). For the mixture of PF/MC, the LT_{gel} determined by viscosity was slightly lower than the sol-to-gel transition temperature where $G'=G''$ (Fig. 2.11). This may be due to the increase in viscosity of the solutions resulting from the influence of MC. However, as the concentration of PF in the blend increased, the LT_{gel} of PF/MC mixtures was closer to the crossover temperature of G' and G''.

The viscosity after UT_{gel} began to drop on further heating, refecting the breaking down of networks and phase separation (105-107). The temperatures between LT_{gel} and UT_{gel} yielded a hard gel state as previously described (105) . Li and Hyun reported that when temperatures were lower than LT_{gel} and higher than UT_{gel}, the neat PF systems were turned in the sol state (105). In this study, when temperatures were higher than UT_{gel}, the PF and PF/MC systems were not in a sol state but transformed into weaker gels ($G'>G''$) (Figs 2.10 and 2.11). As shown in Fig. 2.9, LT_{gel} of PF and PF/MC decreased with increase in PF concentrations, and UT_{gel} increased with increase in PF concentrations. The UT_{gel} of 20PF and 20PF/MC (high PF concentrations) was not observed because the temperature range of this study was not high enough to detect their UT_{gel}. The UT_{gel} of 20PF was previously reported to be about 75 °C (105).

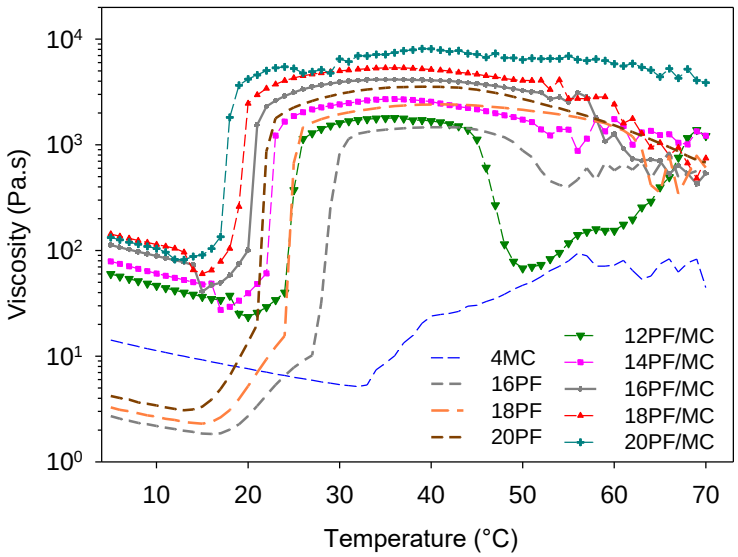

Fig. 2.9 Viscosity as a function of temperature upon heating at a rate of 1.0°C/min of MC, 16PF, 18PF and 20PF and the mixtures of MC and various concentrations of PF.

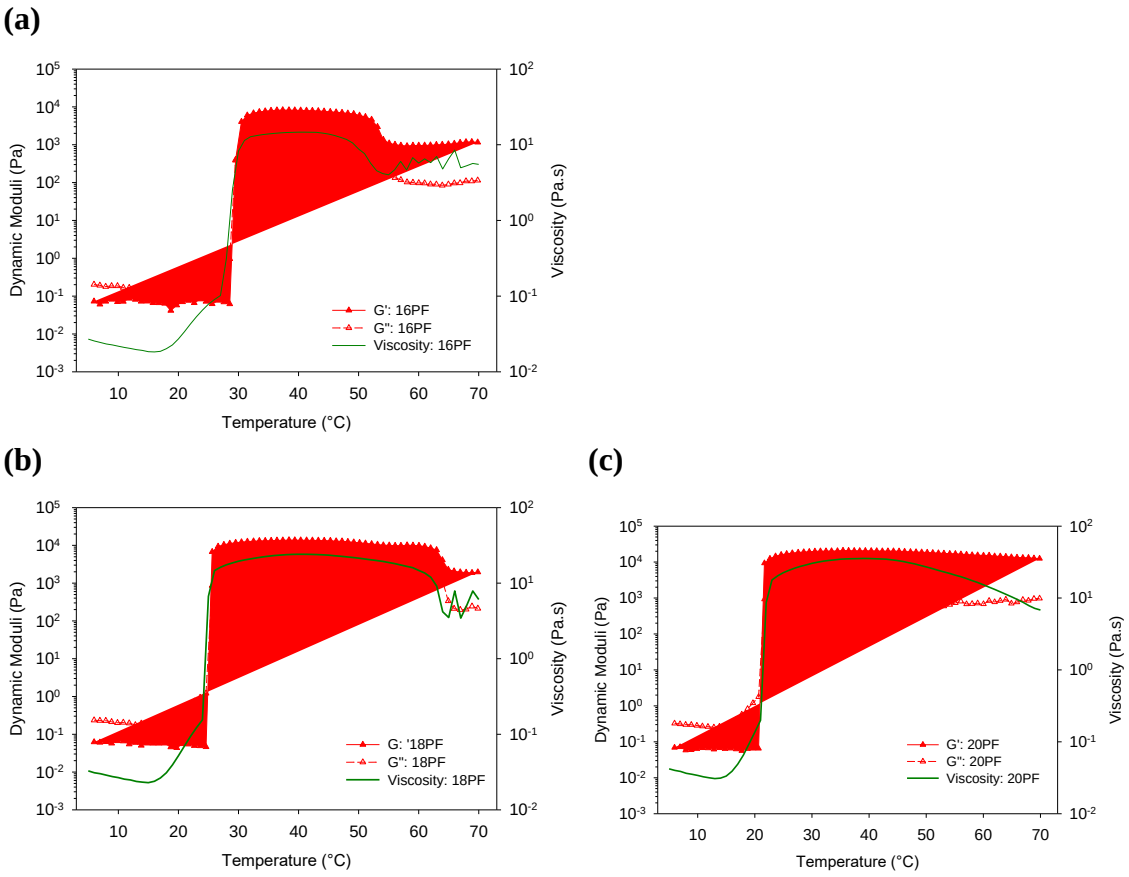

Fig. 2.10 Storage modulus G′ (closed symbols), loss modulus G″ (open symbols) and viscosity as a function of temperature of (a)16PF, (b)18PF, and (c) 20PF.

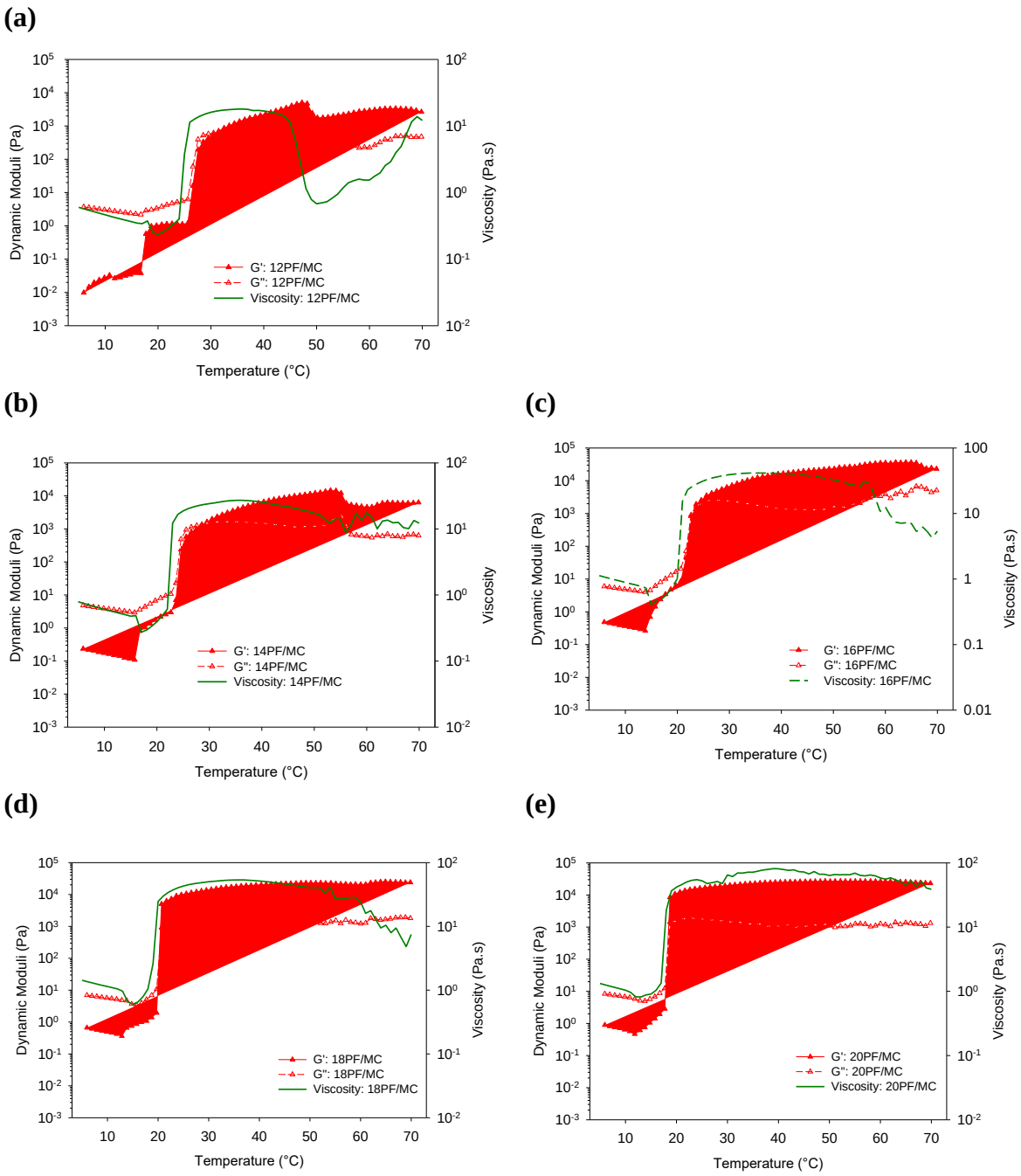

Fig. 2.11 Storage modulus G′ (closed symbols), loss modulus G″ (open symbols) and viscosity as a function of temperature of (a) 12PF/MC, (b) 14PF/MC, (c) 16PF/MC, (d) 18PF/MC, and (e) 20PF/MC

2.7 Summary

MC, various concentrations of PF (12PF, 14PF, 16PF, 18PF, and 20PF) and their blends (12PF/MC, 14PF/MC, 16PF/MC, 18PF/MC, and 20PF/MC) including the blends present EDS were investigated. TTM, turbidity, DSC and rheological analyses were systematically performed to determine the temperature-induced micellization and gelation of PF/MC systems. The clouding phenomenon observed in the PF/MC blends may reflect the efficient dehydration of PEO moiety of the micelles by MC. The CMT and the enthalpy of micellization were reduced by including MC into PF. The sol-to-gel temperature can be modulated and decreased by increasing PF concentrations.

The mixtures of 12PF/MC and 14PF/MC were in sol state near ambient temperature of (24 °C) and developed *in situ* gels at body temperature (37 °C). These mixtures were found to be suitable as injectable implant matrices. These mixtures were selected for further investigation in next chapter.

CHAPTER 3

RESULTS AND DISCUSSION

FOR PLURONIC F127/METHYLCELLULOSE/DOXYCYCLINE

This chapter aims to investigate the pluronic F127 and methylcellulose blends of 12PF/MC and 14PF/MC. Both blends were suitable as injectable implant matrices that exhibited a solution state at ambient temperature and gelation at the physiological temperature. Mucoadhesive property and biocompatibility of selected blends were initially demonstrated. Then, doxycycline hyclate (DX), a model drug for treatment periodontitis were incorporated in both matrices. Finally, their gelation properties and antimicrobial activity of PF/MC containing DX were evaluated.

3.1 Samples preparation

MC (4% w/w), 12PF, 14 PF, 12PF/MC and 14PF/MC were prepared following method that previous explained in chapter 1. 12PF/MC and 14PF/MC comprising DX were prepared by dispersing DX powder into homogenous 12PF/MC and 14PF/MC on ice bath with continuous vigorously stirring to obtained final concentrations of DX at 0.25 and 0.5% w/w, respectively. All blends were further stirred and then cooled until clear yellowish solutions were observed. These separately blends were name as 12PF/MC/0.25DX, 12PF/MC/0.5DX, 14PF/MC/0.25DX, and 14PF/MC/0.5DX, respectively. All samples were stored in refrigerator prior to further examine.

For mucoadhesive investigation, appropriate amount of mucin powder was dispersed in Milli-Q water or the PF/MC solutions to obtain 10% w/w of mucin in water, 12PF/MC or 14PF/MC. All samples were kept in the refrigerator at 4 °C. These samples were evaluated within 2 days of preparation.

3.2 Gelation temperature analysis

Test tube inversion method (TTM) was explored for finding estimate the gelation temperature and qualitative analysis of the transition from clear gel to turbid gel. Samples were heated at temperature ranging from 20 °C to 70 °C and allowed to equilibrate for 20 min after each increment. Effect of heating on gelation of 12PF/MC and 14PF/MC containing DX are shown in Fig. 3.1.

After finished preparation, PF/MC blends containing DX were clear yellowish solution (4 °C). The yellowish color was increased depending on increasing of DX. Based on TTM, gelation temperature of 12PF/MC, 12PF/MC/0.25DX, and 12PF/MC/0.5DX were 26, 30, and 30 °C, respectively. While gelation temperature of 14PF/MC, 14PF/MC/0.25DX, and 14PF/MC/0.5DX were 23, 25, and 25 °C, respectively. This TTM result showed that DX influenced on gelation by delaying the gel formation temperature. After samples were equilibrated at 25 °C for 20 min, 12PF/MC were high viscous solution (did not gel). 12PF/MC/0.25DX, and 12PF/MC/0.5DX exhibited yellowish clear soft gel. In contrast, 14PF/MC were slightly turbid hard gel. 14PF/MC/0.25DX, and 14PF/MC/0.5DX were yellowish slightly hard turbid gel. At body temperature (37 °C), all combination turned to yellowish turbid hard gel. At high temperature (50-70 °C), gel hardness of 12PF/MC, 12PF/MC/0.25DX, and 12PF/MC/0.5DX were decreased but remained gel. On the other hand, 14PF/MC, 14PF/MC/0.25DX, and 14PF/MC/0.5DX were preserved strong gel and increased in turbidity. This study demonstrated that DX at concentration of 0.25 and 0.5% w/w increased gelation temperature of both blends (12PF/MC and 14PF/MC) and decreased gel strength of 12PF/MC blend. Nevertheless, required gelation temperature and gel strength were found at the range covering the body temperature.

3.3 Mucoadhesive evaluation

Since 12PF/MC and 14PF/MC mixtures are sol near ambient temperature (about 24 °C), both mixtures were investigated as injectable implant matrices. Mucoadhesive behavior of both mixtures was investigated and compared to that of 12PF, 14PF and MC. The value of $\Delta G'_{relative}$ is considered to be an indicative parameter of the mucoadhesive strength of different polymeric platforms (34, 108).

The $\Delta G'_{relative}$ values of MC, 12PF, 14PF, 12PF/MC and 14PF/MC are shown in Fig. 3.2. Based on the $\Delta G'_{relative}$ values, MC demonstrated considerable mucoadhesive behavior, while the mucoadhesive property of 12PF and 14PF was relatively poor. Meanwhile, the mucoadhesive characteristics of PF correlated well with their concentrations (14PF > 12PF). These results are in general agreement with the property of both polymers reported in studies (109, 110). Methylcellulose has been recognized as a mucoadhesive polymer (109, 111). In contrast, a major drawback of PF is its poor mucoadhesive strength (110). The $\Delta G'_{relative}$ value of 14PF/MC is slightly higher than 12PF/MC. Both are significantly higher than their concentration of the pure PF (12PF and 14PF) ($p<0.005$), respectively. This may indicate that blending PF with MC improves the mucoadhesive property of PF-based thermosensitive gels.

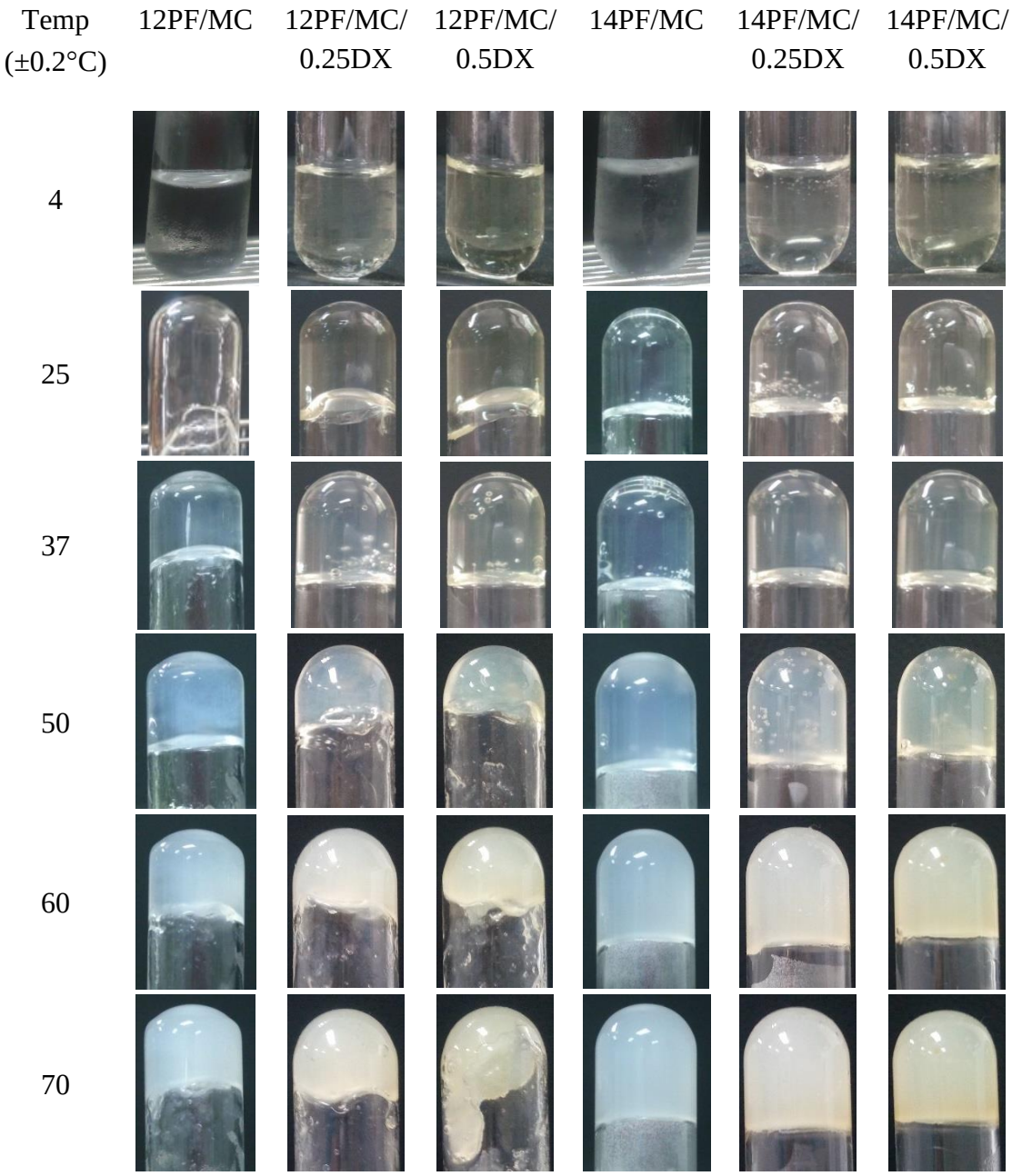

Fig. 3.1 Macroscopic visual detection of 12PF/MC hydrogels containing 0.25 and 0.5%DX, and 14PF/MC hydrogels containing 0.25 and 0.5%DX after heating over different time points.

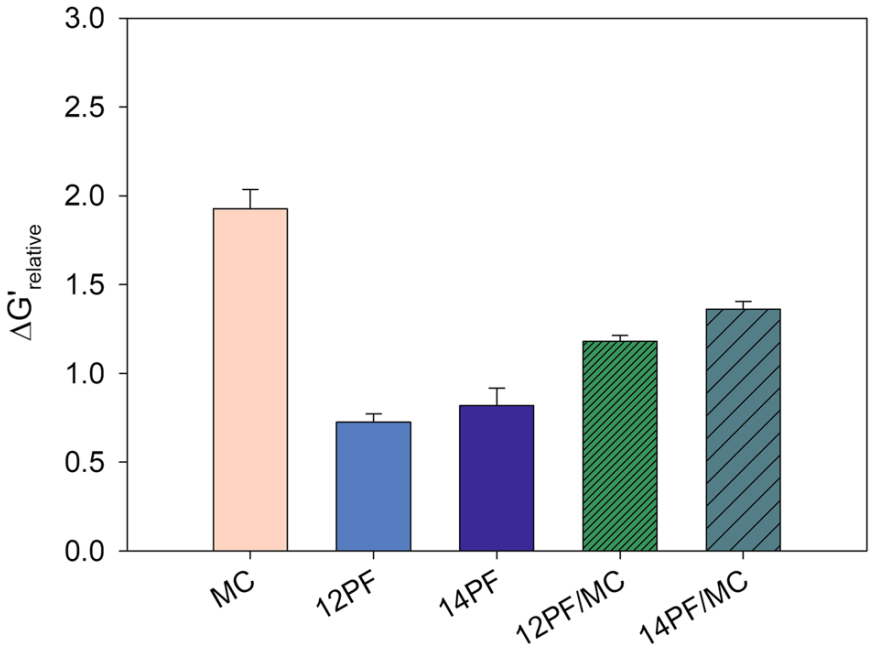

Fig. 3.2 Relative rheological synergism (ΔG′relative) at an angular frequency of 6.28 rad/s of MC, 12PF, 14PF, 12PF/MC and 14PF/MC in 10% w/v mucin at 37 °C (mean±s.d, n = 3)

3.4 Cytotoxicity assay

Cytotoxicity analysis was performed according to ISO 109903-5:2009 (E) using mouse fibroblast cell line (L929 cells). Cytotoxicity effect of 12PF/MC and 14PF/MC hydrogels on L929 is shown in Fig. 3.3. Cell culture media as a negative control was presented cell viability at 100.00±1.40. 25% Ethanol as a positive control was very toxic to the cells (5.52±1.81%). Cell viability of 12PF/MC and 14PF/MC hydrogels were 92.70±1.81 and 88.58±2.48, respectively. Both hydrogels showed cell viability significantly decreased ($p<0.05$) compared to control. However, increasing of cell viability by more than 70% is generally considered a noncytotoxic effect following ISO 109903-5:2009 (E) – Biological Evaluation of Medical Devices by MTT cytotoxicity test and other related publications (112-114). Thus, 12PF/MC and 14PF/MC hydrogels were noncytotoxic to L929 fibroblasts. This study demonstrated the biocompatibility of 12PF/MC and 14PF/MC based hydrogels.

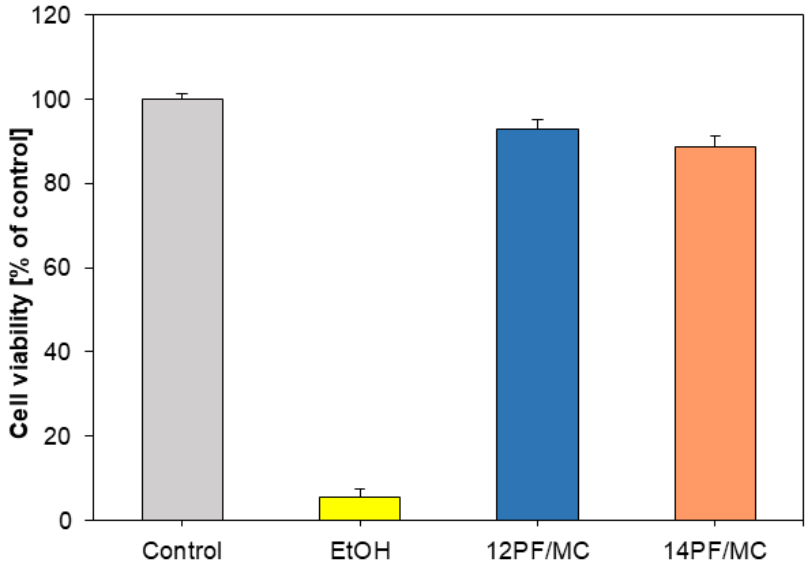

Fig. 3.3 Percentage of cell viability of 12PF/MC and 14PF/MC (mean±s.d, n = 8)

3.5 Rheological measurement

The sol-to-gel transition of 12PF/MC and 14PF/MC hydrogels: present and absent DX were investigated by comparing their viscoelasticities as a function of temperature. Viscoelastic moduli, G′ and G″ of samples upon heating are shown in Fig. 3.4. G′ was smaller than G″ at low temperature (5-16 °C). Then, the increase of both G′ and G″ was observed. This two-step occurred before crossover point and hydrogels exhibited liquid-like state (G′<G″). The crossover point (G′=G″) was implied the sol-to-gel transition temperature of samples upon heating. The sol-to-gel transition temperature of 12PF/MC, 12PF/MC/0.25DX, and 12PF/MC/0.5DX were 30.8, 34.5, and 34.6 °C, respectively (Fig. 3.4a-c). The sol-to-gel transition temperature of 14PF/MC, 14PF/MC/0.25DX, and 14PF/MC/0.5DX were 24.6, 31.1, and 31.6 °C, respectively (Fig. 3.4d-f). These results were found that the sol-to-gel transition temperature of 12PF/MC and 14PF/MC were lower than those containing DX. While 12PF/MC and 14PF/MC hydrogels containing DX at different concentrations (0.25DX and 0.5DX) were not found changing in sol-to-gel transition temperature. Therefore, this finding was demonstrated that DX affected on gelation temperature of 12PF/MC and 14PF/MC based hydrogels by delaying gel forming temperature. Although, Dx delayed the gelation temperature of 12PF/MC and 14PF/MC hydrogels, these gelation temperatures were nearby the body temperature (37 °C). All hydrogels exhibited solid-like state.

Viscosity of 12PF/MC and 14PF/MC hydrogels comprising different DX concentrations was concurrently investigated as also presented in Fig. 3.4. Viscosity of

all samples decreased slightly at low temperature (5-17 °C). The sharp increase in viscosity around the sol- to-gel transition lower T_{gel} (LT_{gel}) were seen as same as in each sample. When the temperature was further increased, the viscosity of samples plateaued upon heating to 45 °C excepted 12PF/MC/0.25DX and 12PF/MC/0.5DX. The viscosity upper T_{gel} (UT_{gel}) of 12PF/MC/0.25DX and 12PF/MC/0.5DX were declined about 40 and 38 °C, respectively. These studies were revealed that DX at different concentrations (0.25DX and 0.5DX) interfered viscosity of 12PF/MC based hydrogel at temperature higher than 38 °C. In addition, viscosity of 12PF/MC present DX was decreased depending on increasing of DX concentrations.

3.6 Viscosity measurement

Fig. 3.5. is showed viscosity of hydrogels upon heating from 5-45 °C. Viscosity of all hydrogels were compared for prediction the gels strength which previously described that the temperatures between LT_{gel} and UT_{gel} yielded a hard gel state (105). As comparing hard gel by viscosity, 14PF/MC, 14PF/MC/0.25DX, and 14PF/MC/0.5DX were stronger gel than 12PF/MC, 12PF/MC/0.25DX, and 12PF/MC/0.5DX, respectively. In addition, 12PF/MC and 14PF/MC hydrogels were stronger gel than DX-loaded gels. The gel strength of 12PF/MC/0.5DX was weaker than 12PF/MC/0.25DX. These both weak hydrogels were different among DX-loaded hydrogels which observed after heating above 38 °C. These studies discovered that gelation temperature and gel strength of 12PF/MC and 14PF/MC hydrogels were interfered by DX. Nevertheless, all tested hydrogels were solution at ambient temperature and turn to gel at body temperature. These polymeric matrices could be use as injectable drug delivery of DX.

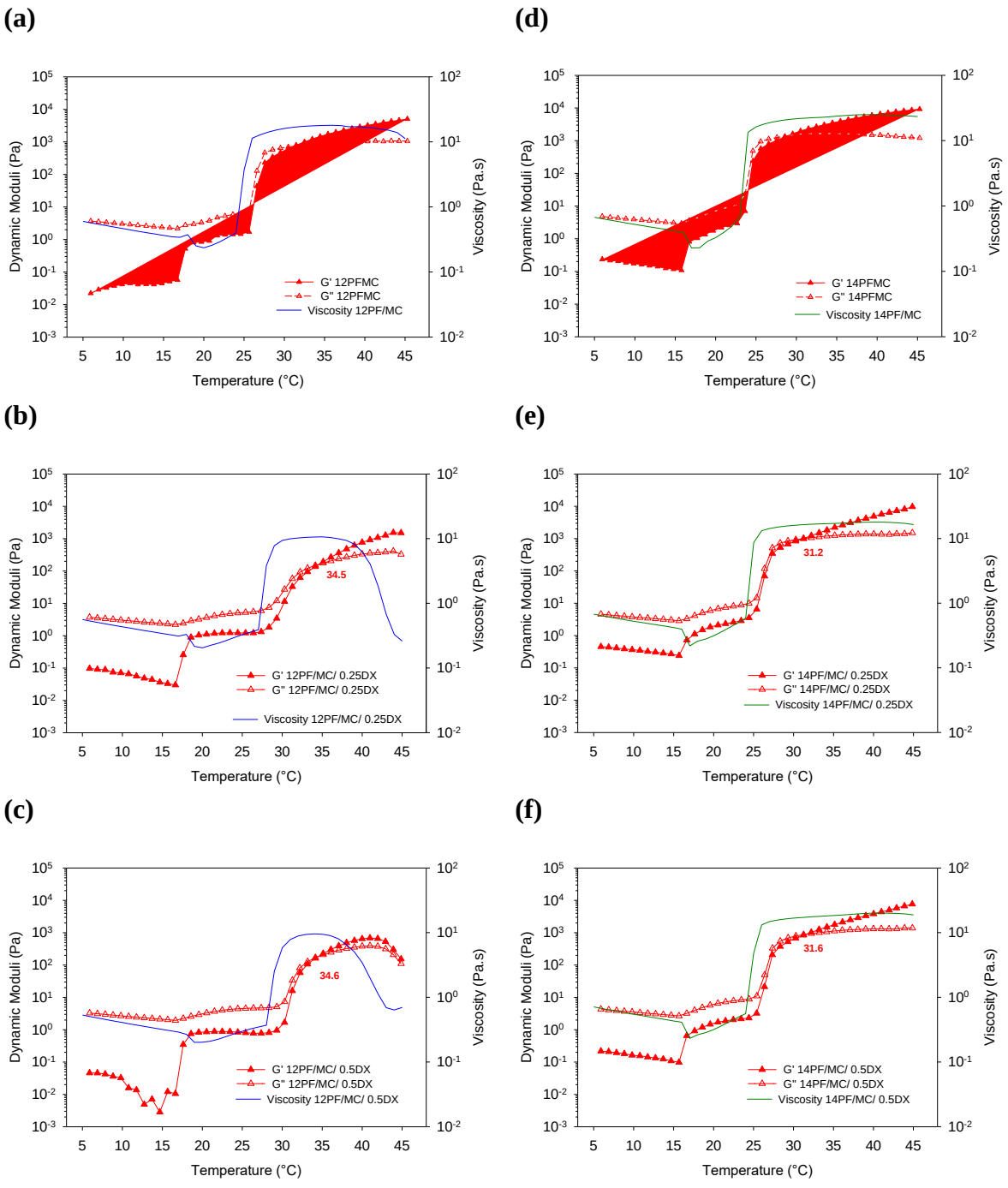

Fig. 3.4 Storage modulus G′ (closed symbols), loss modulus G″ (open symbols) as a function of temperature as well as viscosity of: (a) 12PF/MC, (b) 12PF/MC/0.25DX, (c) 12PF/MC/0.25DX, (d) 14PF/MC, (e) 14PF/MC/0.25DX, and (f) 14PF/MC/0.5DX, respectively. Samples were heated at a rate of 1 °C/min.

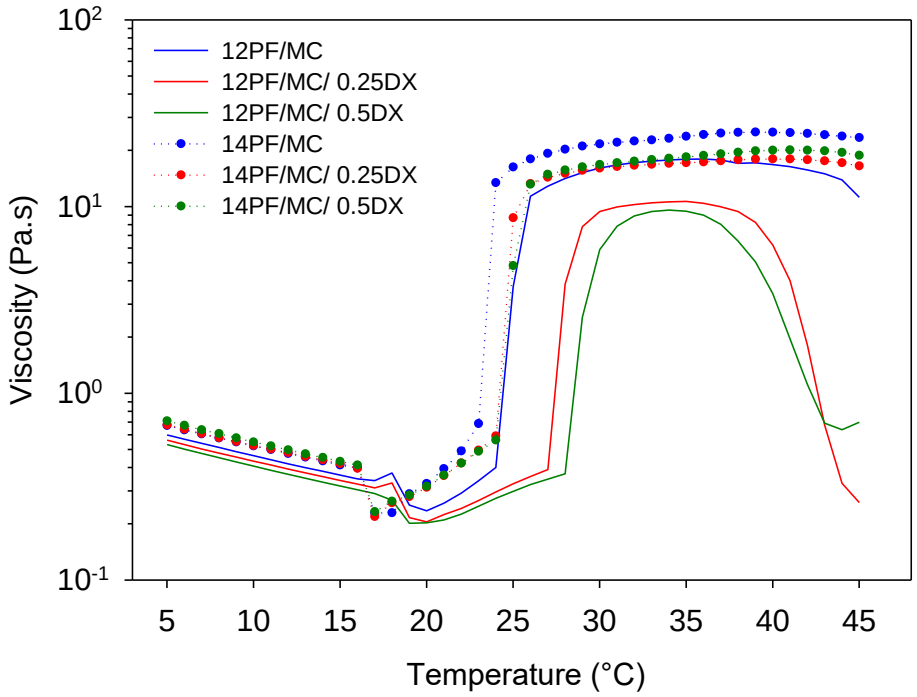

Fig. 3.5 Viscosity as a function of temperature upon heating at a rate of 1.0 °C/min of 12PF/MC, 12PF/MC/0.25DX, 12PF/MC/0.25DX, 14PF/MC, 14PF/MC/0.25DX, and 14PF/MC/0.5DX, respectively.

3.7 Antimicrobial activity analysis

Some of the notable drugs typically used in the management of periodontitis include tetracycline, DX, metronidazole and macrolides (115). The major causes of periodontitis are growth and accumulation of gram-negative anaerobes in the periodontal pockets including *P. gingivalis, A. actinomycetemcomitans and P. intermedia*. These anaerobic pathogens release toxins and enzymes which can stimulate inflammatory response causing the destruction of connective tissues around the teeth and alveolar bone (60). In addition, these pathogens are the most predominant etiological agents for periodontitis associated with the chronic and aggressive form of the disease (116). Therefore, these three pathogens were selected for investigating the activity of DX incorporated in 12PF/MC and 14PF/MC matrices compared to the pure drug. The photographs of inhibition zone of *P. gingivalis, P. intermedia*, and *A. actinomycetemcomitans* after treated with samples are presented in Fig. 3.6, 3.7, and 3.8, respectively. Moreover, the diameter of the zone of inhibition against the three microbes exposed to 0.25DX, 0.5DX, 12PF/MC/0.25DX, 14PF/MC/0.25DX, 12PF/MC/0.5DX and 14PF/MC/0.5DX is displayed in Fig. 3.9. The zone of inhibition diameter of 0.5DX was significantly greater than that of 0.25DX ($p<0.05$) against all microbes. The microbial susceptibility was in the order of *A. actinomycetemcomitans > P. Intermedia > P. gingivalis*. The zone of inhibition diameters of the DX-loaded hydrogels was not significantly different from the corresponding concentration of pure DX. There were no significant differences among the inhibition zones of 0.25DX, 12PF/MC/0.25DX and 14PF/MC/0.25DX ($p>0.05$) as well as those of 0.5DX, 12PF/MC/0.5DX and 14PF/MC/0.5DX ($p>0.5$) against all microbes. These findings indicate that the polymeric matrices did not inhibit the biological activity of the drug.

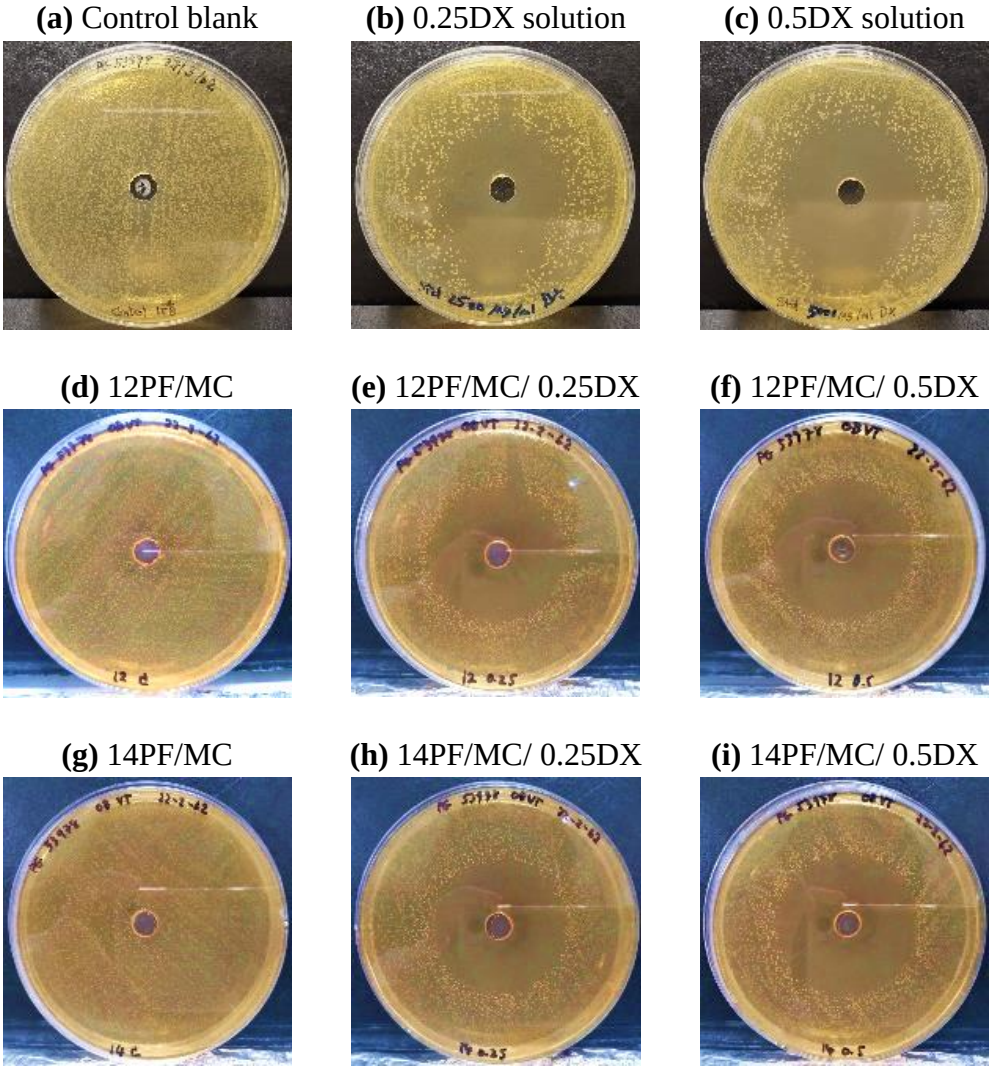

Fig. 3.6 Photograph shows inhibition zone of 0.25DX and 0.5DX solutions as well as both DX concentrations in the 12PF/MC and 14PF/MC hydrogels on *P. gingivalis (ATCC 53978).*

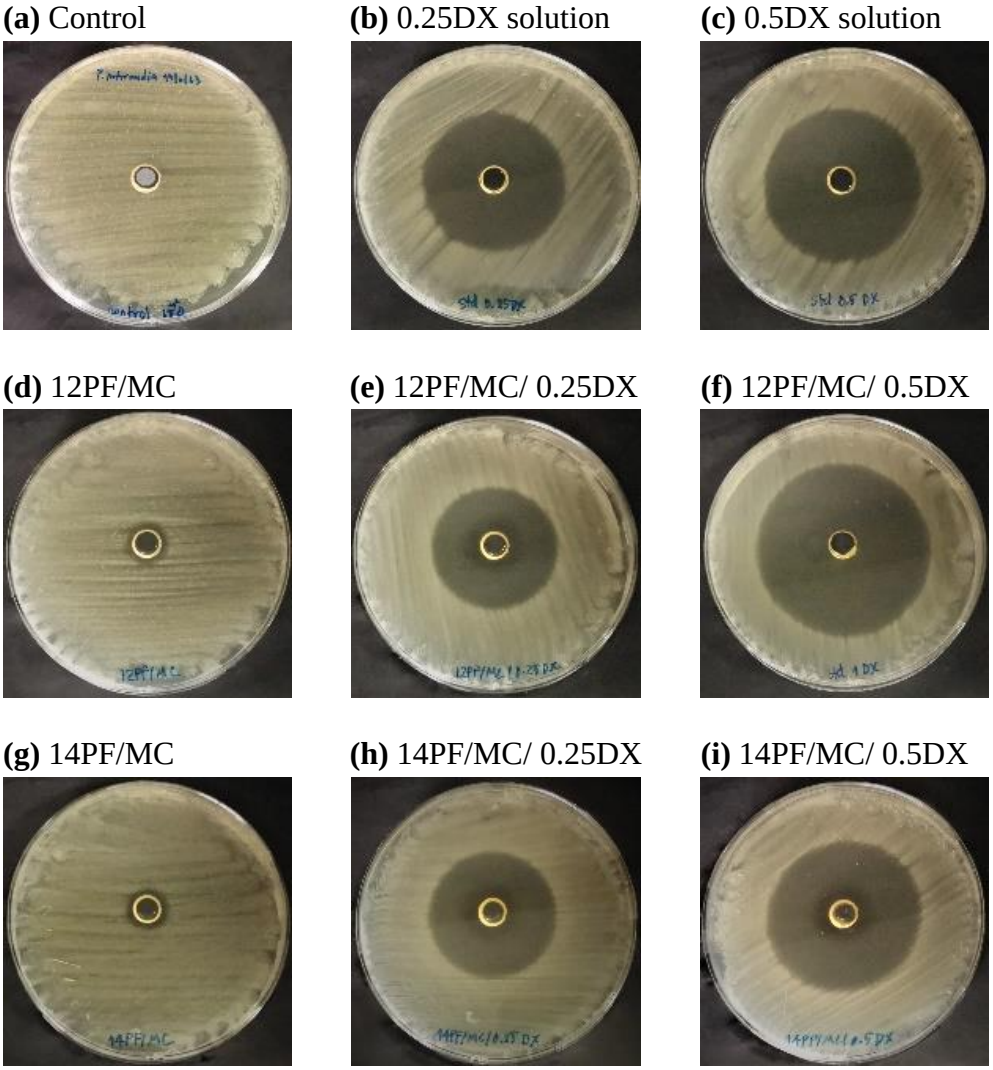

Fig. 3.7 Photograph shows inhibition zone of 0.25DX and 0.5DX solutions as well as both DX concentrations in the 12PF/MC and 14PF/MC hydrogels on *P. intermedia (ATCC 25611).*

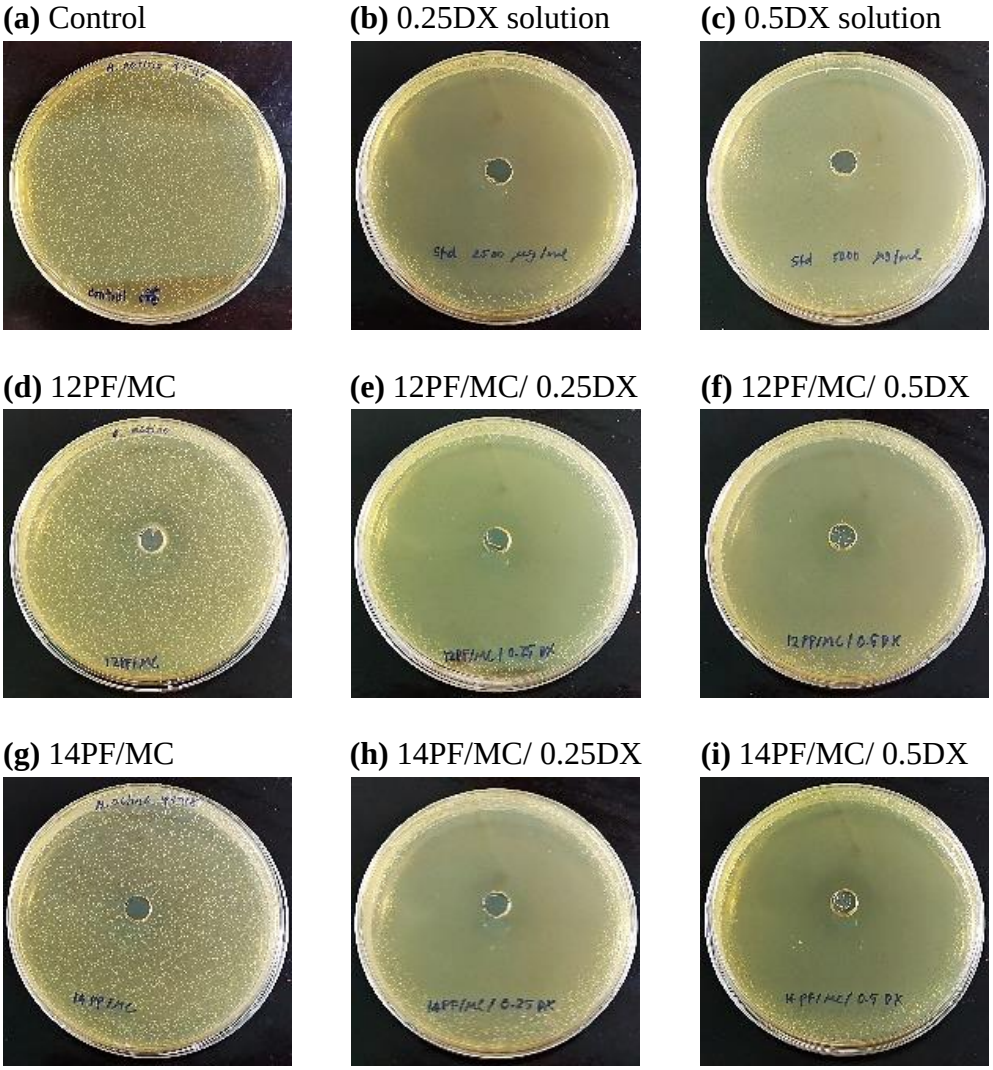

Fig. 3.8 Photograph shows inhibition zone of 0.25DX and 0.5DX solutions as well as both DX concentrations in the 12PF/MC and 14PF/MC hydrogels on *A.actinomycetemcomitans (ATCC 43718).*

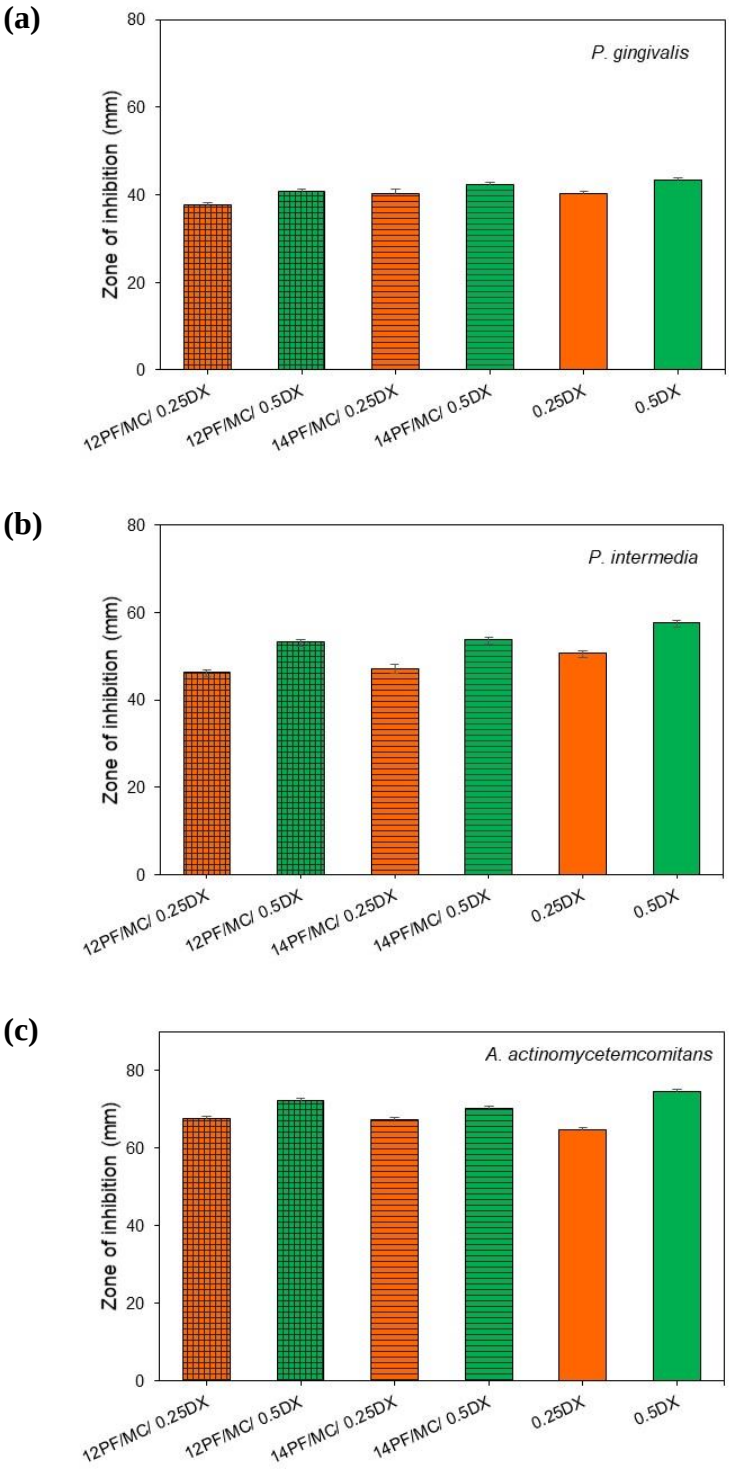

Fig. 3.9 Effect of 0.25DX and 0.5DX solutions as well as both DX concentrations in the 12PF/MC and 14PF/MC hydrogels on inhibition zone of (a) *P. gingivalis*, (b) *P. Intermedia*, and (c) *A. actinomycetemcomitans* (mean±s.d., n = 3)

3.8 Scanning Electron Microscopy analysis

Morphology of 12PF/MC and 14PF/MC incorporating 0.25%DX and 0.5%DX was investigated. Scanning Electron Microscopy (SEM) images of gel samples were performed at different magnifications (300x and 1000x) as shown in Fig. 3.10a-b. The result was found that pore size of 12PF/MC was larger than 14PF/MC because of amount of PF in the blend of 12PF/MC less than 14PF/MC blend. Smooth shape of pore size was also observed in 14PF/MC blend. Moreover, pore size of 12PF/MC and 14PF/MC loading 0.25%DX and 0.5%DX were found denser than their based. Decreasing in porosity was depending on concentration of DX. In addition, porosity of blends at high concentration of DX was more disorganized. This study may relate with the viscosity and gel strength of blends.

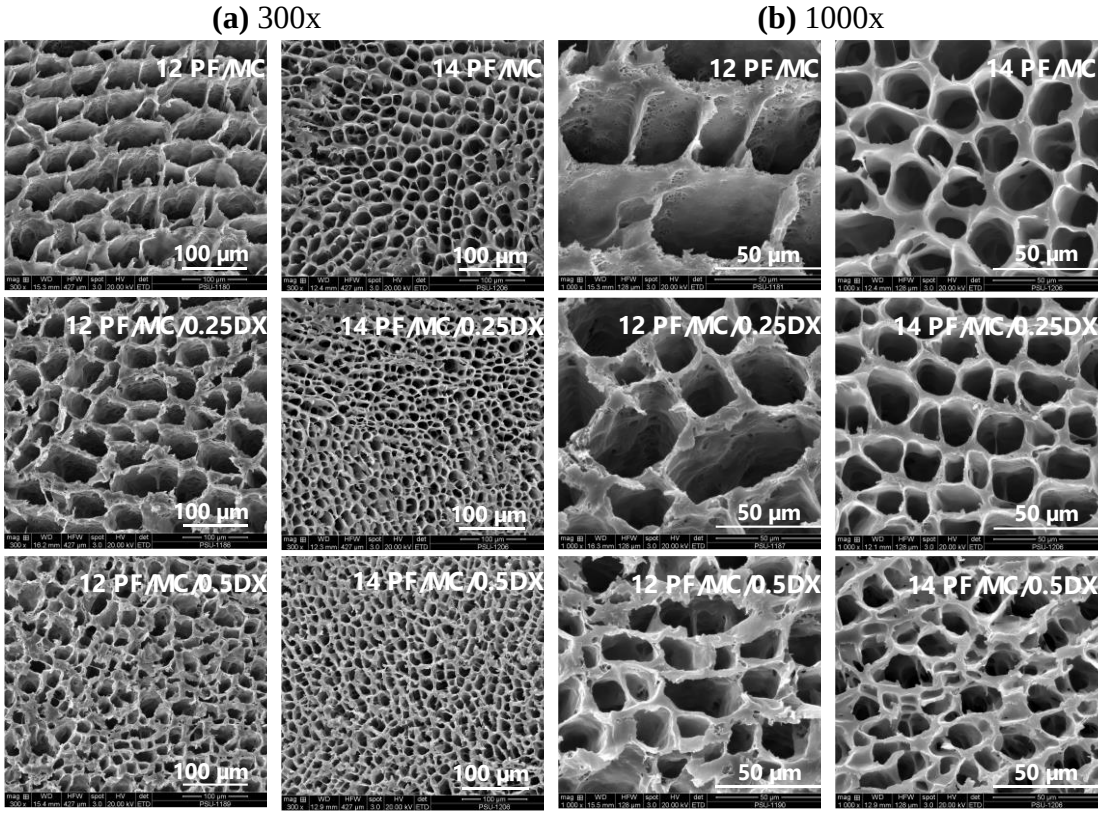

Fig. 3.10 SEM images at 37 °C (gel state) of 12PF/MC and 14PF/MC hydrogels containing 0.25 and 0.5%DX at different magnifications: (a) 300x and (b) 1000x.

3.9 *In vitro* drug release study

In vitro drug release of 0.25DX and 0.5DX from 12PF/MC and 14PF/MC was investigated using dialysis membrane in PBS (pH 7.4) at 37 °C. The *in vitro* release profile of 12PF/MC/0.25DX, 12PF/MC/0.5DX, 14PF/MC/0.25DX and 14PF/MC/0.5DX is shown in Fig. 3.10. The 12PF/MC and 14PF/MC prolonged the release of DX. Comparatively, the drug was released faster from 12PF/MC than from 14PF/MC. This may be due to the fact that the pore size of 12PF/MC was larger than that of 14PF/MC (Fig. 3.11). The higher amount of PF increased the compactness of the gel and slowed the release of DX. In addition, the viscosity at 37 °C of 12PF/MC was lower than that of 14PF/MC (Fig. 3.5). The greater the viscosity of the gel layer, the more resistant the gel layer is to diffusion, and the drug release is prolonged as previously described (117). This slow release in an extended period may have potential positive implications for the treatment of periodontitis.

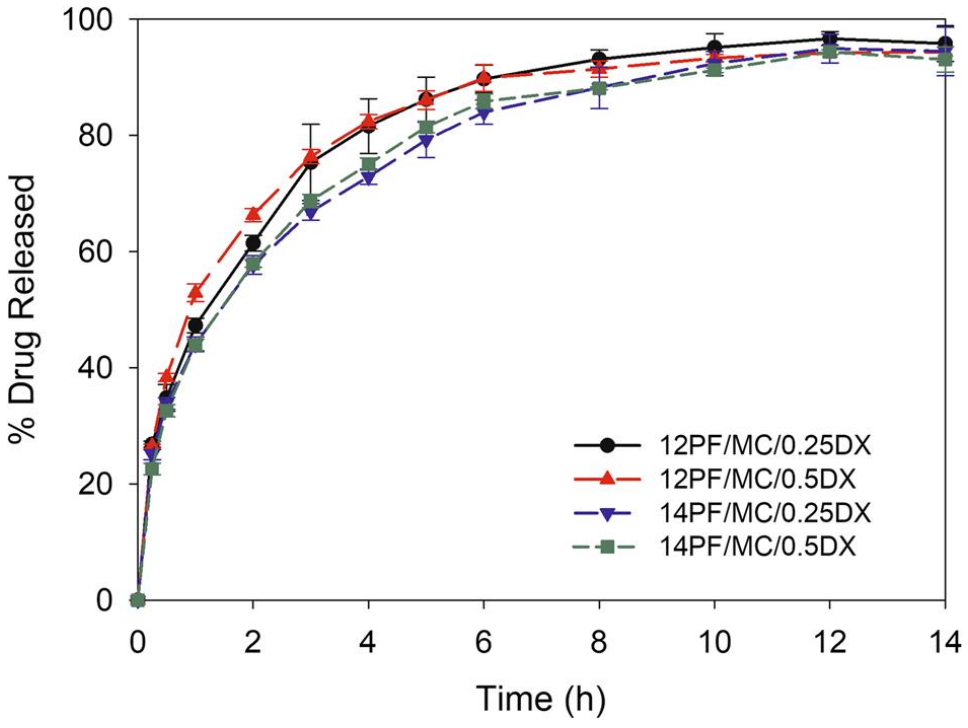

Fig. 3.11 *In vitro* release of DX at 37 °C from 12PF/MC and 14PF/MC hydrogels containing 0.25 and 0.5%DX (mean ± s.d., n = 3)

3.10 Summary

Results in this chapter demonstrated that 12PF/MC and 14PF/MC blends exhibited mucoadhesive property and well biocompatible with fibroblasts. Besides, the incorporation of DX in 12PF/MC and 14PF/MC blends displayed gelation temperature and gel strength covering ambient and body temperature. In addition, the DX-loaded 12PF/MC and 14PF/MC blends revealed the same antibacterial activity as the pure drug solution. This indicated that both PF/MC matrices did not obstruct the antibacterial activity of the drug. The 12PF/MC and 14PF/MC exhibited slow release of DX. Taken together, these findings demonstrated that the appropriate mixtures of PF/MC are promising matrices for the development of efficient periodontal drug delivery system.

CHAPTER 4

RESULTS AND DISCUSSION

CHARACTERIZATION OF PLURONIC F127/METHYLCELLULOSE

This chapter explained the structural characteristics and gelation behaviors of PF/MC hydrogel blends by using macroscopic visual detection, small-angle X-ray scattering (SAXS) and rheological measurement.

4.1 Sample preparation

The PF solutions were prepared at concentrations of 11 and 17% (w/w) using a cold method as previously described (38). Briefly, an appropriate amount of PF was dissolved in Mill-Q water at 4 °C and refrigerated overnight to ensure that PF was entirely dissolved to obtain 11 and 17% (w/w) of PF (referred to as 11PF and 17PF, respectively). The required amount of methylcellulose was dispersed in hot water with vigorous stirring by magnetic stirrer. After the methylcellulose powder was completely dispersed, the remainder of the water was added to produce 4% w/w of methylcellulose and then cooled in an ice bath until a transparent solution was obtained (referred to as MC). The required amount of PF (11 g or 17 g) was dispersed in 50 mL of cold methylcellulose solution containing 4 g of methylcellulose. Subsequently, the cold water was added to each sample to produce a mixture with the final weight of 100 g. These 11 and 17% w/w of PF in 4% w/w of MC were referred to as 11PF/MC and 17PF/MC, respectively. The resulting blend was mixed thoroughly and refrigerated until it was completely dissolved. For the samples containing EDS, the required amount of the drug to obtain the final concentration of 0.1% (w/w) was dispersed to the 11PF/MC and 17PF/MC solutions and mixed until the drug was completely dissolved. These mixtures were referred to as 11PF/MC/EDS and 17PF/MC/EDS, respectively.

4.2 Macroscopic visual detection

The gelation temperatures of the samples were visually detected using a TTM as previously described (34, 118-120). The samples were heated from 15 to 70 °C in a temperature-controlled water bath at an increment of 1 °C. The samples were allowed to equilibrate for 25 min after each increase in temperature. Phase transition was

evaluated by tilting the tube after the incubation period. The temperature at which the samples became solid but slightly flowed at the surface when tilting the tube was recorded as gelation temperature of a soft gel (119). With further heating, the temperature at which samples did not flow was recorded as a transition temperature of a hard or strong gel (119).

All samples were clear solution at 4 °C. During heating at a rate 1°C/min, the low concentration of 11PF were solution under heating condition. Gelation temperature of 17PF were detected as clear strong gel at 27 °C. After equilibrating for 25 min, mixing of 11PF with MC (11PF/MC) was exhibited the gel-like characteristic. 11PF/MC was slightly turbid soft gel at 27 °C and became turbid strong gel at 32 °C. 17PF/MC was clear soft gel at 23 °C and turned clear hard gel at 27 °C. Gelation temperature of 11PF/MC/EDS and 17PF/MC/EDS were found as same as those corresponding blends without EDS. The macroscopic visual detection by TTM of samples during heating from 15 to 70 °C are shown in Fig. 4.1. At 25 °C, 17PF, and 11PF/MC were remained solution. As temperature rising to 37 °C, all blends were turbid strong gel. Blended hydrogels turned turbid gel depending on increasing temperature. This study was found that blending PF with MC (11PF/MC and 17PF/MC) were provided strong gel during heating at high temperature (70 °C) by visual investigation.

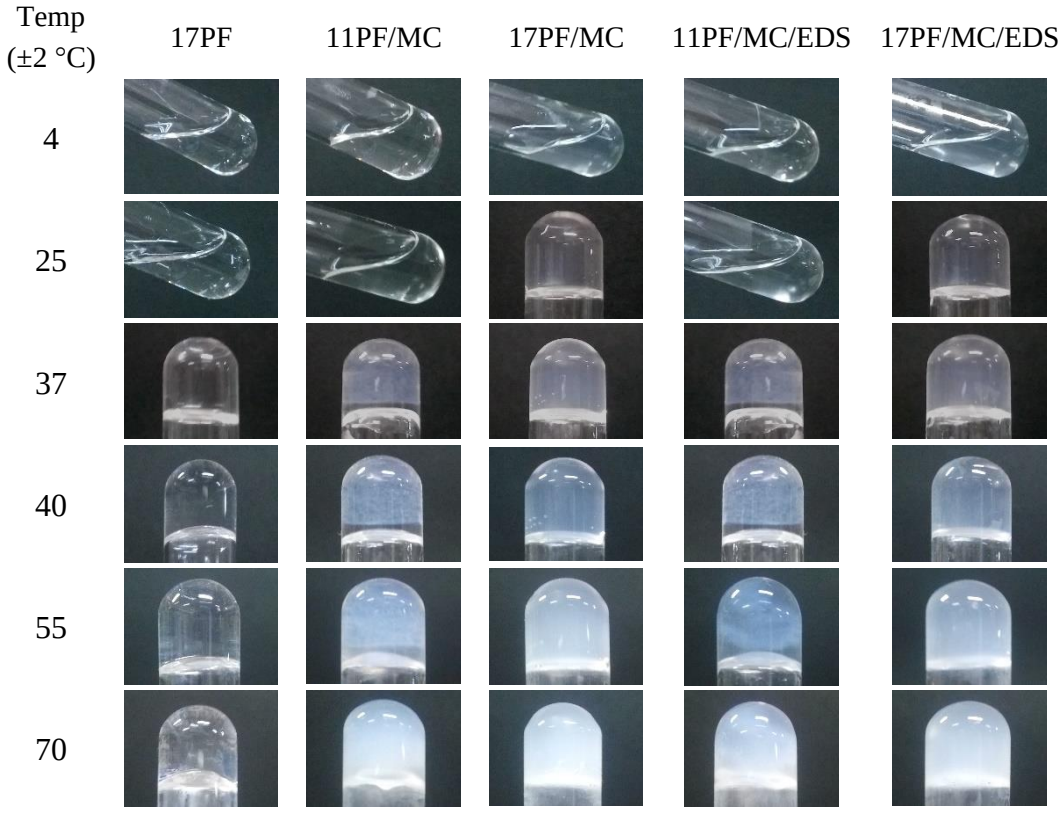

Fig. 4.1 The macroscopic visual detection by TTM of hydrogel samples during heating from 15 to 70 °C.

4.3 Rheological measurements

Generally, the gelation of methylcellulose occurred in two steps during heating. The first step is a clear soft gel, and the second step is a turbid hard (strong) gel. The temperature dependence of dynamic moduli, G′ (elastic modulus) and G″ (viscous modulus) during heating from 5 to 70 °C at the rate of 1 °C/min of MC, is shown in Fig. 4.2a.

MC solution behaved as a viscoelastic fluid with G″ > G′ at low temperatures. Based on TTM and rheological property which showed G′ > G″, a clear soft gel was found at 45–50 °C due to progressive chain association of a few chains of highly methylated zones which is the most hydrophobic zones (54). Over 50 °C, a turbid gel was formed due to phase separation. Turbidity increased strongly with a fully turbid gel at about 55 °C. PF (a PEO-PPO-PEO triblock copolymer) in aqueous solutions can self-assemble into micelles above the critical micelle temperature (CMT) or the critical micelle concentration (CMC) (121). Increasing the temperature of PF solution caused the reducing aqueous solubility of relatively hydrophobic (PPO) segments and initiated micelle formation with relatively hydrophobic PPO cores and relatively hydrophilic PEO coronas (shells) (122). This core–shell structure is known as a micelle. The formation of micelles strongly depends on temperature and concentration. PF underwent a transition from sol-to-gel with increasing temperature through three different stages: sol, soft gel and strong gel. In general, the transition from sol-to-soft gel occurred when micelle density reached a certain value and produced a sufficient ordered structure to trigger the characteristic rheological effect (123-125), or soft gel corresponded to a defective version of hard gel as previously described (126). As previously explained, soft gel was identified between micellar liquid and hard gel (solid crystal phase). Soft gel was characterized by G′ > G″ and both increased rapidly, and G′ was relatively small compared to G″, but in sol, G″ > G′ and both were much smaller. For strong gel, G′ > G″ and both G′ and G″ are large and immobility of the solution in the TTM test. For 11PF, the G′ values were always lower than G″ values (Fig. 4.3a), demonstrating that this low concentration could not form a gel at any temperature. This is consistent with previous reports that CGC (critical gelation concentration) of PF is about 16% w/w (38, 121). For 17PF, at the beginning of heating, both G′ and G″ were very small and G″ > G′ (Fig. 4.2b), and the system was in a sol state. The interaction of the PEO blocks on the micelle corona with water became less favorable upon heating. Further increasing temperature, both G′ and G″ increase rapidly, and a crossover of G′ and G″ appeared at 25 °C, and this crossover point was defined as the rheological gel temperature. Based on TTM, a clear soft gel was formed at about 26–27 °C. After about 27 °C, strong gel was detected by viscoelastic analysis (Fig. 4.2b) and also recognized by immobility in TTM. This is further discussed with the SAXS analysis.

In general, PF gel in aqueous solution is a clear gel (127) ; in this study, soft and strong gels of 17PF were clear, but the PF solutions could become turbid to the

eyes when blending with methylcellulose (11PF/MC and 17PF/MC). Although 11PF could not form gel, 11PF/MC solution turned to gel as shown in Fig. 4.2c. The crossover of G′ and G″ was detected at 26.5 °C. After the crossover, G′ > G″ was shown, based on TTM, a soft gel was detected between 27 and 31 °C. Further increasing the temperature, a strong gel was detected (immobility in TTM test). Both 11PF/MC soft and strong gels were turbid, and turbidity increased with increasing temperature.

The temperature dependence of dynamic modulus for 17PF and 17PF/MC systems was comparable as shown in Fig. 4.2b, d, respectively. Nevertheless, the effect of adding MC was to move the onset of gel formation to a lower temperature; gelation temperature was 22 °C for 17PF/MC but 25 °C for 17PF. At the crossover temperature (22 °C to about 24 °C), 17PF/MC developed a clear soft gel. Clear strong gel was detected from 24 to 27 °C, and over 27 °C the turbid strong gel was developed. Viscoelastic behaviors of 17PF, 11PF/MC and 17PF/MC in the presence of EDS were comparable to those corresponding systems without EDS as shown in Figs. 4.3b-d. In addition, characteristics of 17PF/EDS, 11PF/MC/EDS and 17PF/MC/EDS are similar to those of the neat PF/MC blends when tested by TTM experiments. This indicated that EDS did not change the sol-to-gel transitions of PF and PF/MC systems.

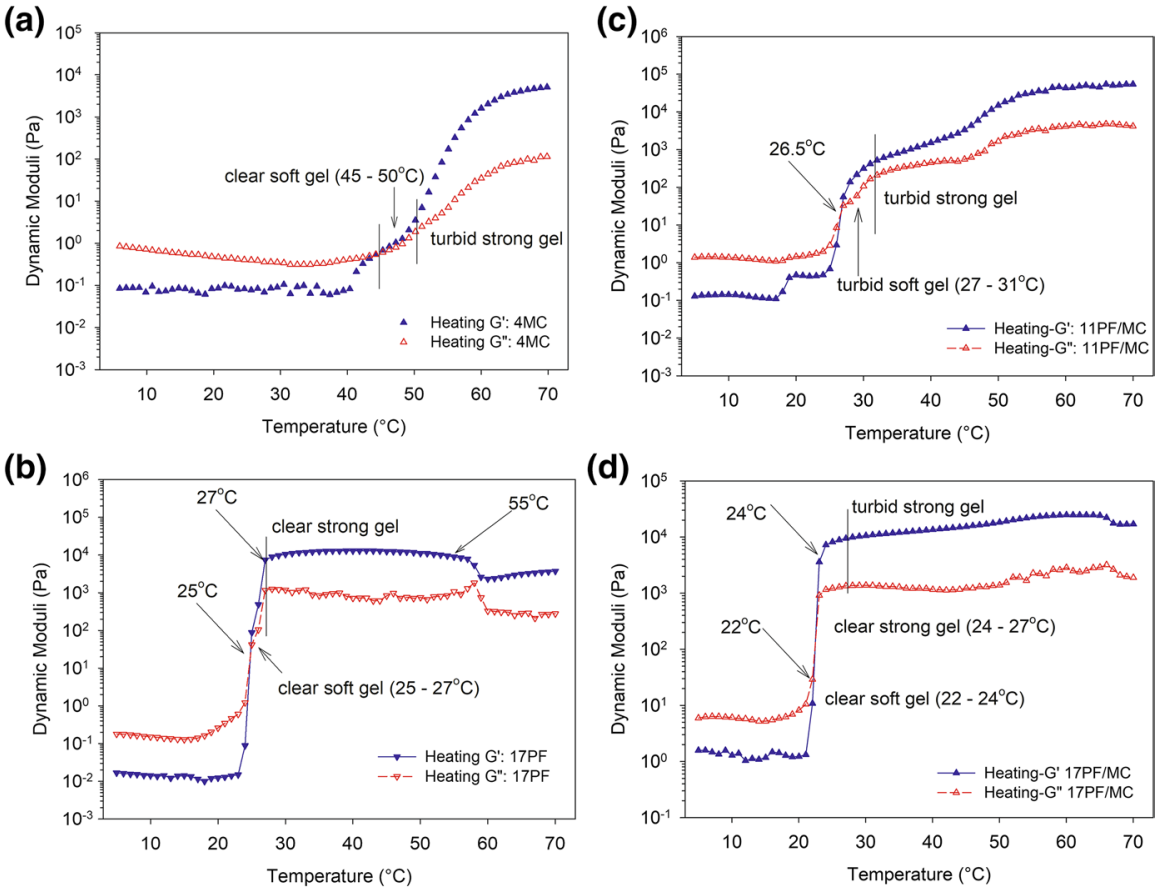

Fig. 4.2 Temperature dependence of dynamic moduli, G′ (closed) and G″ (opened), during heating from 5 to 70 °C at the rate of 1 °C/min of (a) 4MC, (b) 17PF, (c) 11PF/MC and (d) 17PF/MC.

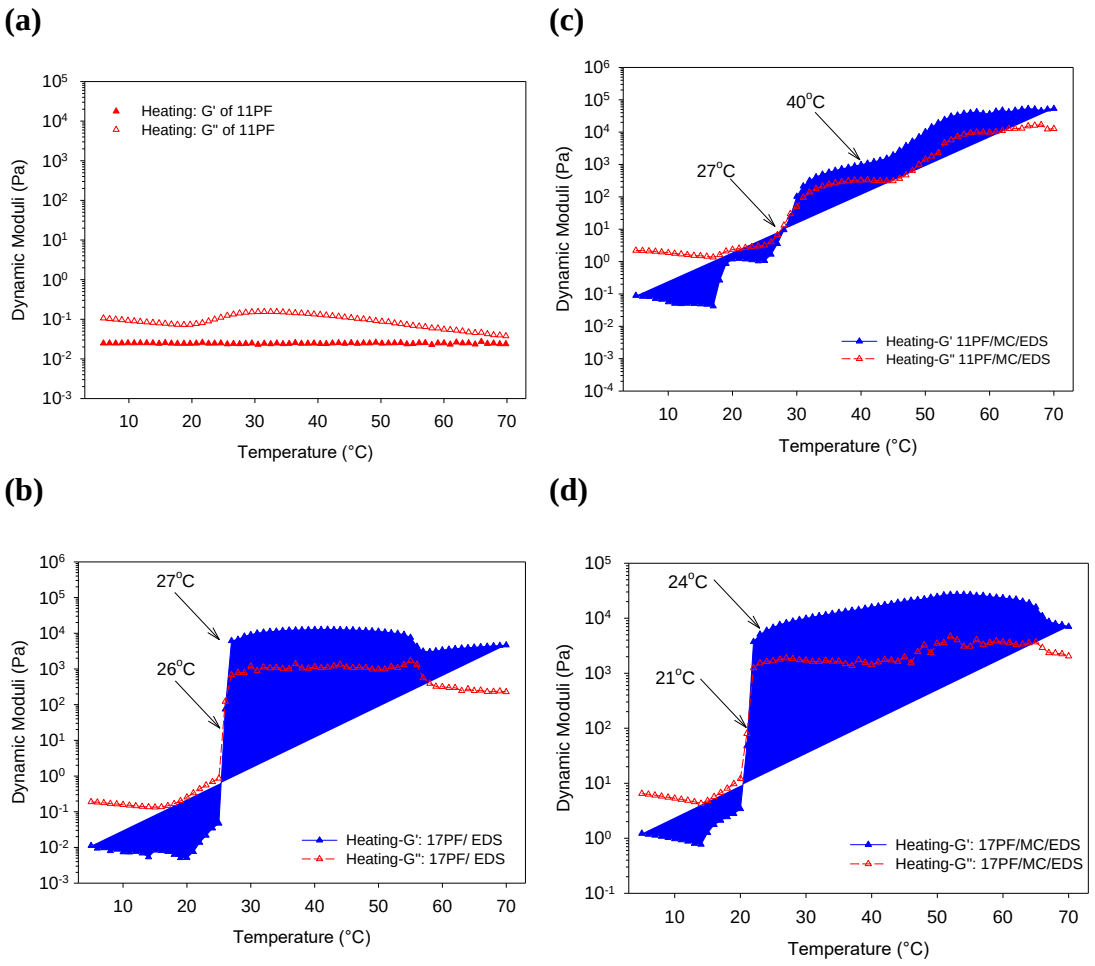

Fig. 4.3 Temperature dependence of dynamic moduli, G′ (closed) and G″ (opened), during heating from 5 to 70 °C at the rate of 1 °C/min of (a) 11PF, (b) 17PF/EDS, (c) 11PF/MC/EDS and (d) 17PF/MC/EDS

4.4 Small-angle X-ray scattering (SAXS) Analysis

SAXS experiments were performed at the BL 1.3W of the Siam Photon Laboratory, Synchrotron Light Research Institute, Nakhon-Ratchasima, Thailand. The liquid cell with Kapton windows was used to contain the samples, while the sample temperature was controlled by a Eurotherm 2216E Temperature Controller. The beam energy was set at 9 keV. The scattering patterns were recorded using the CCD camera, and the sample to detector distance was 2500 mm. The scattering intensities were computed by circularly averaging the scattering patterns after subtracting the scattering of the background from that of samples either in the gel or in the solution states. Data corrections and determinations were performed using the SAXSIT program.

In this study, the SAXS technique was used to determine the structural characteristic of PF, MC and their blends. As shown in Fig. 4.4, SAXS profiles of MC at 25 and 37 °C showed low scattering intensity. At these temperatures, MC was sol. The scattering intensity at low q range of MC increased when the temperature increased as revealed by the SAXS scattering at 40 °C in which MC sample turned out to be a clear soft gel. A very steep upturn of the SAXS curve at small q values was observed in the profiles of MC at the higher temperatures of 55 °C and 70 °C (Fig. 4.4). MC was a turbid strong gel at these two high temperatures. MC became gel at elevated temperatures due to intermolecular associations between the hydrophobic residues of the polymers that led to the formation of gel networks resulting in a significant increase in the scattering intensities at the low scattering angles as previously described (128, 129).

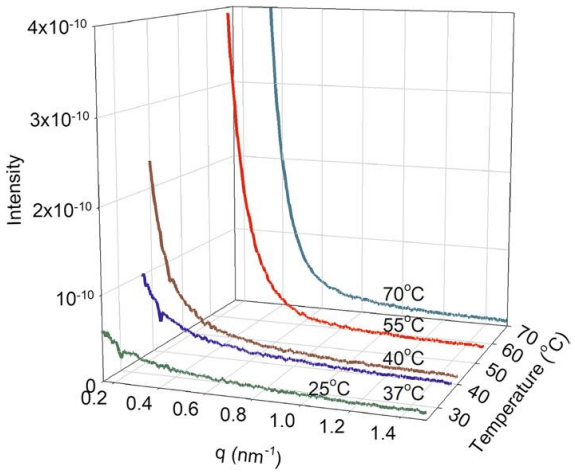

Fig. 4.4 Small-angle X-ray scattering curves of 4% w/w of methylcellulose at various temperature.

SAXS profiles of 11PF and 17PF at various temperatures are shown in Fig. 4.5a and 4.5b, respectively. According to the results obtained from TTM and rheological measurements, 17PF showed gel behavior at 25–70 °C, but 11PF did not form gel at any temperature. At the low concentration of 11PF, all scattering functions at 25, 37, 40, 55 and 70 °C indicated a disordered structure (Fig. 4.5a). In general, the dominated cubic lattice structure observed for PF gels is face-centered cubic (FCC)(130).The gel structures with an FCC close packed structure have been reported as 18–40% PF in water(130-132). As shown in Fig. 4.5b, SAXS profiles of 17PF at 25, 37, 40 and 55 °C were consistent with SAXS data previously reported for FCC structure (131, 132). As mentioned above, at 25 °C, 17PF formed soft gel, and the low diffraction intensities might be interpreted as an existence of a defected FCC structure as previously described (125, 126, 133). As shown in Fig. 4.2b, G′ curve of 17PF dropped

at about 55 °C, and SAXS profile showed a somewhat less ordered structure as compared to the SAXS profiles at 37 and 40 °C. At 70 °C, however, 17PF show a broad peak reflecting a disordered system. The change to a disordered system at this high temperature has been previously reported by Meznarich *et al*. (123). Therefore, temperature plays an important role in the formation of ordered micelles and the stability of a gel structure. Although the scattering function revealed the order-to-disorder transition, 17PF gel did not transform to sol at this high temperature as revealed by TTM and rheological investigation (Fig. 4.2b). According to the rheological measurements, G′ slightly decreased compared to the G′ at 27–55 °C. This slight drop of G′ indicated the lower gel strength compared to the lower-temperature gel. This transition to lower gel strength may be due to the decrease in solubility of PEO blocks at high temperature which caused a part of PEO to be merged into the core of micelles. Subsequently, the size of micellar cores was larger and the degree of shell overlapping decreased, resulting in the decrease in entanglement density of PEO in the overlapped shell and decrease in gel strength as previously explained (122).

SAXS profiles of 11PF/MC at various temperatures are displayed in Fig. 4.5c. SAXS profile of 11PF/MC at 25 °C revealed a disordered structure, and the system was in a sol state (G″ > G′, Fig. 4.2c) at this temperature. Based on rheological measurement, G′ was higher than G″ after 26.5 °C. A transition from the disordered state (sol state) at 25 °C to the FCC-ordered state occurred at the higher temperature of 37 °C. SAXS profiles showed a slightly less ordered structure at 40 °C and disordered structures at 55 and 70 °C. The samples were gels, although less ordered or disordered structures were developed at these high temperatures. The same observations have also been previously reported for the neat PF gels (124) .For 17PF/MC, SAXS profiles indicated FCC-ordered structures at 25, 37, 40 and 55 °C (Fig. 4.5d) since the sample was gel at 22 °C (G′ > G″) during heating (Fig. 4.2d). The presence of MC lowered the gelation temperature compared to the neat 17PF. SAXS profile revealed a disordered structure at 70 °C, but that the sample still existed as gel. As shown in Fig. 4.5e–f, SAXS profiles of 11PF/MC/EDS and 17PF/MC/EDS were similar to those of the corresponding PF/MC blends without EDS (Fig. 4.5c, d). This demonstrated that EDS did not cause the change of order structures and gel behaviors of 11PF/MC and 17PF/MC.

Fig. 4.6 summarizes SAXS profiles of samples at room (25 °C) and body (37 °C) temperatures. At 25 °C, SAXS profiles of 11PF, MC, 11PF/MC and 11PF/MC/EDS indicated disordered structures and these samples were in sol state based on TTM and rheological data. However, 17PF, 17PF/MC and 17PF/MC/EDS exhibited ordered structures, and all were in gel state. At body temperature, all samples except MC presented as ordered structures and these samples were in gel state. Therefore, 11PF/MC could be used for *in situ* gelling preparation. The material could be injected as a sol at room temperature and become gel at body temperature and possibly sustained release the required drug at site of injection. In addition, the

thermosensitive sol–gel transition of PF/MC blends did not change when adding a drug such as EDS.

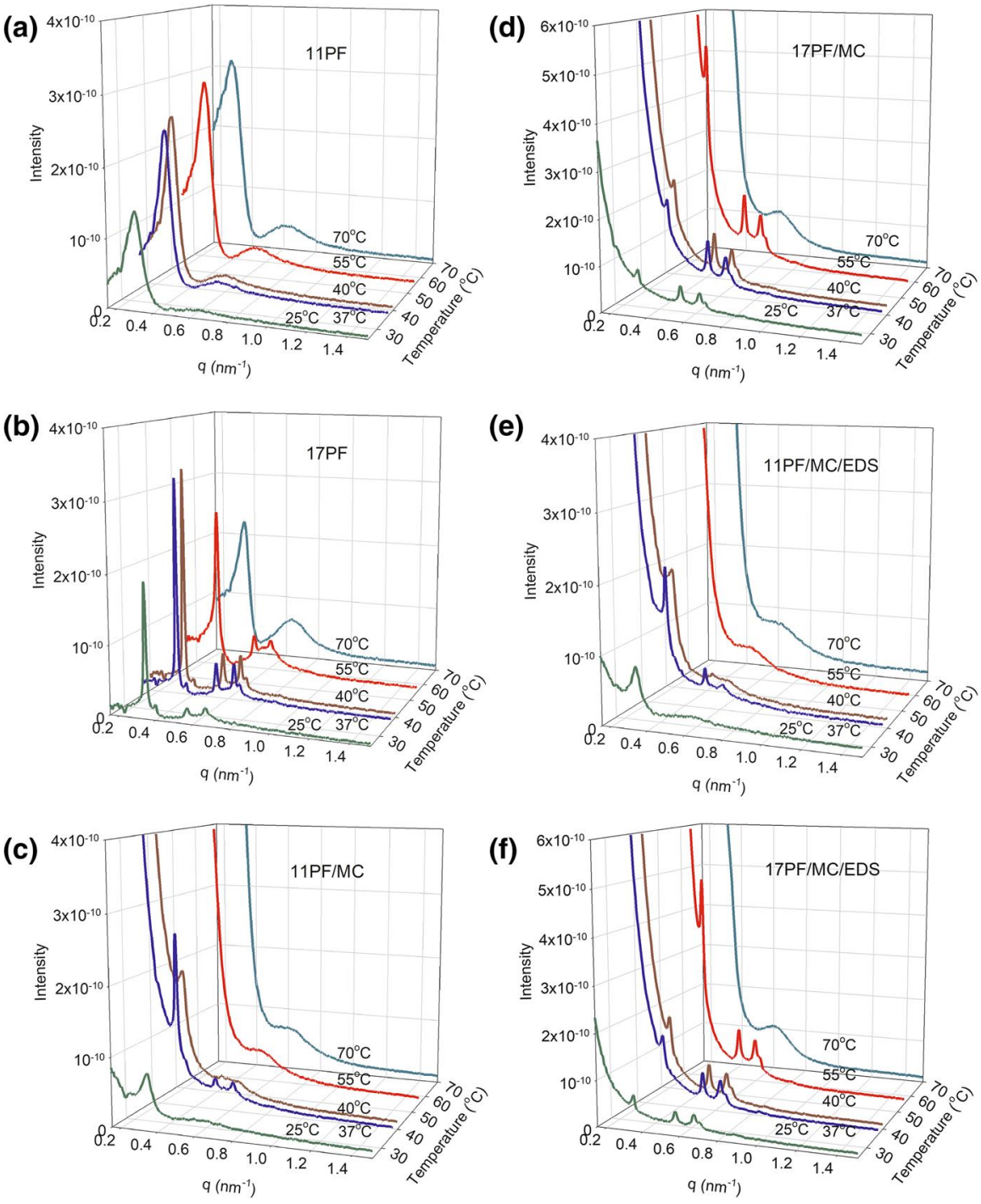

Fig. 4.5 Small-angle X-ray scattering curves of (a) 11PF, (b) 17PF, (c) 11PF/MC, (d) 17PF/MC, (e) 11PF/MC/EDS and (f) 17PF/MC/EDS at various temperatures.

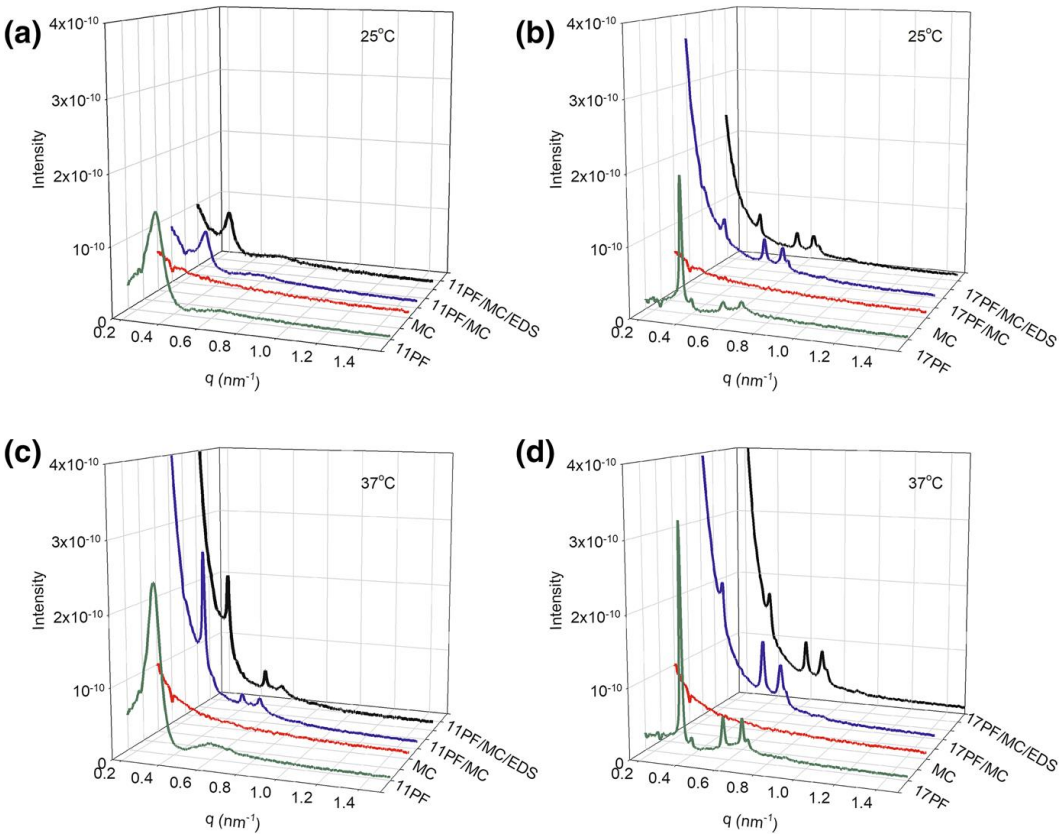

Fig. 4.6 Small-angle X-ray scattering curves of 11PF, MC, 11PF/MC and 11PF/MC/EDS at (a) 25 °C and (c) 37 °C; and 17PF, MC, 17PF/MC and 17PF/MC/EDS at (b) 25 °C and (d) 37 °C.

In the presence of MC, the decrease of sol-to-gel temperature of 17PF and the ability to form gel of 11PF were probably caused by increasing the interaction between PF and MC, and/or from decreasing the intermolecular hydrogen bond between PF and water as well as between MC and water molecules, causing the decrease in water activity or “salt-out like” effect as previously described (38, 122, 134). When the temperature is below its CMT, PF chains exist as unimer. Upon heating, dehydration of the PPO blocks occurred, and micellization started (Fig. 4.7). Due to low micellar density of the low concentration of 11PF, the dispersed micelles were unable to be packed into an ordered structure, so 11PF solution was in a liquid state. Nevertheless, when adding MC into 11PF solution, the dehydrated MC chains may be able to act as bridges to connect PF micelles to form a gel network (Fig. 4.7) as previously described for Pluronic-R 25R4-assisted gelation of PF (122). MC assisted interconnected network of micelles also created turbidity to the system. For higher concentration of 17PF, the dispersed micelles may be able to form a closely packed crystalline lattice or an ordered structure by themselves and trigger the sol-to- gel transition. However, the dispersed micelles of 17PF/MC could form a closely packed crystalline lattice, which corresponded to the sol-to-gel transition, at temperatures lower

than the neat 17PF probably due to the “salt-out like” effect from MC. At the 22-27 °C temperature range, the system formed clear gels. Over 27 °C, MC chains could connect PF micelles and a turbid gel was formed. Furthermore, SAXS profiles of the neat PF (Fig. 4.5b) were different from that of PF/MC blends (Fig. 4.5c, d); in the presence of MC, the steep upturns of the SAXS curves at small q values was observed at high temperatures of 55 and 70 °C which was similar to that of the neat MC (Fig. 4.4). Therefore, gelling process in the presence of MC at high temperatures might involve the gelation of the MC-assisted network connection of PF and also the gel network of MC.

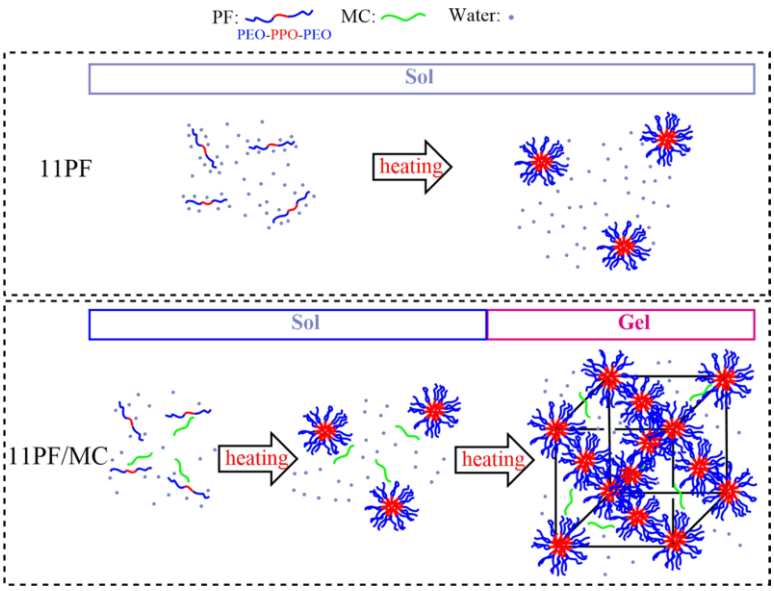

Fig. 4.7 Schematic diagrams for the microstructure formation in aqueous solution of 11PF and 11PF/MC upon heating.

4.5 Summary

PF gel formation on heating was modulated by mixing this block copolymer with MC. Although 11PF still existed as sol at all temperature ranges (15–70 °C), 11PF/MC exhibited viscoelastic sol–gel transition upon heating and it remained as sol at room temperature (25 °C). Over 27 °C, the turbid soft gel of 11PF/MC was detected up to around 31 °C. At higher temperatures, 11PF/MC became turbid strong gel. For 17PF/MC, the presence of MC lowered the gelation temperature. At 22 °C, the clear soft gel was observed. Above 27 °C, the gel became cloudy. At the intermediate temperatures above the gelation temperature, the FCC packing of the micelles was dominant. The MC-assisted interconnected network of PF micelles might trigger the sol–gel transition. Although the less ordered structure of intermicellar organization was

observed at high temperatures, the blends still exhibited gel-like characteristics. In addition, the steep upturn of the scattering curves appeared in the small q range. The MC network might dominate the gel of the blends at high temperature. The presence of the model drug, EDS, did not alter the thermosensitive gelation and the phase behavior of the blends. In addition, this study indicates that blending PF with MC is a potential strategy for modulating the thermosensitive characteristics of the *in situ* gel forming matrices.

CHAPTER 5

CONCLUDING REMARKS

In 2016, our research group reported that EDS-loaded 12PF/MC, 14PF/MC, 16PF/MC, 18PF/MC, and 20PF/MC were more functional for a sustained drug delivery for osteogenesis. Nevertheless, hydrogels characteristics and gel formation mechanisms should be additional studied. Therefore, the characterizations associated with the gel forming mechanism was carried out in this thesis work.

In this study, novel thermo-responsive hydrogels comprising various Pluronic F127 (PF) concentrations (12, 14, 16, 18, and 20% w/w) with 4% w/w Methylcellulose (MC) were successfully developed and characterized. All hydrogel blends were evaluated to obtain the optimized matrices most suited for *in situ* implant drug delivery system. This work performed to find the optimized hydrogels as follows:

Firstly, the thermo-responsive hydrogels containing various PF concentrations (12, 14, 16, 18, and 20% w/w) were blended with 4% w/w MC and characterized. MC, various PF concentrations (12, 14, 16, 18, and 20% w/w) and their blends (12PF/MC, 14PF/MC, 16PF/MC, 18PF/MC, and 20PF/MC) were systematically performed by TTM, turbidity, DSC and rheological analyses. As a first result, PF/MC blending provided clear solution at ambient temperature and became turbid gel at the range of body temperature. Second, the clouding phenomenon observed in the PF/MC blends may reflect the efficient dehydration of PEO moiety of the micelles by MC. Thus, turbidity was the result of MC into PF system. Third, the CMT and the enthalpy of micellization were reduced by including MC into PF. Lastly, the viscoelasticity results were related with the temperature-induced micellization and gelation of PF/MC systems. As these characterizations, gel formation mechanisms of hydrogels blends were more well understand and their characteristics suited for *in situ* implant drug delivery system.

Next, optimized blends from the first research part were selected and then loaded with an antibiotic drug for evaluation the effectiveness for periodontal treatment. Among of blends, 12PF/MC and 14PF/MC were well suited. Since their characteristics were in solution state near ambient temperature of (24 °C) and formed *in situ* gels at body temperature (37 °C). 12PF/MC and 14PF/MC shown substantially better mucoadhesive property than pure 12PF and 14PF, respectively. Furthermore, biocompatibility of these mixtures was well shown on mouse fibroblasts. In the next study, doxycycline hyclate (DX) was added at concentrations of 0.25 and 0.5% w/w into 12PF/MC and 14PF/MC. Although, the gelation temperature and viscosity of the DX-loaded blends were changed at high temperatures range. However, all blends still exhibited gel-like characteristics covering the ambient and body temperature. Moreover, DX-incorporated 12PF/MC and 14PF/MC blends presented the same

antibacterial activity as the pure drug solution. This indicated that both PF/MC matrices did not prohibit the antibacterial activity of the drug. The 12PF/MC and 14PF/MC also exhibited slow-release profile of DX. Therefore, in the present study demonstrated that the appropriate mixtures of thermo-responsive PF/MC are promising matrices for the development of efficient periodontal drug delivery system.

Furthermore, the structural transformation of PF/MC was investigated using small-angle X-ray scattering (SAXS), which is a powerful technique used for determining the structural organization of micellar and polymeric systems. The thermo-responsive hydrogels containing 4% w/w MC and various concentrations of PF at 11 and 17% w/w (11PF and 17PF) were prepared. In this study, etidronate sodium (EDS) were added on those samples and investigated. As a result of TTM and viscoelasticity, 11PF still existed as sol at all temperature ranges (15–70 ℃). The blend of 11PF/MC remained solution at room temperature (25 ℃) and became turbid soft gel (27 ℃) and turbid strong gel at temperature above 27 ℃, respectively. 17PF developed clear gel at 25 ℃. The blend of 17PF/MC exhibited soft gel and strong gel at temperature 27 and 25 ℃, respectively. The gelation temperature of blending hydrogels with EDS were not differ from those correspondent concentrations. As a result of SAXS, at the intermediate temperatures above the gelation temperature, the FCC packing of the micelles was dominant. The MC-assisted interconnected network of PF micelles might trigger the sol–gel transition. Although the less ordered structure of intermicellar organization was observed at high temperatures, the blends still exhibited gel-like characteristics. In addition, the steep upturn of the scattering curves appeared in the small q range. The MC network might dominate the gel of the blends at high temperature. The presence of the model drug, EDS, did not alter the thermosensitive gelation and the phase behavior of the blends. In addition, this study indicates that blending PF with MC is a potential strategy for modulating the thermosensitive characteristics of the *in situ* gel forming matrices.

In conclusion, blending of polymeric co-solution of PF and MC such as 11PF/MC, 12PF/MC, 14PF/MC, 16PF/MC, 18PF/MC, and 20PF/MC could employ for *in situ* implant drug delivery system. All blends were advantageous used for EDS delivery system. Moreover, 12PF/MC and 14PF/MC blends were effectiveness as an injectable delivery system of DX for treatment periodontitis. However, this research outcomes could suggest that Dx concentration less than 0.25% w/w was an attractive approach to improve viscoelasticity of blends (12PF/MC and 14PF/MC). Therefore, the selection of blends, the model drug, and drug concentration should be well considered depending on the targeted organs.

BIBLIOGRAPHY

1. Peppas NA, Bures P, Leobandung W, Ichikawa H. Hydrogels in pharmaceutical formulations. European Journal of Pharmaceutics and Biopharmaceutics. 2000;50(1):27-46.
2. Hoffman AS. Hydrogels for biomedical applications. Advanced Drug Delivery Reviews. 2002;65:18-23.
3. Parhi R. Cross-linked hydrogel for pharmaceutical applications: A Review. Advanced Pharmaceutical Bulletin. 2017;7(4):515-30.
4. Caló E, Khutoryanskiy VV. Biomedical applications of hydrogels: A review of patents and commercial products. European Polymer Journal. 2015;65:252-67.
5. Pyarasani RD, Jayaramudu T, John A. Polyaniline-based conducting hydrogels. Journal of Materials Science. 2019;54(2):974-96.
6. Hoare TR, Kohane DS. Hydrogels in drug delivery: Progress and challenges. Polymer. 2008;49(8):1993-2007.
7. Harrison IP, Spada F. Hydrogels for atopic dermatitis and wound management: A superior drug delivery vehicle. Pharmaceutics. 2018;10(2).
8. Masteikova R, Chalupova Z, Sklubalova Z. Stimuli-sensitive hydrogels in controlled and sustained drug delivery. Medicina (Kaunas, Lithuania). 2003;39 Suppl 2:19-24.
9. Parodi A, Khaled Z, Yazdi I, Evangelopoulos M, Toledano Furman N, Wang X, et al. Smart hydrogels. In: Bharat Bhushan, editor. Encyclopedia of nanotechnology: Berlin (Germany): Springer Science+Business Media Dordrecht; 2015. p. 1-13.
10. Fajardo A, Pereira A, Rubira A, Valente A, Muniz E. Chapter 9 - Stimuli-responsive polysaccharide-based hydrogels. In: Pietro Matricardi, Franco Alhaique, Tommasina Coviello, editors. Polysaccharide hydrogels: Characterization and biomedical applications, New Delhi (India): Pan Stanford; 2015. p. 325-66.
11. Klouda L. Thermoresponsive hydrogels in biomedical applications: A seven-year update. European Journal of Pharmaceutics and Biopharmaceutics. 2015;97:338-49.
12. Matanović MR, Kristl J, Grabnar PA. Thermoresponsive polymers: Insights into decisive hydrogel characteristics, mechanisms of gelation, and promising biomedical applications. International Journal of Pharmaceutics. 2014;472(1):262-75.
13. Klouda L, Mikos AG. Thermoresponsive hydrogels in biomedical applications. European Journal of Pharmaceutics and Biopharmaceutics. 2008;68(1):34-45.
14. Hoffman AS. Hydrogels for biomedical applications. Advanced Drug Delivery Reviews. 2002;54(1):3-12.

15. Li Z, Guan J. Thermosensitive hydrogels for drug delivery. Expert Opinion on Drug Delivery. 2011;8(8):991-1007.
16. Chen D, Guo P, Chen S, Cao Y, Ji W, Lei X, et al. Properties of xyloglucan hydrogel as the biomedical sustained-release carriers. Journal of Materials Science: Materials in Medicine. 2012;23(4):955-62.
17. Liu W-F, Kang C-Z, Kong M, Li Y, Su J, Yi A, et al. Controlled release behaviors of chitosan/α, β-glycerophosphate thermo-sensitive hydrogels. Frontiers of Materials Science. 2012;6(3):250-8.
18. Nie S, Hsiao WLW, Pan W, Yang Z. Thermoreversible Pluronic® F127-based hydrogel containing liposomes for the controlled delivery of paclitaxel: in vitro drug release, cell cytotoxicity, and uptake studies. International Journal of Nanomedicine. 2011;6:151-66.
19. da Silva JB, Cook MT, Bruschi ML. Thermoresponsive systems composed of poloxamer 407 and HPMC or NaCMC: mechanical, rheological and sol-gel transition analysis. Carbohydrate Polymers. 2020;240:116268.
20. Ekerdt BL, Fuentes CM, Lei Y, Adil MM, Ramasubramanian A, Segalman RA, et al. Thermoreversible hyaluronic acid-PNIPAAm hydrogel systems for 3D stem cell culture. Advanced Healthcare Materials. 2018;7(12):e1800225.
21. Kaur K, Paiva SS, Caffrey D, Cavanagh BL, Murphy CM. Injectable chitosan/collagen hydrogels nano-engineered with functionalized single wall carbon nanotubes for minimally invasive applications in bone. Materials Science and Engineering C: Materials for Biological Applications. 2021;128:112340.
22. Dalvi A, Ravi PR, Uppuluri CT. Rufinamide-loaded chitosan nanoparticles in xyloglucan-based thermoresponsive in situ gel for direct nose to brain delivery. Frontiers in Pharmacology. 2021;12.
23. Velazquez N, Turino L, Luna J, Mengatto L. Progesterone loaded thermosensitive hydrogel for vaginal application: Formulation and in vitro comparison with commercial product. Saudi Pharmaceutical Journal. 2019;27.
24. Arafa MG, El-Kased RF, Elmazar MM. Thermoresponsive gels containing gold nanoparticles as smart antibacterial and wound healing agents. Scientific Reports. 2018;8(1):13674.
25. Morochnik S, Zhu Y, Duan C, Cai M, Reid RR, He TC, et al. A thermoresponsive, citrate-based macromolecule for bone regenerative engineering. Journal of Biomedical Materials Research Part A. 2018;106(6):1743-52.
26. Schilling AL, Kulahci Y, Moore J, Wang EW, Lee SE, Little SR. A thermoresponsive hydrogel system for long-acting corticosteroid delivery into the paranasal sinuses. Journal of Controlled Release. 2021;330:889-97.
27. Wang B, Shao J, Jansen JA, Walboomers XF, Yang F. A novel thermoresponsive gel as a potential delivery system for Lipoxin. Journal of Dental Research. 2019;98(3):355-62.

28. Soga O, van Nostrum CF, Fens M, Rijcken CJF, Schiffelers RM, Storm G, et al. Thermosensitive and biodegradable polymeric micelles for paclitaxel delivery. Journal of Controlled Release. 2005;103(2):341-53.
29. Andrews GP, Gorman SP, Jones DS. Rheological characterisation of primary and binary interactive bioadhesive gels composed of cellulose derivatives designed as ophthalmic viscosurgical devices. Biomaterials. 2005;26(5):571-80.
30. Cho JH, Kim S-H, Park KD, Jung MC, Yang WI, Han SW, et al. Chondrogenic differentiation of human mesenchymal stem cells using a thermosensitive poly(N-isopropylacrylamide) and water-soluble chitosan copolymer. Biomaterials. 2004;25(26):5743-51.
31. Sá-Lima H, Tuzlakoglu K, Mano JF, Reis RL. Thermoresponsive poly(N-isopropylacrylamide)-g-methylcellulose hydrogel as a three-dimensional extracellular matrix for cartilage-engineered applications. Journal of Biomedical Materials Research Part A. 2011;98A(4):596-603.
32. Payne C, Dolan EB, O'Sullivan J, Cryan SA, Kelly HM. A methylcellulose and collagen based temperature responsive hydrogel promotes encapsulated stem cell viability and proliferation in vitro. Drug Delivery and Translational Research. 2017;7(1):132-46.
33. Gaihre B, Unagolla JM, Liu J, Ebraheim NA, Jayasuriya AC. Thermoresponsive injectable microparticle-gel composites with recombinant BMP-9 and VEGF enhance bone formation in rats. ACS Biomaterials Science and Engineering. 2019;5(9):4587-600.
34. Hirun N, Tantishaiyakul V, Sangfai T, Ouiyangkul P, Li L. In situ mucoadhesive hydrogel based on methylcellulose/xyloglucan for periodontitis. Journal of Sol-Gel Science and Technology. 2019;89(2):531-42.
35. Modi D, Mohammad, Warsi MH, Garg V, Bhatia M, Kesharwani P, et al. Formulation development, optimization, and in vitro assessment of thermoresponsive ophthalmic pluronic F127-chitosan in situ tacrolimus gel. Journal of Biomaterials Science Polymer Edition. 2021;32(13):1678-702.
36. Mayol L, Quaglia F, Borzacchiello A, Ambrosio L, Rotonda MIL. A novel poloxamers/hyaluronic acid in situ forming hydrogel for drug delivery: Rheological, mucoadhesive and in vitro release properties. European Journal of Pharmaceutics and Biopharmaceutics. 2008;70(1):199-206.
37. Moreno E, Schwartz J, Larrañeta E, Nguewa PA, Sanmartín C, Agüeros M, et al. Thermosensitive hydrogels of poly(methyl vinyl ether-co-maleic anhydride) – Pluronic® F127 copolymers for controlled protein release. International Journal of Pharmaceutics. 2014;459(1):1-9.
38. Rangabhatla ASL, Tantishaiyakul V, Oungbho K, Boonrat O. Fabrication of pluronic and methylcellulose for etidronate delivery and their application for osteogenesis. International Journal of Pharmaceutics. 2016;499(1):110-8.
39. Kim JK, Won Y-W, Lim KS, Kim Y-H. Low-molecular-weight methylcellulose-based thermo-reversible gel/pluronic micelle combination

system for local and sustained Docetaxel delivery. Pharmaceutical Research. 2012;29(2):525-34.

40. Qiu Y, Park K. Environment-sensitive hydrogels for drug delivery. Advanced Drug Delivery Reviews. 2001;53(3):321-39.
41. Kabanov AV, Batrakova EV, Alakhov VY. Pluronic® block copolymers as novel polymer therapeutics for drug and gene delivery. Journal of Controlled Release. 2002;82(2–3):189-212.
42. He C, Kim SW, Lee DS. In situ gelling stimuli-sensitive block copolymer hydrogels for drug delivery. Journal of Controlled Release. 2008;127(3):189-207.
43. Bercea M, Darie RN, Niţă LE, Morariu S. Temperature responsive gels based on Pluronic F127 and poly(vinyl alcohol). Industrial and Engineering Chemistry Research. 2011;50(7):4199-206.
44. Dumortier G, Grossiord JL, Agnely F, Chaumeil JC. A review of poloxamer 407 pharmaceutical and pharmacological characteristics. Pharmaceutical Research. 2006;23(12):2709-28.
45. Li L, Liu S. Multiple phase transition and scaling law for poly(ethylene oxide)–poly(propylene oxide)–poly(ethylene oxide) triblock copolymer in aqueous Solution. ACS applied materials & interfaces. 2015;7.
46. El-Kamel AH. In vitro and in vivo evaluation of Pluronic F127-based ocular delivery system for timolol maleate. International Journal of Pharmaceutics. 2002;241(1):47-55.
47. Funami T, Kataoka Y, Hiroe M, Asai I, Takahashi R, Nishinari K. Thermal aggregation of methylcellulose with different molecular weights. Food Hydrocolloids. 2007;21(1):46-58.
48. Bodvik R, Dedinaite A, Karlson L, Bergström M, Bäverbäck P, Pedersen JS, et al. Aggregation and network formation of aqueous methylcellulose and hydroxypropylmethylcellulose solutions. Colloids and Surfaces A: Physicochemical and Engineering Aspects. 2010;354(1–3):162-71.
49. Joshi SC, Su JC, Liang CM, Lam YC. Gelation of methylcellulose hydrogels under isothermal conditions. Journal of Applied Polymer Science. 2008;107(4):2101-8.
50. LI L, WANG Q, and , XU Y. Thermoreversible association and gelation of methylcellulose in aqueous solutions. Nihon Reoroji Gakkaishi 2003;31(5):287-96.
51. Bodvik R, Karlson L, Edwards K, Eriksson J, Thormann E, Claesson PM. Aggregation of modified celluloses in aqueous solution: Transition from methylcellulose to hydroxypropylmethylcellulose solution properties induced by a low-molecular-weight oxyethylene additive. Langmuir. 2012;28(38):13562-9.
52. Fairclough JPA, Yu H, Kelly O, Ryan AJ, Sammler RL, Radler M. Interplay between gelation and phase separation in aqueous solutions of methylcellulose and hydroxypropylmethylcellulose. Langmuir. 2012;28(28):10551-7.

53. Nasatto PL, Pignon F, Silveira JLM, Duarte MER, Noseda MD, Rinaudo M. Methylcellulose, a cellulose derivative with original physical properties and extended applications. Polymers. 2015;7(5):777-803.
54. Li L, Thangamathesvaran P, Yue C, Tam K, Hu X, Lam YC. Gel network structure of methylcellulose in water. Langmuir. 2001;17.
55. Itoh K, Hatakeyama T, Shimoyama T, Miyazaki S, D'Emanuele A, Attwood D. In situ gelling formulation based on methylcellulose/pectin system for oral-sustained drug delivery to dysphagic patients. Drug Development and Industrial Pharmacy. 2011;37(7):790-7.
56. Sangfai T, Tantishaiyakul V, Hirun N, Li L. Microphase separation and gelation of methylcellulose in the presence of gallic acid and NaCl as an in situ gel-forming drug delivery system. AAPS PharmSciTech. 2016:1-12.
57. Nasir F, Iqbal Z, Khan A, Khan JA, Khan A, Khuda F, et al. Development and evaluation of pluronic and methylcellulose-based thermoreversible drug delivery system for insulin. Drug Development and Industrial Pharmacy. 2014;40(11):1503-8.
58. Joshi D, Garg T, Goyal AK, Rath G. Advanced drug delivery approaches against periodontitis. Drug Delivery. 2016;23(2):363-77.
59. Jacob S. Global prevalence of periodontitis: A literature review. International Arab Journal of Dentistry. 2012;3(1):26-30.
60. Chen X, Wu G, Feng Z, Dong Y, Zhou W, Li B, et al. Advanced biomaterials and their potential applications in the treatment of periodontal disease. Critical Reviews in Biotechnology. 2016;36(4):760-75.
61. Tabary N, Chai F, Blanchemain N, Neut C, Pauchet L, Bertini S, et al. A chlorhexidine-loaded biodegradable cellulosic device for periodontal pockets treatment. Acta Biomaterialia. 2014;10(1):318-29.
62. Jain N, Jain GK, Javed S, Iqbal Z, Talegaonkar S, Ahmad FJ, et al. Recent approaches for the treatment of periodontitis. Drug Discovery Today. 2008;13(21–22):932-43.
63. Goodson JM, Haffajee A, Socransky SS. Periodontal therapy by local delivery of tetracycline. Journal of Clinical Periodontology. 1979;6(2):83-92.
64. Goodson JM, Holborow D, Dunn RL, Hogan P, Dunham S. Monolithic tetracycline-containing fibers for controlled delivery to periodontal pockets. Journal of Periodontology. 1983;54(10):575-9.
65. Tonetti M, Cugini MA, Goodson JM. Zero-order delivery with periodontal placement of tetracycline-loaded ethylene vinyl acetate fibers. Journal of Periodontal Research. 1990;25(4):243-9.
66. Akncbay H, Senel S, Ay ZY. Application of chitosan gel in the treatment of chronic periodontitis. Journal of Biomedical Materials Research Part B: Applied Biomaterials. 2007;80(2):290-6.

67. Pakzad Y, Ganji F. Thermosensitive hydrogel for periodontal application: in vitro drug release, antibacterial activity and toxicity evaluation. Journal of Biomaterials Applications. 2016;30(7):919-29.
68. Safari J, Zarnegar Z. Advanced drug delivery systems: Nanotechnology of health design A review. Journal of Saudi Chemical Society. 2014;18(2):85-99.
69. Rao SK, Setty S, Acharya AB, Thakur SL. Efficacy of locally-delivered doxycycline microspheres in chronic localized periodontitis and on *Porphyromonas gingivalis*. Journal of Investigative and Clinical Dentistry. 2012;3(2):128-34.
70. Lu Z, Rong K, Li J, Yang H, Chen R. Size-dependent antibacterial activities of silver nanoparticles against oral anaerobic pathogenic bacteria. Journal of Materials Science: Materials in Medicine. 2013;24(6):1465-71.
71. Domínguez-Delgado CL, Rodríguez-Cruz IM, Escobar-Chávez JJ, Calderón-Lojero IO, Quintanar-Guerrero D, Ganem A. Preparation and characterization of triclosan nanoparticles intended to be used for the treatment of acne. European Journal of Pharmaceutics and Biopharmaceutics. 2011;79(1):102-7.
72. Pragati S, Ashok S, Kuldeep S. Recent advances in periodontal drug delivery systems. International Journal of Drug Delivery 2009;1(1):1-14.
73. Higashi K, Matsushita M, Morisaki K, Hayashi S, Mayumi T. Local drug delivery systems for the treatment of periodontal disease. Journal of Pharmacobio-Dynamics. 1991;14(2):72-81.
74. Perugini P, Genta I, Conti B, Modena T, Pavanetto F. Periodontal delivery of ipriflavone: new chitosan/PLGA film delivery system for a lipophilic drug. International Journal of Pharmaceutics. 2003;252(1):1-9.
75. Wang LC, Chen XG, Zhong DY, Xu QC. Study on poly(vinyl alcohol)/carboxymethyl-chitosan blend film as local drug delivery system. Journal of Materials Science: Materials in Medicine. 2007;18(6):1125-33.
76. Senarat S, Wai Lwin W, Mahadlek J, Phaechamud T. Doxycycline hyclate-loaded in situ forming gels composed from bleached shellac, Ethocel, and Eudragit RS for periodontal pocket delivery. Saudi Pharmaceutical Journal. 2021;29(3):252-63.
77. Kogawa AC, Zoppi A, Quevedo MA, Nunes Salgado HR, Longhi MR. Increasing Doxycycline hyclate photostability by complexation with β-cyclodextrin. AAPS PharmSciTech. 2014;15:1209-17.
78. Phaechamud T, Charoenteeraboon J. Antibacterial activity and drug release of chitosan sponge containing doxycycline hyclate. AAPS PharmSciTech. 2008;9(3):829-35.
79. Jain P, Garg A, Farooq U, Panda AK, Mirza MA, Noureldeen A, et al. Preparation and quality by design assisted (Qb-d) optimization of bioceramic loaded microspheres for periodontal delivery of doxycycline hyclate. Saudi Journal of Biological Sciences. 2021;28(5):2677-85.

80. Kopytynska-Kasperczyk A, Dobrzynski P, Pastusiak M, Jarzabek B, Prochwicz W. Local delivery system of doxycycline hyclate based on ϵ-caprolactone copolymers for periodontitis treatment. International Journal of Pharmaceutics. 2015;491(1):335-44.
81. Cover NF, Lai-Yuen SK, Parsons AK, Kumar A. Synergetic effects of doxycycline-loaded chitosan nanoparticles for improving drug delivery and efficacy. International Journal of Nanomedicine. 2012;7:2411 - 9.
82. He Z-x, Wang Z-h, Zhang H-h, Pan X, Su W-r, Liang D, et al. Doxycycline and hydroxypropyl-β-cyclodextrin complex in poloxamer thermal sensitive hydrogel for ophthalmic delivery. Acta Pharmaceutica Sinica B. 2011;1(4):254-60.
83. Li W, Cheong Y-K, Hui W, Ren G, Yang YZ. Neuroprotective effects of etidronate and 2,3,3-trisphosphonate against glutamate-induced toxicity in PC12 cells. Neurochemical research. 2016;41.
84. Fleisch H, Reszka A, Rodan G, Rogers M. Chapter 78 - Bisphosphonates: mechanisms of action. In: Bilezikian JP, Raisz LG, Rodan GA, editors. Principles of Bone Biology (Second Edition). San Diego: Academic Press; 2002. p. 1361-XLIII.
85. Papapetrou PD. Bisphosphonate-associated adverse events. Hormones (Athens). 2009;8(2):96-110.
86. Wells GA, Cranney A, Peterson J, Boucher M, Shea B, Robinson V, et al. Etidronate for the primary and secondary prevention of osteoporotic fractures in postmenopausal women. Cochrane Database of Systematic Reviews. 2008;2008(1):Cd003376.
87. Abrahamsen B. Adverse effects of bisphosphonates. Calcified Tissue International. 2010;86(6):421-35.
88. Gong C, Qi T, Wei X, Qu Y, Wu Q, Luo F, et al. Thermosensitive polymeric hydrogels as drug delivery systems. Current Medicinal Chemistry. 2013;20(1):79-94.
89. Liu Y, Zhu Y-y, Wei G, Lu W-y. Effect of carrageenan on poloxamer-based in situ gel for vaginal use: Improved in vitro and in vivo sustained-release properties. European Journal of Pharmaceutical Sciences. 2009;37(3–4):306-12.
90. Varshosaz J, Tabbakhian M, and, Salmani Z. Designing of a thermosensitive chitosan/poloxamer in situ gel for ocular delivery of ciprofloxacin. The Open Drug Delivery Journal. 2008;2(1):61-70.
91. de Lima CM, Siqueira SMC, de Amorim AFV, Costa KBS, de Brito DHA, Ribeiro MENP, et al. Effects of polypropylene glycol 400 (PPG400) on the micellization and gelation of Pluronic F127. Macromolecules. 2015;48(21):7978-82.
92. Zheng P, Li L, Hu X, Zhao X. Sol–gel transition of methylcellulose in phosphate buffer saline solutions. Journal of Polymer Science Part B: Polymer Physics. 2004;42(10):1849-60.

93. Silva RCd, Loh W. Effect of additives on the cloud points of aqueous solutions of ethylene oxide–propylene oxide–ethylene oxide block copolymers. Journal of Colloid and Interface Science. 1998;202(2):385-90.
94. Sharma R, Bahadur P. Effect of different additives on the cloud point of a polyethylene oxide-polypropylene oxide-polyethylene oxide block copolymer in aqueous solution. Journal of Surfactants and Detergents. 2002;5(3):263-8.
95. Park MJ, Char K, Kim HD, Lee C-H, Seong B-S, Han Y-S. Phase behavior of a PEO-PPO-PEO triblock copolymer in aqueous solutions: Two gelation mechanisms. Macromolecular Research. 2002;10(6):325-31.
96. Pham Trong LC, Djabourov M, Ponton A. Mechanisms of micellization and rheology of PEO–PPO–PEO triblock copolymers with various architectures. Journal of Colloid and Interface Science. 2008;328(2):278-87.
97. Oshiro A, da Silva DC, de Mello JC, de Moraes VWR, Cavalcanti LP, Franco MKKD, et al. Pluronics F-127/L-81 binary hydrogels as drug-delivery systems: Influence of Physicochemical Aspects on Release Kinetics and Cytotoxicity. Langmuir. 2014;30(45):13689-98.
98. Pragatheeswaran AM, Chen SB. The influence of poly(acrylic acid) on micellization and gelation characteristics of aqueous Pluronic F127 copolymer system. Colloid and Polymer Science. 2016;294(1):107-17.
99. Pothan LA, George CN, John MJ, Thomas S. Dynamic mechanical and dielectric behavior of banana-glass hybrid fiber reinforced polyester composites. Journal of Reinforced Plastics and Composites. 2010;29(8):1131-45.
100. Hirun N, Tantishaiyakul V, Sangfai T, Boonlai W, Soontaranon S, Rugmai S. The effect of poly(acrylic acid) on temperature-dependent behaviors and structural evolution of poloxamer 407. Polymer International. 2021;70(9):1282-9.
101. Curnutt A, Smith K, Darrow E, Walters KB. Chemical and microstructural characterization of pH and [Ca^{2+}] dependent sol-gel transitions in mucin biopolymer. Scientific Reports. 2020;10(1):8760.
102. Prud'homme RK, Wu G, Schneider DK. Structure and rheology studies of poly(oxyethylene-oxypropylene-oxyethylene) aqueous solution. Langmuir. 1996;12(20):4651-9.
103. Zhang J, Gassmann M, Chen X, Burger C, Rong L, Ying Q, et al. Characterization of a reversible thermoresponsive gel and its application to oligonucleotide separation. Macromolecules. 2007;40(15):5537-44.
104. Wu C, Liu T, Chu B. Viscosity-adjustable block copolymer for DNA separation by capillary electrophoresis. ELECTROPHORESIS. 1998;19(2):231-41.
105. Li X, Hyun K. Rheological study of the effect of polyethylene oxide (PEO) homopolymer on the gelation of PEO-PPO-PEO triblock copolymer in aqueous solution. Korea-Australia Rheology Journal. 2018;30(2):109-25.
106. Bromberg L. Temperature-sensitive star-branched poly(ethylene oxide)–b-poly(propylene oxide)–b-poly(ethylene oxide) networks. Polymer. 1998;39(23):5663-9.

107. Wang Y, Tan Y, Huang X, Xu G. Gelation behavior of thermo-responsive poly(ethylene oxide) and poly(propylene oxide) multiblock polycarbonates. Journal of Macromolecular Science, Part A. 2009;46(4):397-404.
108. Duggan S, Hughes H, Owens E, Duggan E, Cummins W, O' Donovan O. Synthesis and characterisation of mucoadhesive thiolated polyallylamine. International Journal of Pharmaceutics. 2016;499(1):368-75.
109. Barakat NS. In vitro and in vivo characteristics of a thermogelling rectal delivery system of etodolac. AAPS PharmSciTech. 2009;10(3):724-31.
110. Ci L, Huang Z, Liu Y, Liu Z, Wei G, Lu W. Amino-functionalized poloxamer 407 with both mucoadhesive and thermosensitive properties: preparation, characterization and application in a vaginal drug delivery system. Acta Pharmaceutica Sinica B. 2017;7(5):593-602.
111. Roy S, Pal K, Anis A, Pramanik K, Prabhakar B. Polymers in mucoadhesive drug-delivery systems: A brief note. Designed Monomers and Polymers. 2009;12(6):483-95.
112. 10993-5:2009(E) ISI. Biological evaluation of medical devices—Part 5: Tests for in vitro cytotoxicity. Available online: https://www.iso.org/standard/36406.html (accessed on 1 November 2021).
113. Sobolewska E, Makowiecki P, Drozdowska J, Dziuba I, Nowicka A, Wyganowska-Świątkowska M, et al. Cytotoxic potential of denture adhesives on human fibroblasts—In vitro study. Materials. 2022;15:1583.
114. Markstedt K, Mantas A, Tournier I, Martínez Ávila H, Hägg D, Gatenholm P. 3D bioprinting human chondrocytes with nanocellulose–Alginate bioink for cartilage tissue engineering applications. Biomacromolecules. 2015;16(5):1489-96.
115. Prakasam A, Elavarasu SS, Natarajan RK. Antibiotics in the management of aggressive periodontitis. Journal of Pharmacy And Bioallied Sciences. 2012;4(Suppl 2):S252-S5.
116. AlJehani YA. Risk factors of periodontal disease: Review of the literature. International Journal of Dentistry. 2014;2014:9.
117. Cheong LWS, Heng PWS, Wong LF. Relationship between polymer viscosity and drug release from a matrix system. Pharmaceutical Research. 1992;9(11):1510-4.
118. Behera B, Patil V, Sagiri SS, Pal K, Ray SS. Span-60-based organogels as probable matrices for transdermal/topical delivery systems. Journal of Applied Polymer Science. 2012;125(2):852-63.
119. Kwon K-W, Park MJ, Hwang J, Char K. Effects of alcohol addition on gelation in aqueous solution of poly(ethylene oxide)-Poly(propylene oxide)-poly(ethylene oxide) triblock copolymer. Polymer Journal. 2001;33(5):404-10.
120. de Oliveira AC, Vilsinski BH, Bonafé EG, Monteiro JP, Kipper MJ, Martins AF. Chitosan content modulates durability and structural homogeneity of

chitosan-gellan gum assemblies. International Journal of Biological Macromolecules. 2019;128:114-23.

121. Sun K, Raghavan SR. Thermogelling aqueous fluids containing low concentrations of Pluronic F127 and laponite nanoparticles. Langmuir. 2010;26(11):8015-20.
122. Liu S, Li L. Molecular interactions between PEO–PPO–PEO and PPO–PEO–PPO triblock copolymers in aqueous solution. Colloids and Surfaces A: Physicochemical and Engineering Aspects. 2015;484:485-97.
123. Meznarich N, Juggernauth K, Batzli K, Love B. Structural changes in PEO-PPO-PEO gels induced by methylparaben and dexamethasone observed using time-resolved SAXS. Macromolecules. 2011;44.
124. Chaibundit C, Ricardo NMPS, Ricardo NMPS, Muryn CA, Madec M-B, Yeates SG, et al. Effect of ethanol on the gelation of aqueous solutions of Pluronic F127. Journal of Colloid and Interface Science. 2010;351(1):190-6.
125. Castelletto V, Caillet C, Fundin J, Hamley IW, Yang Z, Kelarakis A. The liquid–solid transition in a micellar solution of a diblock copolymer in water. The Journal of Chemical Physics. 2002;116(24):10947-58.
126. Hamley IW, Pople JA, Fairclough JPA, Terrill NJ, Ryan AJ, Booth C, et al. Effect of shear on cubic phases in gels of a diblock copolymer. The Journal of Chemical Physics. 1998;108(16):6929-36.
127. Ricardo NMPS, Ricardo NMPS, Costa FdMLL, Bezerra FWA, Chaibundit C, Hermida-Merino D, et al. Effect of water-soluble polymers, polyethylene glycol and poly(vinylpyrrolidone), on the gelation of aqueous micellar solutions of Pluronic copolymer F127. Journal of Colloid and Interface Science. 2012;368(1):336-41.
128. Tomšič M, Prossnigg F, Glatter O. A thermoreversible double gel: Characterization of a methylcellulose and κ-carrageenan mixed system in water by SAXS, DSC and rheology. Journal of Colloid and Interface Science. 2008;322(1):41-50.
129. Tomšič M, Guillot S, Sagalowicz L, Leser ME, Glatter O. Internally self-assembled thermoreversible gelling emulsions: ISAsomes in methylcellulose, κ-carrageenan, and mixed hydrogels. Langmuir. 2009;25(16):9525-34.
130. Mortensen K, Batsberg W, Hvidt S. Effects of PEO-PPO diblock impurities on the cubic structure of aqueous PEO-PPO-PEO pluronics micelles: Fee and bcc ordered structures in F127. Macromolecules. 2008;41:1720–7.
131. Wu C, Liu A, Chu B, and DKS, Graziano V. Characterization of the PEO−PPO−PEO triblock copolymer and its application as a separation medium in capillary electrophoresis. Macromolecules. 1997;30:4574-83.
132. Jiang J, Li C, Lombardi J, Colby RH, Rigas B, Rafailovich MH, et al. The effect of physiologically relevant additives on the rheological properties of concentrated Pluronic copolymer gels. Polymer. 2008;49(16):3561-7.

133. Efrat R, Aserin A, Kesselman E, Danino D, Wachtel EJ, Garti N. Liquid micellar discontinuous cubic mesophase from ternary monoolein/ethanol/water mixtures. Colloids and Surfaces A: Physicochemical and Engineering Aspects. 2007;299(1):133-45.
134. Pandit NK, Kisaka J. Loss of gelation ability of Pluronic® F127 in the presence of some salts. International Journal of Pharmaceutics. 1996;145(1):129-36.

APPENDICES

Paper 1

Boonrat, O., Tantishaiyakul, V., and Hirun, N. 2021. Structural characterization using SAXS and rheological behaviors of pluronic F127 and methylcellulose blends. Polymer Bulletin (78): 1175–1187. https://doi.org/10.1007/s00289-020-03154-y.

Polymer Bulletin (2021) 78:1175–1187
https://doi.org/10.1007/s00289-020-03154-y

ORIGINAL PAPER

Structural characterization using SAXS and rheological behaviors of pluronic F127 and methylcellulose blends

Onpreeya Boonrat[1] · Vimon Tantishaiyakul[1,2] · Namon Hirun[3] · Supagorn Rugmai[4] · Siriwat Soontaranon[4]

Received: 10 December 2019 / Revised: 20 January 2020 / Accepted: 2 March 2020 /
Published online: 9 March 2020

Abstract

Binary polymeric mixtures containing pluronic F127 (PF) and methylcellulose were prepared to generate new thermosensitive matrices. The small-angle X-ray scattering (SAXS) behavior of PF/MC blends was investigated in relation to the temperature-dependent phase transition and rheological characteristic. Although 11% w/w PF (11PF) cannot form gel, the test tube tilting method and rheological analysis showed that the incorporation of 4% w/w methylcellulose (MC) into 11PF (11PF/MC) enabled the system to form gel upon heating. In addition, adding MC lowered the gelation temperature of 17% w/w PF (17PF). The ordered structure of these gels exhibited a face-centered cubic phase at intermediate temperature above the gelation temperature; the steep upturn of the SAXS curves was observed in the small scattering vector range at high temperatures (55–70 °C). The presence of MC might cause an MC-assisted interconnected network of micelles. At high temperatures, the gelation possibly involved MC-assisted intermicellar organization of PF as well as the gel network of MC. Etidronate sodium was incorporated into the matrices, and the drug did not significantly affect the thermosensitive gelation and the ordered structure of the polymeric systems. Furthermore, this study indicated that 11PF/MC was sol at 25 °C and became gel at body temperature of 37 °C. Therefore, blending PF with MC is a potential strategy for tailoring the thermosensitive performance of the in situ gelling preparation for drug delivery.

Keywords Pluronic F127 · Methylcellulose · SAXS · Rheological property

Electronic supplementary material The online version of this article (https://doi.org/10.1007/s00289-020-03154-y) contains supplementary material, which is available to authorized users.

✉ Vimon Tantishaiyakul
vimon.t@psu.ac.th

Extended author information available on the last page of the article

Introduction

Hydrogels are of special importance in the area of pharmaceuticals, cosmetics and food applications. Hydrogels can facilitate sustained or controlled release of drugs and various functional molecules [1] and present desired properties of the systems. One of the more recent interests in hydrogel research is in situ formation of injectable hydrogels because of their ease of administration. Physical hydrogels can easily be employed to form in situ hydrogels. Physical hydrogels can change in their transition from solution (sol) to gel state using external stimuli such as temperature, pH and solvent composition [1]. Physical hydrogels are different from chemical hydrogels since their chains are held together by non-covalent bonds, i.e., ionic, hydrogen bonding and dipole interactions, but the chains of chemical hydrogels are joined by covalent cross-linking. Therefore, the network junctions of physical hydrogels are transient or reversible rather than permanent.

If the system is sol at room temperature and turns to gel at body temperature, it will facilitate the injection and provide in situ gel forming drug depot at the site of injection. This makes the thermoreversible or thermosensitive hydrogels attractive as an injectable drug delivery matrix since the sol-to-gel transition of polymer solutions is principally induced by temperature. Various polymers have been investigated as thermoreversibly in situ gelling materials [2]. Our interest lies in pluronic F 127 (PF) and methylcellulose which are well-known excipients used for gelation in various drug delivery systems. PF is a triblock copolymer consisting of poly(ethylene oxide)-polypropylene oxide-poly(ethylene oxide), PEO-PPO-PEO [3]. PF, a nonionic surfactant, exhibits gelation based on micellization above the critical micelle temperature (CMT) or the critical micelle concentration (CMC) in water [4]. Methylcellulose is a gellifying polymer derived from cellulose which is extensively used as a drug excipient. PF and methylcellulose undergo thermoreversible gelation upon heating. Both can form soft gel and strong (hard) gel depending on temperatures. Recently, we have prepared and investigated the blends of PF and methylcellulose for injectable implant drug delivery systems [5]. Etidronate sodium (EDS) was added into the blends for producing an osteogenic effect. The viability of two cell lines, MC3T3-E1 (a murine osteoblast cell line) and C2C12 (a murine myoblast cell line), in the presence of PF substantially increased in the presence of MC.

An understanding of the temperature-dependent gelation and structural organization plays an important role in developing new polymeric platform as thermosensitive matrices [6–9]. Although the gelation and structural organization of plain PF and plain MC have been investigated [9–12], there is a paucity of study that has described the contribution of the structural evolution to the thermosensitive gelation of PF/MC. In this study, we were interested in determining whether the presence of MC has any effect on the temperaturedependent structural transformation of the low concentration of PF (11PF), below the typical gelation concentration. In addition, we wanted to know whether the gelation mechanism and structural organization of the high concentration of PF (17PF), above the gelation concentration, were affected by MC. Therefore, new mixtures of MC with

PF (11PF/MC and 17PF/MC) were selected. In addition, the plain PF solutions at concentrations of 11 and 17% w/w were also investigated and compared with the corresponding PF concentrations in the presence of MC. Here, the structural transformation of PF/MC was investigated using small-angle X-ray scattering (SAXS), which is a powerful technique used for determining the structural organization of micellar and polymeric systems [6]. In order to understand the relationship between the scattering behavior and the gelation, the boundary between the sol and gel phases was described using a test tube tilting method (TTM), and the temperature-dependent phase transition and rheological characteristic were also determined. Furthermore, it is known that some additives can influence the PF and MC gelation behaviors [6, 13, 14]. The effect of EDS on PF/MC was also investigated.

Experimental

Materials

Methylcellulose (methoxy content 27.5–31.5%, viscosity 10–25 mPa.S for a 2% solution in H_2O at 18 °C) and PF (PEO_{99}-PPO_{65}-PEO_{99}) were purchased from Sigma (St. Louis, MO, USA) and used as received. All other chemicals and reagents used were of analytical grade.

Sample preparation

The PF solutions were prepared at concentrations of 11 and 17% (w/w) using a cold method as previously described [5]. Briefly, an appropriate amount of PF was dissolved in MillQ water at 4 °C and refrigerated overnight to ensure that PF was entirely dissolved to obtain 11 and 17% (w/w) of PF (referred to as 11PF and 17PF, respectively). The required amount of methylcellulose was dispersed in hot water with vigorous stirring by magnetic stirrer. After the methylcellulose powder was completely dispersed, the remainder of the water was added to produce 4% w/w of methylcellulose and then cooled in an ice bath until a transparent solution was obtained (referred to as MC). The required amount of PF (11 g or 17 g) was dispersed in 50 mL of cold methylcellulose solution containing 4 g of methylcellulose. Subsequently, the cold water was added to each sample to produce a mixture with the final weight of 100 g. These 11 and 17% w/w of PF in 4% w/w of MC were referred to as 11PF/MC and 17PF/MC, respectively. The resulting blend was mixed thoroughly and refrigerated until it was completely dissolved. For the samples containing EDS, the required amount of the drug to obtain the final concentration of 0.1% (w/w) was dispersed to the 11PF/MC and 17PF/MC solutions and mixed until the drug was completely dissolved. These mixtures were referred to as 11PF/MC/EDS and 17PF/MC/EDS, respectively.

Macroscopic visual detection

The gelation temperatures of the samples were visually detected using a TTM as previously described [15–18]. The samples were heated from 15 to 70 °C in a temperature-controlled water bath at an increment of 1 °C. The samples were allowed to equilibrate for 25 min after each increase in temperature. Phase transition was evaluated by tilting the tube after the incubation period. The temperature at which the samples became solid but slightly flowed at the surface when tilting the tube was recorded as gelation temperature of a soft gel [17]. With further heating, the temperature at which samples did not flow was recorded as a transition temperature of a hard or strong gel [17].

Rheological measurements

All rheological behaviors were measured with a Discovery Hybrid Rheometer (DHR2, TA Instruments, USA) using a 40-mm parallel plate equipped with a Peltier plate temperature control system. Samples in the liquid state were loaded onto the bottom plate of the rheometer at 5 °C, and the periphery of the samples was covered by a layer of silicone oil to prevent evaporation. For oscillatory rheological measurements, the amplitude sweep test for each sample was first tested to investigate the linear viscoelastic range (LVR). Subsequently, the suitable strain value for each sample was selected to perform other oscillatory tests within LVR. The temperature dependence of the elastic modulus (G') and viscous modulus (G'') was analyzed using the parallel plate geometry and a gap of 1 mm at an angular frequency of 6.28 rad/s (1 Hz) over the range 5–70 °C at a temperature scanning rate of 1 °C/min.

Small-angle X-ray scattering (SAXS) Analysis

SAXS experiments were performed at the BL 1.3W of the Siam Photon Laboratory, Synchrotron Light Research Institute, Nakhon-Ratchasima, Thailand. The liquid cell with Kapton windows was used to contain the samples, while the sample temperature was controlled by a Eurotherm 2216E Temperature Controller. The beam energy was set at 9 keV. The scattering patterns were recorded using the CCD camera, and the sample to detector distance was 2500 mm. The scattering intensities were computed by circularly averaging the scattering patterns after subtracting the scattering of the background from that of samples either in the gel or in the solution states. Data corrections and determinations were performed using the SAXSIT program.

Results and discussion

Viscoelastic analysis

Generally, the gelation of methylcellulose occurred in two steps during heating. The first step is a clear soft gel, and the second step is a turbid hard (strong) gel [19]. The temperature dependence of dynamic moduli, G' (elastic modulus) and G'' (viscous modulus) during heating from 5 to 70 °C at the rate of 1 °C/min of MC, is shown in Fig. 1a. MC solution behaved as a viscoelastic fluid with $G'' > G'$ at low temperatures. Based on TTM and rheological property which showed $G' > G''$, a clear soft gel was found at 45–50 °C due to progressive chain association of a few chains of highly methylated zones which is the most hydrophobic zones [10]. Over 50 °C, a turbid gel was formed due to phase separation. Turbidity increased strongly with a fully turbid gel at about 55 °C.

PF (a PEO-PPO-PEO triblock copolymer) in aqueous solutions can self-assemble into micelles above the critical micelle temperature (CMT) or the critical micelle concentration (CMC) [4]. Increasing the temperature of PF solution caused the reducing aqueous solubility of relatively hydrophobic (PPO) segments and initiated micelle formation with relatively hydrophobic PPO cores and relatively hydrophilic PEO coronas (shells) [20]. This core–shell structure is

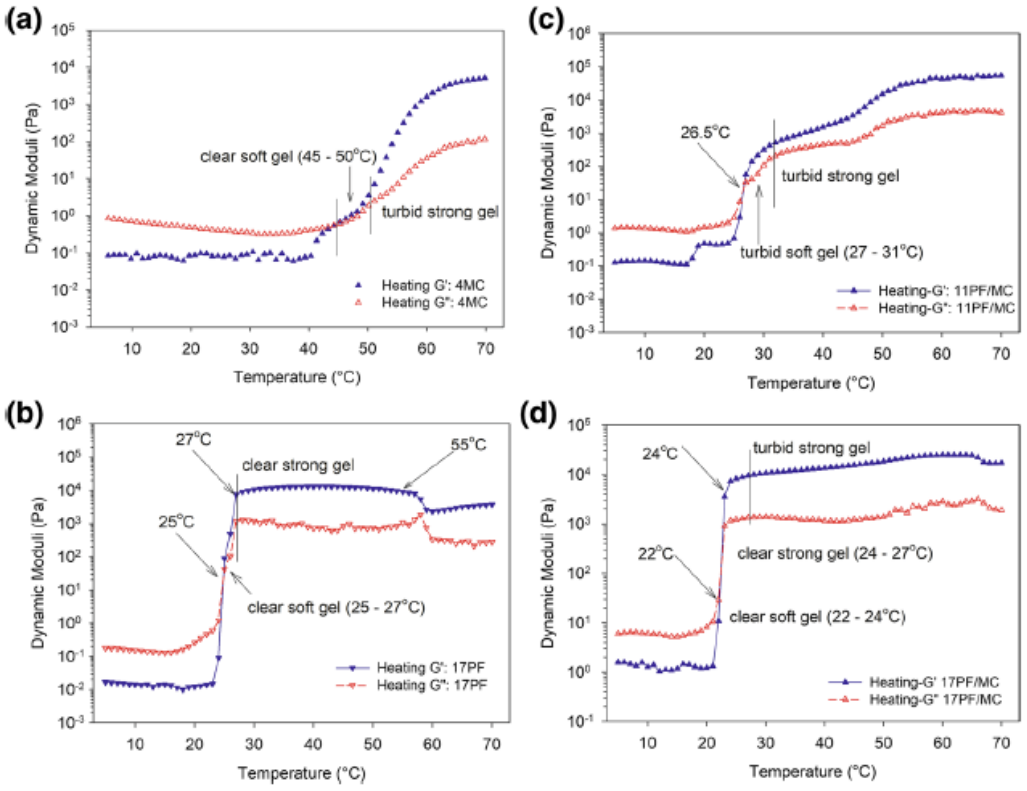

Fig. 1 Temperature dependence of dynamic moduli, G' (closed) and G'' (opened), during heating from 5 to 70 °C at the rate of 1 °C/min of **a** 4MC, **b** 17PF, **c** 11PF/MC and **d** 17PF/MC

known as a micelle. The formation of micelles strongly depends on temperature and concentration. PF underwent a transition from sol-to-gel with increasing temperature through three different stages: sol, soft gel and strong gel. In general, the transition from sol-to-soft gel occurred when micelle density reached a certain value and produced a sufficient ordered structure to trigger the characteristic rheological effect [6, 21, 22], or soft gel corresponded to a defective version of hard gel as previously described [23]. As previously explained, soft gel was identified between micellar liquid and hard gel (solid crystal phase). Soft gel was characterized by $G' > G''$ and both increased rapidly, and G' was relatively small compared to G'', but in sol, $G'' > G'$ and both were much smaller. For strong gel, $G' > G''$ and both G' and G'' are large and immobility of the solution in the TTM test.

For 11PF, the G' values were always lower than G'' values (Supplementary material Fig. A1), demonstrating that this low concentration could not form a gel at any temperature. This is consistent with previous reports that CGC (critical gelation concentration) of PF is about 16% w/w [4, 5]. For 17PF, at the beginning of heating, both G' and G'' were very small and $G'' > G'$ (Fig. 1b), and the system was in a sol state. The interaction of the PEO blocks on the micelle corona with water became less favorable upon heating. Further increasing temperature, both G' and G'' increase rapidly, and a crossover of G' and G'' appeared at 25 °C, and this crossover point was defined as the rheological gel temperature. Based on TTM, a clear soft gel was formed at about 26–27 °C. After about 27 °C, strong gel was detected by viscoelastic analysis (Fig. 1b) and also recognized by immobility in TTM. This is further discussed with the SAXS analysis.

In general, PF gel in aqueous solution is a clear gel [8]; in this study, soft and strong gels of 17PF were clear, but the PF solutions could become turbid to the eyes when blending with methylcellulose (11PF/MC and 17PF/MC). Although 11PF could not form gel, 11PF/MC solution turned to gel as shown in Fig. 1c. The crossover of G' and G'' was detected at 26.5 °C. After the crossover, $G' > G''$ was shown, based on TTM, a soft gel was detected between 27 and 31 °C. Further increasing the temperature, a strong gel was detected (immobility in TTM test). Both 11PF/MC soft and strong gels were turbid, and turbidity increased with increasing temperature.

The temperature dependence of dynamic modulus for 17PF and 17PF/MC systems was comparable as shown in Fig. 1b, c, respectively. Nevertheless, the effect of adding MC was to move the onset of gel formation to a lower temperature; gelation temperature was 22 °C for 17PF/MC but 25 °C for 17PF. At the crossover temperature (22 °C to about 24 °C), 17PF/MC developed a clear soft gel. Clear strong gel was detected from 24 to 27 °C, and over 27 °C the turbid strong gel was developed. Viscoelastic behaviors of 17PF, 11PF/MC and 17PF/MC in the presence of EDS were comparable to those corresponding systems without EDS as shown in Figs.A2, A3, A4 in Supplementary material. In addition, characteristics of 17PF/EDS, 11PF/MC/EDS and 17PF/MC/EDS are similar to those of the neat PF/MC blends when tested by TTM experiments. This indicated that EDS did not change the sol-to-gel transitions of PF and PF/MC systems.

SAXS analysis

In this study, the SAXS technique was used to determine the structural characteristic of PF, MC and their blends. As shown in Fig. 2, SAXS profiles of MC at 25 and 37 °C showed low scattering intensity. At these temperatures, MC was sol. The scattering intensity at low q range of MC increased when the temperature increased as revealed by the SAXS scattering at 40 °C in which MC sample turned out to be a clear soft gel. A very steep upturn of the SAXS curve at small q values was observed in the profiles of MC at the higher temperatures of 55 °C and 70 °C (Fig. 2 and Supplementary material Fig. A5). MC was a turbid strong gel at these two high temperatures. MC became gel at elevated temperatures due to intermolecular associations between the hydrophobic residues of the polymers that led to the formation of gel networks resulting in a significant increase in the scattering intensities at the low scattering angles as previously described [9, 24].

SAXS profiles of 11PF and 17PF at various temperatures are shown in Fig. 3a and 3b, respectively. According to the results obtained from TTM and rheological measurements, 17PF showed gel behavior at 25–70 °C, but 11PF did not form gel at any temperature. At the low concentration of 11PF, all scattering functions at 25, 37, 40, 55 and 70 °C indicated a disordered structure (Fig. 3a). In general, the dominated cubic lattice structure observed for PF gels is face-centered cubic (FCC) [25]. The gel structures with an FCC close packed structure have been reported as 18–40% PF in water [25–27]. As shown in Fig. 3b, SAXS profiles of 17PF at 25, 37, 40 and 55 °C were consistent with SAXS data previously reported for FCC structure [26, 27]. As mentioned above, at 25 °C, 17PF formed soft gel, and the low diffraction intensities might be interpreted as an existence of a defected FCC structure as previously described [22, 23, 28]. As shown in Fig. 1b, G' curve of 17PF dropped at about 55 °C, and SAXS profile showed a somewhat less ordered structure as compared to the SAXS profiles at 37 and 40 °C. At 70 °C, however, 17PF show a broad peak reflecting a disordered system. The change to a disordered system at this high temperature has been previously reported by Meznarich et al. [6]. Therefore, temperature plays an important role in the formation of ordered micelles and the stability of a gel structure.

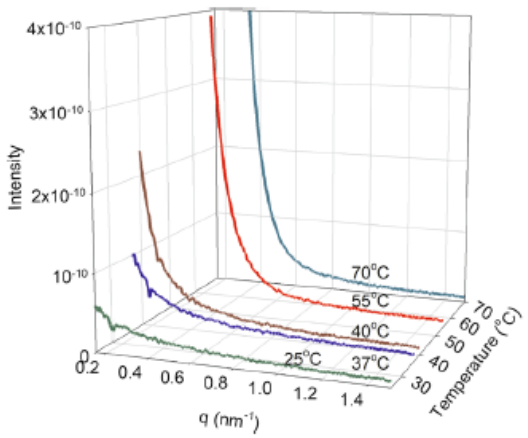

Fig. 2 Small-angle X-ray scattering curves of 4% w/w of methylcellulose at various temperature

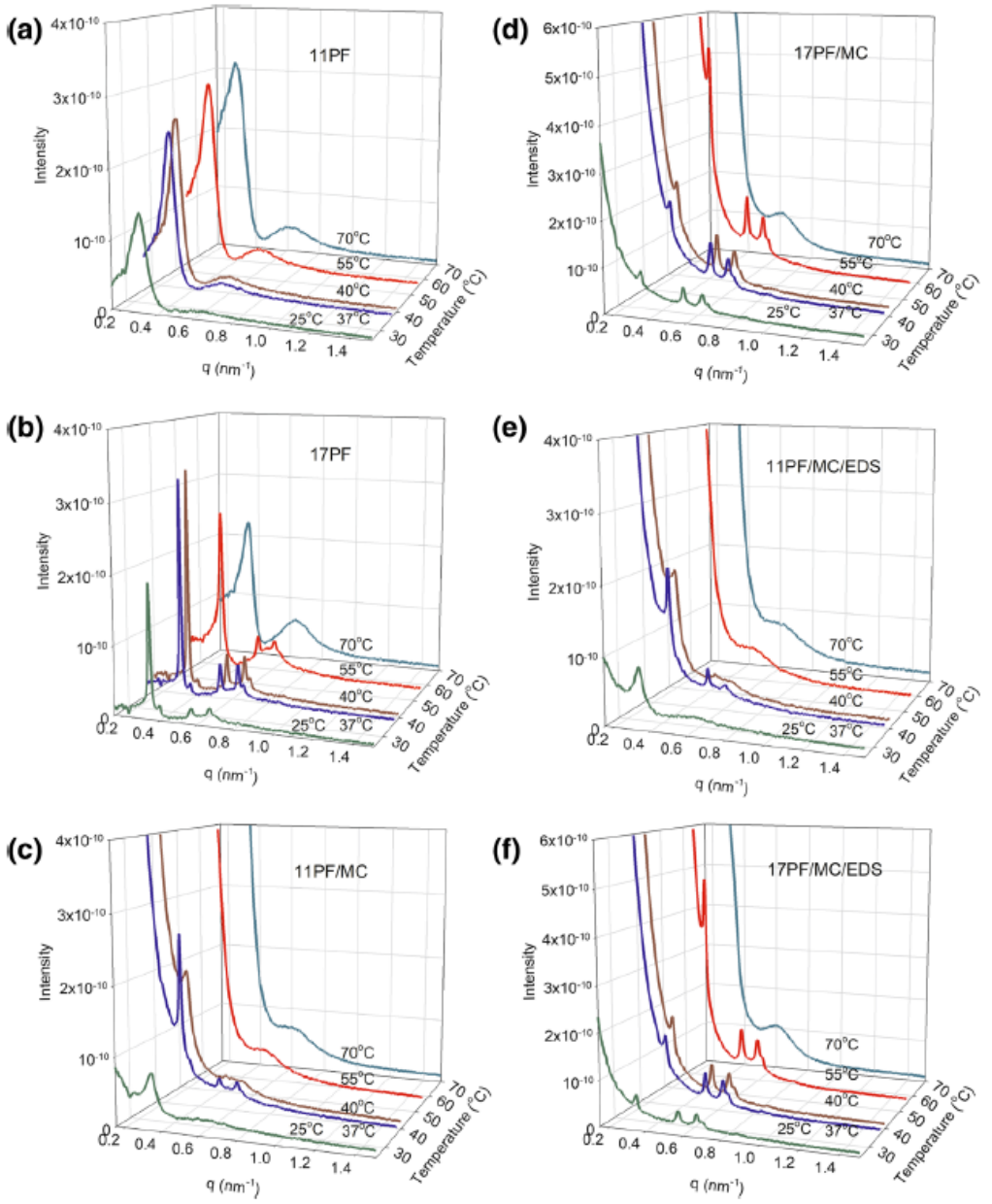

Fig. 3 Small-angle X-ray scattering curves of **a** 11PF, **b** 17PF, **c** 11PF/MC, **d** 17PF/MC, **e** 11PF/MC/EDS and **f** 17PF/MC/EDS at various temperatures

Although the scattering function revealed the order-to-disorder transition, 17PF gel did not transform to sol at this high temperature as revealed by TTM and rheological investigation (Fig. 1b). According to the rheological measurements, G' slightly decreased compared to the G' at 27–55 °C. This slight drop of G' indicated the lower gel strength compared to the lower-temperature gel. This transition to lower gel strength may be due to the decrease in solubility of PEO blocks at high temperature which caused a part of PEO to be merged into the core of micelles. Subsequently, the size of micellar cores was larger and the degree of

shell overlapping decreased, resulting in the decrease in entanglement density of PEO in the overlapped shell and decrease in gel strength as previously explained [20].

SAXS profiles of 11PF/MC at various temperatures are displayed in Fig. 3c. SAXS profile of 11PF/MC at 25 °C revealed a disordered structure, and the system was in a sol state ($G'' > G'$, Fig. 1c) at this temperature. Based on rheological measurement, G' was higher than G'' after 26.5 °C. A transition from the disordered state (sol state) at 25 °C to the FCC-ordered state occurred at the higher temperature of 37 °C. SAXS profiles showed a slightly less ordered structure at 40 °C and disordered structures at 55 and 70 °C. The samples were gels, although less ordered or disordered structures were developed at these high temperatures. The same observations have also been previously reported for the neat PF gels [21].

For 17PF/MC, SAXS profiles indicated FCC-ordered structures at 25, 37, 40 and 55 °C (Fig. 3d) since the sample was gel at 22 °C ($G' > G''$) during heating (Fig. 1d). The presence of MC lowered the gelation temperature compared to the neat 17PF. SAXS profile revealed a disordered structure at 70 °C, but that the sample still existed as gel.

As shown in Fig. 3e–f, SAXS profiles of 11PF/MC/EDS and 17PF/MC/EDS were similar to those of the corresponding PF/MC blends without EDS (Fig. 3c, d). This demonstrated that EDS did not cause the change of order structures and gel behaviors of 11PF/MC and 17PF/MC.

Figure 4 summarizes SAXS profiles of samples at room (25 °C) and body (37 °C) temperatures. At 25 °C, SAXS profiles of 11PF, MC, 11PF/MC and 11PF/MC/EDS indicated disordered structures and these samples were in sol state based on TTM and rheological data. However, 17PF, 17PF/MC and 17PF/MC/EDS exhibited ordered structures, and all were in gel state. At body temperature, all samples except MC presented as ordered structures and these samples were in gel state. Therefore, 11PF/MC could be used for in situ gelling preparation. The material could be injected as a sol at room temperature and become gel at body temperature and possibly sustained release the required drug at site of injection. In addition, the thermosensitive sol–gel transition of PF/MC blends did not change when adding a drug such as EDS.

In the presence of MC, the decrease of sol-to-gel temperature of 17PF and the ability to form gel of 11PF were probably caused by increasing the interaction between PF and MC, and/or from decreasing the intermolecular hydrogen bond between PF and water as well as between MC and water molecules, causing the decrease in water activity or "salt-out like" effect as previously described [5, 20, 29]. When the temperature is below its CMT, PF chains exist as unimer. Upon heating, dehydration of the PPO blocks occurred, and micellization started (Fig. 5). Due to low micellar density of the low concentration of 11PF, the dispersed micelles were unable to be packed into an ordered structure, so 11PF solution was in a liquid state. Nevertheless, when adding MC into 11PF solution, the dehydrated MC chains may be able to act as bridges to connect PF micelles to form a gel network (Fig. 5) as previously described for Pluronic-R 25R4-assisted gelation of PF [20]. An MC-assisted interconnected network of micelles also created turbidity to the system. For higher concentration of 17PF, the dispersed micelles may be able to form a closely

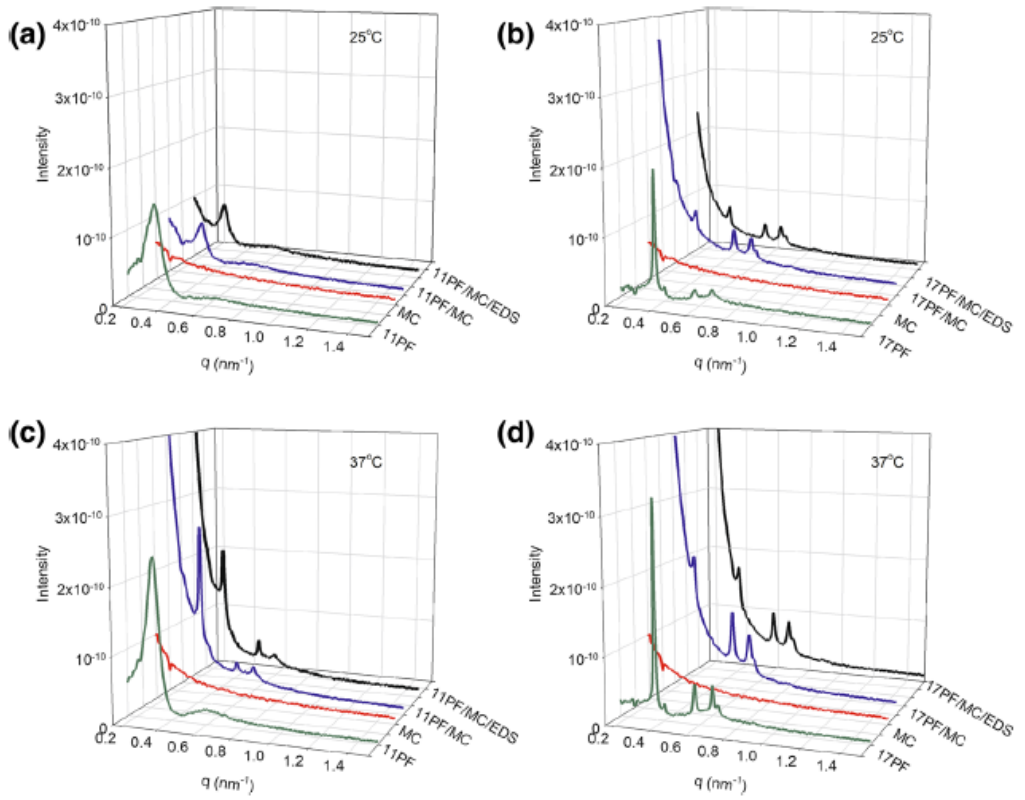

Fig. 4 Small-angle X-ray scattering curves of 11PF, MC, 11PF/MC and 11PF/MC/EDS at **a** 25 °C and **c** 37 °C; and 17PF, MC, 17PF/MC and 17PF/MC/EDS at **b** 25 °C and **d** 37 °C

packed crystalline lattice or an ordered structure by themselves and trigger the sol-to-gel transition. However, the dispersed micelles of 17PF/MC could form a closely packed crystalline lattice, which corresponded to the sol-to-gel transition, at temperatures lower than the neat 17PF probably due to the "salt-out like" effect from MC. At the 22–27 °C temperature range, the system formed clear gels. Over 27 °C, MC chains could connect PF micelles and a turbid gel was formed. Furthermore, SAXS profiles of the neat PF (Fig. 3b) were different from that of PF/MC blends (Fig. 3c, d); in the presence of MC, the steep upturns of the SAXS curves at small q values was observed at high temperatures of 55 and 70 °C (Supplementary material Figs. A6, A7, A8 and A9) which was similar to that of the neat MC (Supplementary material Fig. A5). Therefore, gelling process in the presence of MC at high temperatures might involve the gelation of the MC-assisted network connection of PF and also the gel network of MC.

Conclusion

PF gel formation on heating was modulated by mixing this block copolymer with MC. Although 11PF still existed as sol at all temperature ranges (15–70 °C), 11PF/MC exhibited viscoelastic sol–gel transition upon heating and it remained

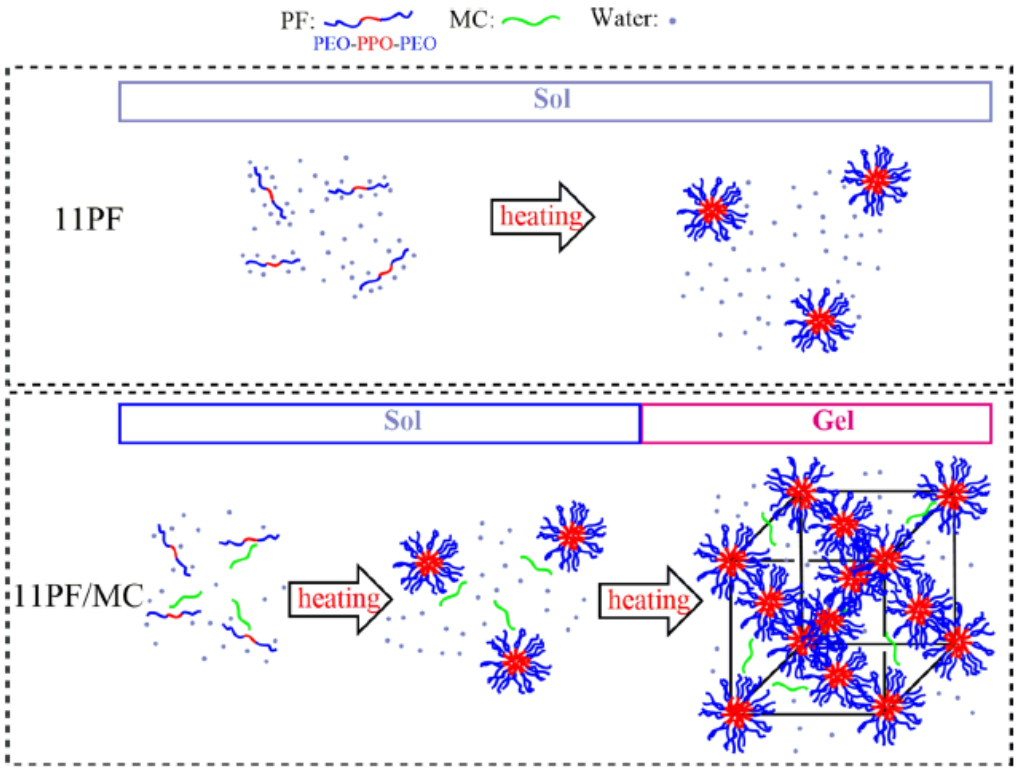

Fig. 5 Schematic diagrams for the microstructure formation in aqueous solution of 11PF and 11PF/MC upon heating

as sol at room temperature (25 °C). Over 27 °C, the turbid soft gel of 11PF/MC was detected up to around 31 °C. At higher temperatures, 11PF/MC became turbid strong gel. For 17PF/MC, the presence of MC lowered the gelation temperature. At 22 °C, the clear soft gel was observed. Above 27 °C, the gel became cloudy. At the intermediate temperatures above the gelation temperature, the FCC packing of the micelles was dominant. The MC-assisted interconnected network of PF micelles might trigger the sol–gel transition. Although the less ordered structure of intermicellar organization was observed at high temperatures, the blends still exhibited gel-like characteristics. In addition, the steep upturn of the scattering curves appeared in the small q range. The MC network might dominate the gel of the blends at high temperature. The presence of the model drug, EDS, did not alter the thermosensitive gelation and the phase behavior of the blends. In addition, this study indicates that blending PF with MC is a potential strategy for modulating the thermosensitive characteristics of the in situ gel forming matrices.

Acknowledgements This work was supported by the Thailand Science Research and Innovation (TSRI) Grant No. RSA6280027.

References

1. Dimatteo R, Darling NJ, Segura T (2018) In situ forming injectable hydrogels for drug delivery and wound repair. Adv Drug Deliv Rev 127:167–184
2. Jeong B, Kim SW, Bae YH (2012) Thermosensitive sol–gel reversible hydrogels. Adv Drug Deliv Rev 64:154–162
3. Escobar-Chávez JJ, López-Cervantes M, Naïk A, Kalia YN, Quintanar-Guerrero D, Ganem-Quintanar A (2006) Applications of thermo-reversible pluronic F-127 gels in pharmaceutical formulations. J Pharm Pharm Sci 9:339–358
4. Sun K, Raghavan SR (2010) Thermogelling aqueous fluids containing low concentrations of pluronic F127 and laponite nanoparticles. Langmuir 26:8015–8020
5. Rangabhatla ASL, Tantishaiyakul V, Oungbho K, Boonrat O (2016) Fabrication of pluronic and methylcellulose for etidronate delivery and their application for osteogenesis. Int J Pharm 499:110–118
6. Meznarich NAK, Juggernauth KA, Batzli KM, Love BJ (2011) Structural changes in PEO-PPO-PEO gels induced by methylparaben and dexamethasone observed using time-resolved SAXS. Macromolecules 44:7792–7798
7. Nascimento MHM, Franco MKKD, Yokaichyia F, de Paula E, Lombello CB, de Araujo DR (2018) Hyaluronic acid in Pluronic F-127/F-108 hydrogels for postoperative pain in arthroplasties: influence on physico-chemical properties and structural requirements for sustained drug-release. Int J Biol Macromol 111:1245–1254
8. Ricardo NM, Ricardo NM, Costa Fde M, Bezerra FW, Chaibundit C, Hermida-Merino D et al (2012) Effect of water-soluble polymers, polyethylene glycol and poly(vinylpyrrolidone), on the gelation of aqueous micellar solutions of Pluronic copolymer F127. J Colloid Interface Sci 368:336–341
9. Tomšič M, Prossnigg F, Glatter O (2008) A thermoreversible double gel: Characterization of a methylcellulose and κ-carrageenan mixed system in water by SAXS, DSC and rheology. J Colloid Interface Sci 322:41–50
10. Li L, Thangamathesvaran PM, Yue CY, Tam KC, Hu X, Lam YC (2001) Gel network structure of methylcellulose in water. Langmuir 17:8062–8068
11. Wu C, Liu T, Chu B (1998) A new separation medium for DNA capillary electrophoresis: self-assembly behavior of Pluronic polyol E99P69E99 in 1X TBE buffer. J Non-Cryst Solids 235–237:605–611
12. Zhang M, Djabourov M, Bourgaux C, Bouchemal K (2013) Nanostructured fluids from pluronic® mixtures. Int J Pharm 454:599–610
13. Itoh K, Hatakeyama T, Kimura T, Shimoyama T, Miyazaki S, D'Emanuele A et al (2010) Effect of D-sorbitol on the thermal gelation of methylcellulose formulations for drug delivery. Chem Pharm Bull 58:247–249
14. Sangfai T, Tantishaiyakul V, Hirun N, Li L (2017) Microphase separation and gelation of methylcellulose in the presence of gallic acid and nacl as an in situ gel-forming drug delivery system. AAPS PharmSciTech 18:605–616
15. Hirun N, Tantishaiyakul V, Sangfai T, Ouiyangkul P, Li L (2019) In situ mucoadhesive hydrogel based on methylcellulose/xyloglucan for periodontitis. J Sol-Gel Sci Technol 89:531–542
16. Behera B, Patil V, Sagiri SS, Pal K, Ray SS (2012) Span-60-based organogels as probable matrices for transdermal/topical delivery systems. J Appl Polym Sci 125:852–863
17. Kwon KW, Park MJ, Hwang J, Char K (2001) Effects of alcohol addition on gelation in aqueous solution of poly(ethylene oxide)-poly(propylene oxide)-poly(ethylene oxide) triblock copolymer. Polym J 33:404–410
18. de Oliveira AC, Vilsinski BH, Bonafe EG, Monteiro JP, Kipper MJ, Martins AF (2019) Chitosan content modulates durability and structural homogeneity of chitosan-gellan gum assemblies. Int J Biol Macromol 128:114–123
19. Nasatto PL, Pignon F, Silveira JLM, Duarte MER, Noseda MD, Rinaudo M (2015) Methylcellulose, a cellulose derivative with original physical properties and extended applications. Polymers 7:777–803
20. Liu SJ, Li L (2015) Molecular interactions between PEO-PPO-PEO and PPO-PEO-PPO triblock copolymers in aqueous solution. Colloid Surface A 484:485–497

21. Chaibundit C, Ricardo N, Ricardo N, Muryn CA, Madec MB, Yeates SG et al (2010) Effect of ethanol on the gelation of aqueous solutions of Pluronic F127. J Colloid Interface Sci 351:190–196
22. Castelletto V, Caillet C, Fundin J, Hamley IW, Yang Z, Kelarakis A (2002) The liquid–solid transition in a micellar solution of a diblock copolymer in water. J Chem Phys 116:10947–10958
23. Hamley IW, Pople JA, Fairclough JPA, Terrill NJ, Ryan AJ, Booth C et al (1998) Effect of shear on cubic phases in gels of a diblock copolymer. J Chem Phys 108:6929–6936
24. Tomsic M, Guillot S, Sagalowicz L, Leser ME, Glatter O (2009) Internally self-assembled thermoreversible gelling emulsions: ISAsomes in methylcellulose, K-carrageenan, and mixed hydrogels. Langmuir 25:9525–9534
25. Mortensen K, Batsberg W, Hvidt S (2008) Effects of PEO-PPO diblock impurities on the cubic structure of aqueous PEO-PPO-PEO pluronics micelles: fcc and bcc ordered structures in F127. Macromolecules 41:1720–1727
26. Wu C, Liu T, Chu B (1997) Characterization of the PEO-PPO-PEO triblock copolymer and its application as a separation medium in capillary electrophoresis. Macromolecules 4574–4583:4574–4583
27. Jiang J, Li C, Lombardi J, Colby RH, Rigas B, Rafailovich MH et al (2008) The effect of physiologically relevant additives on the rheological properties of concentrated Pluronic copolymer gels. Polymer 49:3561–3567
28. Efrat R, Aserin A, Kesselman E, Danino D, Wachtel EJ, Garti N (2007) Liquid micellar discontinuous cubic mesophase from ternary monoolein/ethanol/water mixtures. Colloids Surf, A 299:133–145
29. Pandit NK, Kisaka J (1996) Loss of gelation ability of Pluronic® F127 in the presence of some salts. Int J Pharm 145:129–136

Affiliations

Onpreeya Boonrat[1] · Vimon Tantishaiyakul[1,2] · Namon Hirun[3] · Supagorn Rugmai[4] · Siriwat Soontaranon[4]

1 Department of Pharmaceutical Chemistry, Faculty of Pharmaceutical Sciences, Prince of Songkla University, Hat-Yai 90112, Thailand

2 Center of Excellence for Drug Delivery System, Prince of Songkla University, Hat-Yai 90112, Thailand

3 Division of Pharmaceutical Sciences, Faculty of Pharmacy, Thammasat University, Pathumthani 12120, Thailand

4 Synchrotron Light Research Institute (Public Organization), Nakhon-Ratchasima 30000, Thailand

Paper 2

Boonrat, O., Tantishaiyakul, V., and Hirun, N. 2022. Micellization and gelation characteristics of different blends of pluronic F127/methylcellulose and their use as mucoadhesive in situ gel for periodontitis. Polymer Bulletin (79): 4515-4534. https://doi.org/10.1007/s00289-021-03722-w.

Polymer Bulletin (2022) 79:4515–4534
https://doi.org/10.1007/s00289-021-03722-w

ORIGINAL PAPER

Micellization and gelation characteristics of different blends of pluronic F127/methylcellulose and their use as mucoadhesive in situ gel for periodontitis

Onpreeya Boonrat[1] · Vimon Tantishaiyakul[1,2] · Namon Hirun[3]

Received: 25 February 2021 / Revised: 25 February 2021 / Accepted: 8 May 2021 /
Published online: 19 May 2021

Abstract

Micellization and gelation phenomena of thermosensitive hydrogels based on various concentrations of Pluronic F127 (PF) and 4% w/w methylcellulose (MC) were investigated by test tube inversion, turbidity, differential scanning calorimetry and rheological analyses. Dehydration of hydrophilic moieties of PF in the presence of MC was demonstrated by the clouding phenomenon. The involvement of MC on self-assembly and micelle formation of PF lowered the critical micelle temperature and enthalpy of micellization. The sol-to-gel temperature of the PF/MC blends decreased with increase PF concentrations. Neat samples of 12 or 14% w/w PF (12PF or 14PF, respectively) did not form gel, but their mixtures with MC (12PF/MC and 14PF/MC) were in sol form at ambient temperature (24 °C) and underwent gelation in situ at body temperature (37 °C). Both PF/MC blends were suitable as injectable implant matrices and their mucoadhesive properties were increased compared to pure PF. Doxycycline hyclate (DX), a model antibacterial drug for periodontitis, was incorporated into the 12PF/MC and 14PF/MC. The mixtures demonstrated the same antibacterial activity as the blend-free DX solution. This revealed that the hydrogel matrices did not impair the antibacterial activity of DX. Furthermore, the incorporation of DX into 12PF/MC and 14PF/MC hydrogels enabled the slow release of DX. These findings indicated that the 12PF/MC and 14PF/MC mixtures hold promise as efficient drug delivery systems for periodontitis.

✉ Vimon Tantishaiyakul
vimon.t@psu.ac.th

1 Department of Pharmaceutical Chemistry, Faculty of Pharmaceutical Sciences, Prince of Songkla University, Hat-Yai 90112, Thailand

2 Center of Excellence for Drug Delivery System, Faculty of Pharmaceutical Sciences, Prince of Songkla University, Hat-Yai 90112, Thailand

3 Thammasat University Research Unit in Smart Materials and Innovative Technology for Pharmaceutical Applications (SMIT-Pharm), Faculty of Pharmacy, Thammasat University, Pathumthani 12120, Thailand

Keywords Pluronic F127 · Methylcellulose · Mucoadhesive · Hydrogel

Introduction

Pluronic F127 (PF) is a triblock copolymer consisting of poly(ethylene oxide)–poly(propylene oxide)–poly(ethylene oxide) [1]. PF exhibits thermoreversible gelation based on micellization above the critical micelle temperature (CMT) or the critical micelle concentration (CMC) in water [2]. When CMT or CMC is reached, the micelle structure consisting of a PPO core and PEO corona is formed. Methylcellulose is derived from cellulose and commonly used as a drug excipient. Methylcellulose exhibits thermoreversible gelation upon heating. The gelation temperature of methylcellulose can be altered with the addition of various materials [3–5]. Recently, we prepared and investigated blends of 12, 14, 16, 18 and 20% w/w pluronic F127 (referred to as 12PF, 14PF, 16PF, 18PF and 20PF, respectively) and 4% w/w methylcellulose (MC) for injectable implant drug delivery systems [6]. In addition, 4 mM etidronate sodium (EDS) was loaded into the blends for generating an osteogenesis effect. The PF/MC blends which are thermoreversible demonstrated significant improvement in their properties compared to PF alone. With the addition of MC, blends with PF concentrations as low as 12% w/w (12PF) could form gel, whereas the lowest gel-forming concentration of PF without MC was 15% w/w [2]. These PF/MC gels or PF/MC/EDS gels were cytocompatible to osteoblast and myoblast cell lines, while PF alone at concentrations of 16, 18 and 20% w/w was very cytotoxic.

The gelation of PF as well as PF in the presence of small molecules and polymers have been extensively studied [2, 6–9]. Recent reports revealed that the nanostructure of PF and PF in the presence of 4% methylcellulose (MC) existed as a face-centered cubic phase at intermediate temperature above the gelation temperature [10]. The aim of this work is to investigate the formation of micelles by various concentrations of PF and PF/MC using differential scanning calorimetry (DSC). Viscoelastic moduli as a function of temperature which may be associated with micelle formation were also determined. Furthermore, turbidity/clouding upon heating of PF and PF/MC was examined using ultraviolet spectrometry. The turbidity determination is expected to reveal the phase transition of the samples. Macroscopic observation of sol (liquid) to gel was also examined using tube inversion method (TTM). Doxycycline hyclate (DX), a model drug for the treatment of periodontitis, was incorporated into the suitable PF/MC blends, i.e., blends that exhibited a sol-to-gel transition at appropriate temperatures (ease of injection at ambient temperature and gelation at the site of administration at body temperature). Furthermore, the antimicrobial activities of these samples were evaluated. Finally, the mucoadhesive properties and release characteristics of the selected PF and PF/MC blends were determined.

Experimental

Materials

Pluronic F127 (PEO_{99}-PPO_{65}-PEO_{99}), methylcellulose (methoxy content 27.5–31.5%, viscosity 10–25 mPa.S for a 2% solution in H_2O at 20 °C) and doxycycline hyclate (DX) were purchased from Sigma-Aldrich (St. Louis, MO, USA). All other chemicals and reagents used were of analytical grade.

Sample preparation

The PF solutions were prepared at various concentrations (12, 14, 16, 18 and 20% w/w) using a cold method as previously described [6]. Briefly, required amount of PF was dissolved in Milli-Q water at 4 °C and refrigerated overnight to ensure that PF was completely dissolved to obtain 12, 14, 16, 18 and 20% w/w. Methylcellulose powder was dispersed in hot water with vigorous stirring. After the powder was completely dispersed, the solution was adjusted with water to produce 4% w/w of methylcellulose (MC) and then cooled in an ice bath until a transparent solution was obtained. Subsequently, PF was dispersed into the methylcellulose solution to obtain 12, 14, 16, 18 and 20% w/w of PF in MC (4% w/w) and these blends were referred to as 12PF/MC, 14PF/MC, 16PF/MC, 18PF/MC and 20PF/MC, respectively. The resultant combinations were mixed thoroughly and refrigerated until the blends were completely dissolved.

The model drug, DX, was incorporated into the selected hydrogels, 12PF/MC and 14PF/MC. Briefly, DX powder was dispersed into the homogenous PF/MC blends with vigorous stirring on ice bath to obtain 0.25 and 0.5% w/w of DX in the 12PF/MC and 14PF/MC blends. These were referred to as 12PF/MC/0.25DX, 12PF/MC/0.5DX, 14PF/MC/0.25DX and 14PF/MC/0.5DX, respectively. All the blends were further stirred and then cooled until clear yellowish solutions were observed. The blends were stored in the refrigerator prior to further analyses.

For mucoadhesive investigation, appropriate amount of mucin powder was dispersed in Milli-Q water or the PF/MC solutions to obtain 10% w/w of mucin in water, 12PF/MC or 14PF/MC. All samples were kept in the refrigerator at 4 °C. These samples were evaluated within 2 days of preparation.

Test tube inversion analysis

Test tube inversion method (TTM) was performed by visual observation as previously described [11, 12], with some modifications. The samples were heated from 16 to 70 °C in a temperature-controlled water bath at increments of 1 °C. The samples were allowed to equilibrate for 20 min after each increment. Any phase transition was evaluated by inverting the tube. The temperature at which the samples became solid but somewhat flowed at the surface after tilting the tube was recorded

as gelation temperature of a soft gel. Upon further heating, the temperature at which samples did not flow was recorded as transition temperature of a hard or strong gel [10].

UV–Visible spectrophotometric analysis

The turbidity measurement was conducted using a Cary 300 UV–Vis spectrometer with a temperature controller from Agilent Technologies (Santa Clara, CA, USA). A cold solution of the sample was placed in a cuvette and covered with a plastic cap. Deionized water was used as a reference. The absorbance was measured at 500 nm [13] in the course of heating from 20 to 70 °C at the same scanning rate as DSC and rheological measurements of 1 °C/min.

Differential scanning calorimetry analyses

Calorimetric experiments were performed using DSC 6000 (Perkin-Elmer, USA). Samples were accurately weighed and sealed in aluminum hermetic liquid pans. An empty pan was employed as reference. Samples were heated from 5 to 70 °C at a rate of 1 °C/min under nitrogen atmosphere. The DSC data were analyzed using Pyris software (Perkin-Elmer, USA). Heat of micellization (ΔH, enthalpy change) of the samples was calculated from the area by integrating the endothermic peak as previously described [7].

Rheological determination

Viscoelastic properties and viscosity of the samples were investigated using a Modular Advanced Rheometer System (HAAKE MARS 60, ThermoFisher Scientific, Germany) with a Peltier temperature controller equipped with a water circulator. Parallel plate geometry (35 mm diameter and a 1 mm gap) was used. To avoid dehydration of the samples, solvent trap and the sample hood were employed, and the sample periphery was covered with a thin layer of low viscosity silicone oil. The oscillatory temperature sweep tests were performed by heating from 5 to 70 °C at a rate of 1 °C/min under an oscillation frequency of 1 Hz. All experiments were carried out within linear viscoelastic regime. The temperature dependence of viscosity was evaluated over the range of 5 to 70 °C. The viscosity was determined at a shear rate of 10 s^{-1} upon heating from 5 to 70 °C at a rate of 1 °C/min.

Mucoadhesive analysis

Mucoadhesive property was measured by testing the adhesion strength in terms of elastic moduli using Discovery Hybrid Rheometer (DHR-2, TA Instruments, USA). A parallel plate sensor with 40 mm in diameter was used for the high viscosity samples, and a cone-plate sensor with 60 mm in diameter with cone angle of 2° was used for the low viscosity fluids. The sample temperature was maintained at 37 °C by using a Peltier temperature-control system. The linear viscoelastic region (LVR) for

each sample was determined through amplitude sweeps at the frequency of 0.1 and 10 Hz. The frequency sweeps were performed in the range of 0.1 to 10 Hz within LVR. The values of the elastic modulus were used to calculate the rheological synergy ($\Delta G'$). The $\Delta G'$ value for the single polymer and the blend was determined using Eqs. (1) and (2), respectively. The $\Delta G'$ value of each sample was normalized with respect to the G' value of the sample, either the mucin and single polymer or the blend to obtain the relative rheological synergism ($\Delta G'_{\text{relative}}$) value (Eqs. (3) and (4)) [14–16].

$$\Delta G'_{\text{Polymer/Mucin}} = G'_{\text{Polymer/Mucin}} - (G'_{\text{Polymer}} + G'_{\text{Mucin}}) \tag{1}$$

$$\Delta G'_{\text{Blend/Mucin}} = G'_{\text{Blend/Mucin}} - (G'_{\text{Blend}} + G'_{\text{Mucin}}) \tag{2}$$

$$\Delta G'_{\text{relative: Polymer/Mucin}} = \frac{\Delta G'_{\text{Polymer/Mucin}}}{G'_{\text{Polymer}} + G'_{\text{Mucin}}} \tag{3}$$

$$\Delta G'_{\text{relative: Blend/Mucin}} = \frac{\Delta G'_{\text{Blend/Mucin}}}{G'_{\text{Blend}} + G'_{\text{Mucin}}} \tag{4}$$

where G'_{Blend}, G'_{Polymer} and G'_{Mucin} represent the elastic moduli at 1 Hz for the blends (12PF/MC and 14PF/MC), the single polymer (4MC, 12PF or 14 PF) and 10% (w/w) mucin dispersion, respectively. The $G'_{\text{Blend/Mucin}}$ represents the elastic moduli for the mixture of the blend and mucin, while $G'_{\text{Polymer/Mucin}}$ represents the elastic moduli for the mixture of single polymer and mucin.

Antimicrobial activity analysis

Periodontal pathogenic bacteria used in this study were obtained from ATCC (American Type Culture Collection, Manassas, VA). These bacterial cells were cultured according to the recommended protocol described in the ATCC data sheet. *Porphyromonas gingivalis* (*P. gingivalis*; ATCC® 53,978™) and *Prevotella intermedia* (*P. intermedia*; ATCC® 25,611™) were cultured in supplemented Tryptic Soy Broth (ATCC® medium 2722), while *Aggregatibacter actinomycetemcomitans* (*A. actinomycetemcomitans*; ATCC® 43,718™) were cultured in Brain Heart Infusion Broth (ATCC® medium 44). The agar medium for *A. actinomycetemcomitans* was prepared by adding 5.2 g of Brain Heart Infusion Agar (BD 211,065) into 100 mL of Milli-Q water. To prepare the agar medium for culturing *P. gingivalis* and *P. intermedia*, 1.5 g of the agar was added into a premixed component comprised of 3.0 g of Tryptic Soy Broth, 0.5 g of yeast extract, 0.05 g of L-cysteine hydrochloride, 0.1 mL of hermin stock, 0.02 mL of vitamin K1 stock and 100 mL of water. Each culture medium was autoclaved before use. All bacterial cultures were incubated under anaerobic conditions at 37 °C.

Antimicrobial activities of 12PF/MC and 14PF/MC with and without DX were determined using agar well diffusion method as previously described with minor modifications [17]. The antimicrobial activities were evaluated from the average diameter of the zone of inhibition ($n = 3$). Briefly, 25 mL of the agar medium was poured into each plate and allowed to solidify. The bacterial cells were inoculated by streaking bacterial suspension on agar. Subsequently, small circular cavities were punctured in the agar medium and filled with 80 µl of each sample. The agar cultures of *A. actinomycetemcomitans* and *P. intermedia* were stored in anaerobic jar at 37 °C for 2–3 days [18, 19]. For *P. gingivalis* cultures, the plates were incubated in anaerobic jar at 37 °C for 5–7 days [20]. The diameter of the zone of inhibition was determined and reported in millimeter (mm). The hydrogel without DX served as negative control, while aqueous solution containing DX at equivalent concentration served as positive control.

Scanning electron microscope

The liquid samples of 12PF/MC and 14PF/MC were placed into a 24-well plate (2 ml/well) and equilibrated at 37 °C for 30 min to form gel. Next, the samples were immersed in liquid nitrogen, and the frozen gels were lyophilized. The lyophilized samples were cut and subsequently coated with gold. The morphology of the cross-sectional samples was investigated by SEM-Quanta 400 (FEI™, Oregon, USA) at 20.0 kV.

Drug release study

In vitro release of DX from PF/MC hydrogels was investigated by dialysis method as previously described [3, 21, 22] with minor modifications. In brief, 1 g of sample in liquid state was introduced into the dialysis bag (MWCO 12,000–14,000 kDa, CelluSep T4) and allowed to gel in an incubator at 37 °C. The dialysis bag was then incubated in 100 mL of 0.01 M phosphate buffer saline (PBS) pH 7.4, which had been prewarmed to 37 °C under continuous shaking at 100 rpm. At predetermined time intervals, 1 ml of release medium was collected and replaced by equal volume of prewarmed fresh PBS to maintain a constant volume. The concentration of DX in release medium was determined by HPLC (Hitachi CM-5000 HPLC System, Hitachi High-Technologies Corporation, Tokyo, Japan) with UV detection at 351 nm [23]. Symmetry® C_8, 5 µm, 4.6 × 250 mm (Water Corporation, Milford, Massachusetts, USA) column was used as the stationary phase, while a solution of 0.05 mM KH_2PO_4 (pH 3) and acetonitrile (55:45, v/v) was used as the mobile phase for the analysis. The flow rate was set at 1.0 mL/ min at 25 °C, and the injection volume was 10 µl. Each sample was filtered through a 0.45 µm membrane before injected. The experiment was carried out in triplicate.

Results and discussion

Pluronic F127, being amphiphilic, can self-assemble and aggregate into micelles, a core–corona structure above CMT or CMC in water. The micelle core comprises of hydrophobic PPO blocks, while the hydrophilic PEO blocks form the shell or corona of the micelle [24]. Increasing the temperature or concentration of the copolymer above the CMT or CMC increases micellization. The sol-to-gel transition is considered to result when the micelle density reaches a certain value, resulting in close packing of the micelles into an ordered structure with the PPO cores connected by PEO strands of the copolymer leading to gelation. In the presence of other polymers, the gelation behavior of PF may be modified, which promises to be beneficial for several applications including drug delivery.

Gelation and turbidimetric gelation

TTM was employed to estimate the gelation temperature and a qualitative assessment of the transition from a transparent or clear gel to a turbid gel. Neat 12PF and 14PF could not form gels since these concentrations were lower than the CMC; however, in the presence of 4% w/w methylcellulose, the blends (12PF/MC and 14PF/MC) formed gels. Based on TTM observations, 16PF, 18PF and 20PF formed clear soft gels at about 28, 24 and 20 °C, respectively. In addition, clear hard gels were developed when the solutions were heated at temperatures above 29, 27 and 21 °C, respectively, for 16PF, 18PF and 20PF. These results concur with what was previously findings by de Lima et al. [25], who noted that PF gels were transparent beyond 100 °C.

At body temperature of 37 °C, 16PF, 18PF and 20PF formed clear gels (Fig. 1S). In the presence of 4% w/w methylcellulose, after samples were equilibrated at 25 °C for 20 min, a clear gel was observed for 14PF/MC but not for 12PF/MC. The 16PF/MC, 18PF/MC and 20PF/MC blends produced slightly turbid (hazy) gels at 25 °C (Fig. 1S). All PF/MC blends including 12PF/MC could form gel at 37 °C. The gels turned turbid at the higher temperature, and all became even more turbid (cloudy) at 60 °C. According to these TTM results, the gels formed by neat PF were all clear. The turbid gels could only be formed when PF was blended with MC. Meanwhile, 4% w/w methylcellulose could not gel below 50 °C.

The appearance of turbidity or cloud point can be detected using various experimental techniques, including visual observation [26–28]. Since slight difference may not be detected by visual observation with the naked eye, UV–Vis spectroscopic method was used in this study to further verify the temperature dependence of turbidity.

As shown in Fig. 1, 4% w/w methylcellulose (MC) became turbid at about 50 °C. The transparent solutions of PF/MC gradually became turbid with the increasing temperature. The blends with low PF concentrations (12PF/MC and 14PF/MC) turned turbid at about 40 °C. The 16PF/MC, 18PF/MC and 20PF/MC blends were found turbid at about 30, 26 and 20 °C, respectively. These clouding temperatures

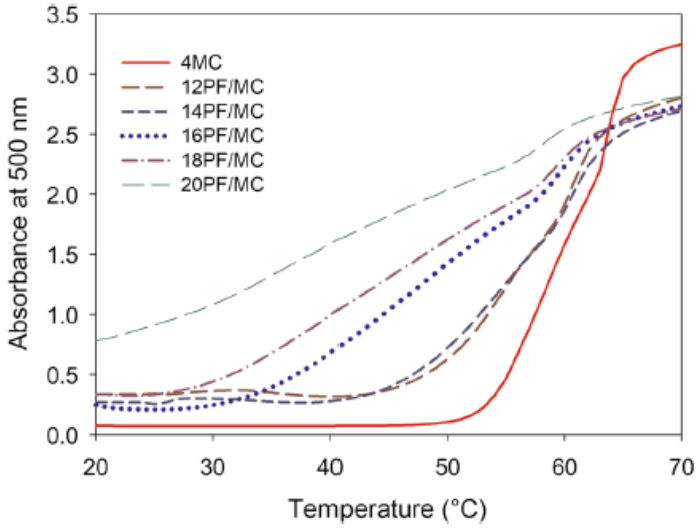

Fig. 1 UV–Vis absorbance (at 500 nm) versus temperature of 4% w/w methylcellulose (MC) and the mixtures of MC and various concentrations of PF during heating at a rate of 1 °C/min

of PF/MC co-solutions are lower than that of MC alone (Fig. 1). Therefore, the turbidity may be caused by the effect of MC on the PF system. Various additives that affect the turbidity of nonionic surfactant including PF has been previously investigated [25, 27, 29]. Typically, additives that increase hydrophobicity of the system decrease the cloud point, while additives that increase hydrophilicity may increase the temperature of clouding [29, 30]. For PF/MC co-solutions, the clouding phenomenon may be ascribed to the efficient dehydration of PEO moiety or hydrophilic moieties of the micelles by MC. These micelles attract or connect each other and form inter-micellar bridges or micellar cluster with the approach of the cloud point as previously described for the block copolymer [31, 32]. As shown in Fig. 1, clouding temperature of PF/MC decreased as the concentration of PF increased. This may result from the higher attractive interaction of micelles with high amounts of PF.

Micellization and gelation

DSC was employed to investigate CMT and heat of micellization (ΔH) of PF solutions and PF/MC co-solutions during heating. The endothermic peak is considered as an indicator for the existence of micellization, with the peak onset and offset temperatures corresponding to the start and end of the process. Increasing either temperature or concentration of PF increased micellization. Thermograms of various concentrations of PF, PF/MC and MC are shown in Fig. 2. The solutions of 12PF, 14PF, 16PF, 18PF and 20PF showed endothermic peaks that were consistent for micellization at 19.8, 17.8, 17.4, 15.9 and 15.0 °C, respectively, during heating (Fig. 2a) [33]. The endothermic peaks shifted to lower temperatures in the presence of MC (Fig. 2b): the endothermic peaks for 12PF/MC, 14PF/MC, 16PF/MC, 18PF/MC and 20PF/MC were detected at 17.2, 16.5, 15.3, 13.0 and 11.5 °C, respectively.

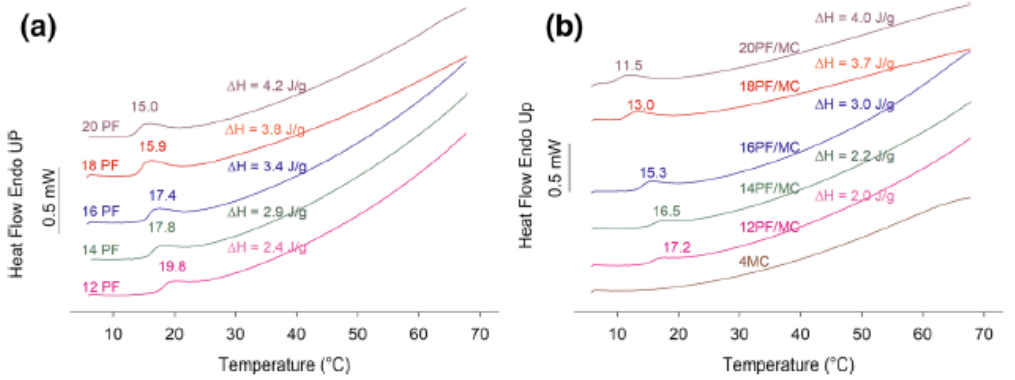

Fig. 2 DSC thermograms of **a** different concentrations of PF and **b** 4% w/w methylcellulose (MC) and the mixtures of MC and various concentrations of PF during heating at a rate of 1 °C/min

At this micellization temperature range, no peak was detected for MC solution since the gelation mechanism of MC does not involve micellization.

The endothermic peak is assigned to the dehydration of PPO blocks which consecutively lead to micelle formation. The area under the endothermic peak (ΔH) is proportional to the amount of formed micelle [34]. The enthalpy of micellization (ΔH) increased with the increase in PF concentrations (Figs. 2a and 3). These results are in accordance with previous findings which asserted that ΔH was proportional to the concentration of PF [34, 35]. However, ΔH of the mixtures of PF/MC was lower than that of the corresponding PF concentration without MC (Figs. 2b and 3). This can be regarded as an indication of the involvement of MC on self-assembly and micellization of PF. The decrease in ΔH is suggestive of a reduction in the energy consumed for PPO dehydration [7]. MC may enhance the dehydration of PPO and consequently lower the micellization temperature and ΔH of the PF/MC

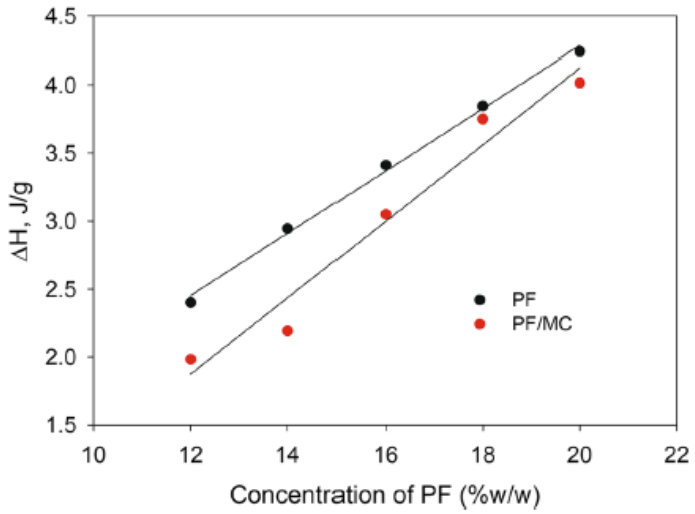

Fig. 3 Enthalpy of PF solution and the co-solution of 4% w/w methylcellulose (MC) and various concentrations of PF during heating ramps

blends, which is not the case for their pure PF counterparts. In general, the appearance of endothermic peak may indicate the formation of micelles but cannot predict whether the system will be able to form gel. For the neat PF, the sol-to-gel transition was considered to occur when the micelle density attained a definite value, resulting in close packing of the micelles into an ordered structure with the PPO cores connected by PEO strands of the copolymer [34]. When MC is present, its interaction with PF and the reduction of the intermolecular hydrogen bonding between the PEO moiety of PF and water may increase the connection between micelles. This may result in the sol-to-gel transition and gel formation of the system even at the low concentrations of PF (12PF and 14PF), which would typically not form gel.

Rheological analyses

The sol-to-gel transition of PF and PF/MC was further investigated by comparing their viscoelasticities as a function of temperature. Viscoelastic moduli, storage modulus (G') and loss modulus (G'') of the aqueous solutions of 12PF, 14PF, 16PF, 18PF and 20PF upon heating are shown in Fig. 4. When the temperature is below their CMT of 17.0 and 15.6 °C for 12PF and 14PF, respectively (Fig. 4a, Region 1), the polymer chains exist as unimers or individual micelles. A constant G' and a slight decrease in G'' with temperature were detected. The micellization started at CMT which is reflected by endothermic onset temperature, and then progressed to attain the endothermic peak temperature at 19.8 and 17.8 °C for 12PF and 14PF, respectively (Fig. 4a, Region 1). Unimers and micelles coexist at the temperature

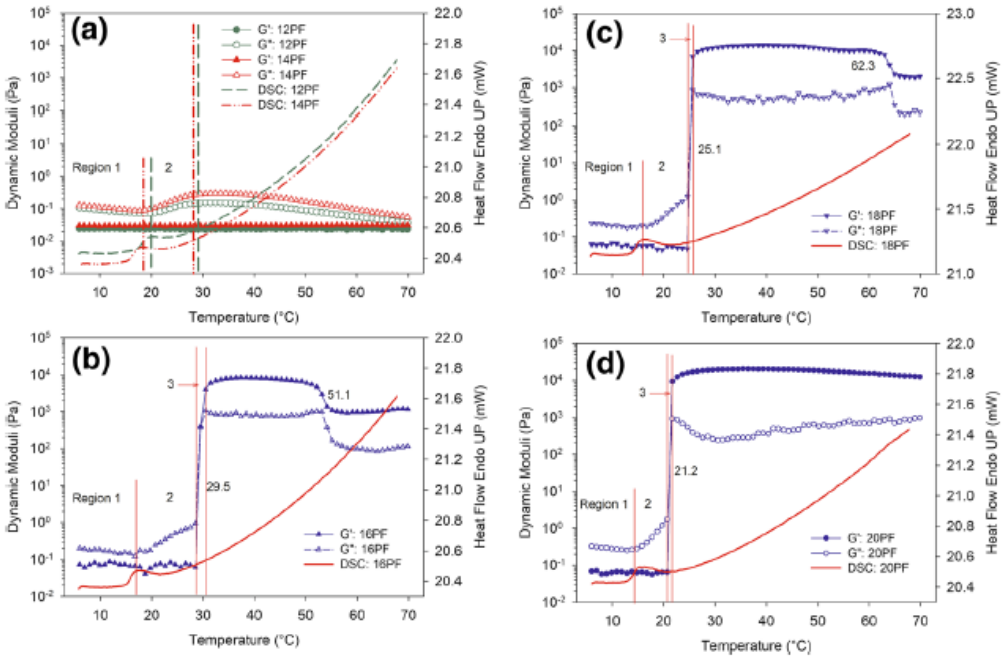

Fig. 4 Storage modulus G', loss modulus G'' and DSC thermograms as a function of temperature of **a** 12PF and 14PF, **b** 16PF, **c** 18PF and **d** 20PF. Samples were heated at a rate of 1 °C/min

range between the CMT and peak temperature as previously described [9]. At this temperature range, G'' curve decreased continuously due to the dehydration of unimers, and the solution is dominated by unimers. As shown in region 2 (Fig. 3a), more micelles are formed with further increase in temperature. G'' gradually increased, while G' remained constant. G'' was maximum close to the offset temperature indicating the end of micellization and all chains exist in micelles. Subsequently, G″ decreased with increase in temperature. For the aqueous solutions of 12PF and 14PF (Fig. 4a), G'' was higher than G' at all temperature range of this study (5–70 °C), indicating that 12PF and 14PF were in a liquid state. In addition, the occurrence of micelle formation was indicated by endothermic peaks from DSC determination in both solutions.

The effect of temperature on G' and G'' for the 16PF, 18PF and 20PF aqueous solutions in regions 1 and 2 (Fig. 4b–d) is the same as described for 12PF and 14PF. While G' remained constant, the gradual increase of G'' with increase in temperature may be caused by the molecular motions occurring in the systems from micelle formation [36] (Fig. 4b–d, region 2). These PF remained as liquid ($G'' > G'$). Subsequently, G' and G'' increased abruptly with crossover at 29.5, 25.1 and 21.2 °C, respectively, for 16PF, 18PF and 20PF (Fig. 4b–d). This sharp increase of both moduli (Fig. 4b–d, region 3) corresponds to the sol-to-gel transition as micelles start to contact each other to form an ordered structure and inter-micellar entanglements as previously described [9]. The end of this region is almost close to the offset temperature of the individual samples. The crossover point is generally considered as the gel point, and it decreased with increase in PF concentrations. After crossover point, G' was larger than G'' and both moduli reached their individual plateaus. Thus, these systems are in a solid-like state. After the sol-to-gel transition, the number of micelles is not changed by temperature and almost all of polymer chains already exist in the micelles. As the temperature increased to 51.1 and 62.3 °C, respectively, for 16PF and 18PF (Fig. 4b–c), the systems entered the second plateau phase. In this region, G' curves declined almost in parallel with G'' curves but are still larger than G'' which indicated that both systems are still elastic. The higher the concentration of PF, the higher the temperature that was needed to decrease the moduli. This decrease of moduli is not observed for 20PF when the system was heated up to 70 °C; therefore, a higher temperature may be required to detect this phenomenon. The decrease of moduli at this temperature was previously ascribed to part of PEO block merging with the cores of micelles. This enhances the size of micellar cores and decreases the corona overlapping amount leading to the reduction in entanglement density of PEO blocks in the overlapped corona and drop of modulus [9].

For 12PF/MC, 14PF/MC, 16PF/MC, 18PF/MC and 20PF/MC, both G' and G'' increased together before reaching the crossover points as shown in Fig. 5, region 2. It is of interest that, at this low temperature range of micelle formation (based on DSC measurements), increase of both G'' and G' was observed. For the neat PF (Fig. 4b-d, region 2) and other pluronic types [9, 33, 37], G' remained constant at this temperature range. The increase of both G' and G'' (Fig. 5, region 2) at this temperature range may be caused by the formation of the free PF micelles in coexistence with the PF micelles with attached MC as well as an increase in the number of micelles. This phenomenon was also observed in the mixture

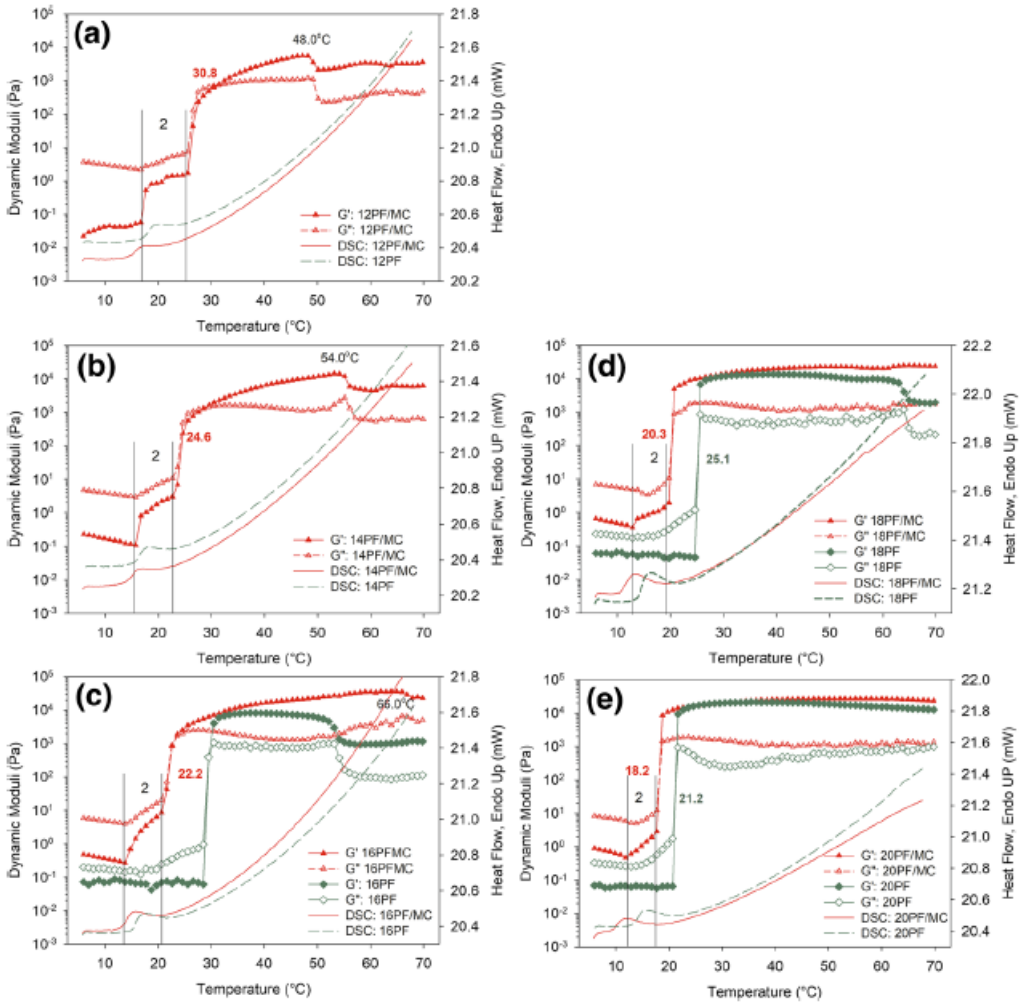

Fig. 5 Storage modulus G' (closed symbols), loss modulus G'' (open symbols) as a function of temperature as well as DSC thermograms: **a** 12PF and 12PF/MC, **b** 14PF and 14PF/MC, **c** 16PF and 16PF/MC, **d** 18PF and 18PF/MC and **e** 20PF and 20PF/MC. Samples were heated at a rate of 1 °C/min

systems of PF and poly(acrylic acid) [38]. MC can promote network formation or increase interface bonding during micelle formation as previously described [36, 39]. Nevertheless, the PF/MC systems at this temperature range exist as solutions as $G'' > G'$. However, all systems can turn to gel as G' is larger than G'' with increase in temperature. The sol-to-gel temperatures for 12PF/MC, 14PF/MC, 16PF/MC, 18PF/MC and 20PF/MC were observed at 30.8, 24.6, 22.2, 20.3 and 18.2 °C, respectively (Fig. 5). Thus, the sol-to-gel temperatures decreased as the concentration of PF in the blend increased. As the temperature increased to 48.0, 54.0 and 66.0 °C, respectively, for 12PF/MC, 14PF/MC and 16PF/MC, the moduli decreased and subsequently G' and G'' were almost parallel (Fig. 5a–c). The drop of moduli for the PF/MC appeared at higher temperatures compared to the PF alone (i.e., 51.1 °C for 16PF and 66.0 °C for 16PF/MC). The drop of G'

and G'' was not observed for 18PF/MC and 20PF/MC (Fig. 5d–e) since the temperature range of this study (5–70 °C) was not high enough for the detection.

Viscosity

The gelation behavior of PF and PF/MC was also examined by measuring viscosity as a function of temperature. The effect of temperature on the viscosity of the samples is shown in Fig. 6. The solution viscosity of all samples decreased slightly at low temperature (5–12 °C) due to shrinkage of coil size or dehydration of the unimers (the dominant species), especially PPO blocks as previously described [24, 40, 41]. Further increase in temperature resulted in micelle formation as the PPO blocks tended to be even more hydrophobic. The sharp increase in viscosity around the sol-to-gel transition temperature of PF was previously described as lower T_{gel} (LT_{gel}) by Li and Hyun [42] and was also observed in this study. When the temperature was further increased, the viscosity plateaued and then declined. The temperature at this point is referred to as the upper T_{gel} (UT_{gel}) [42]. In this study, the sol-to-gel transition was determined by the crossover point ($G'=G''$) which is relatively close to LT_{gel} for the neat PF solutions (Fig. S2). For the mixture of PF/MC, the LT_{gel} determined by viscosity was slightly lower than the sol-to-gel transition temperature where $G'=G''$ (Fig. S3). This may be due to the increase in viscosity of the solutions resulting from the influence of MC. However, as the concentration of PF in the blend increased, the LT_{gel} of PF/MC mixtures was closer to the crossover temperature of G' and G''.

The viscosity after UT_{gel} began to drop on further heating, reflecting the breaking down of networks and phase separation [42–44]. The temperatures between LT_{gel} and UT_{gel} yielded a hard gel state as previously described[42]. Li and Hyun [42] reported that when temperatures were lower than LT_{gel} and higher than UT_{gel}, the neat PF systems were in the sol state. In this study, when temperatures were higher than UT_{gel}, the PF and PF/MC systems were not in a sol state but transformed into weaker gels ($G'>G''$) (Figs S2 and S3). As shown in Fig. 6, LT_{gel} of PF and PF/MC decreased with increase in PF concentrations, and UT_{gel} increased with increase in

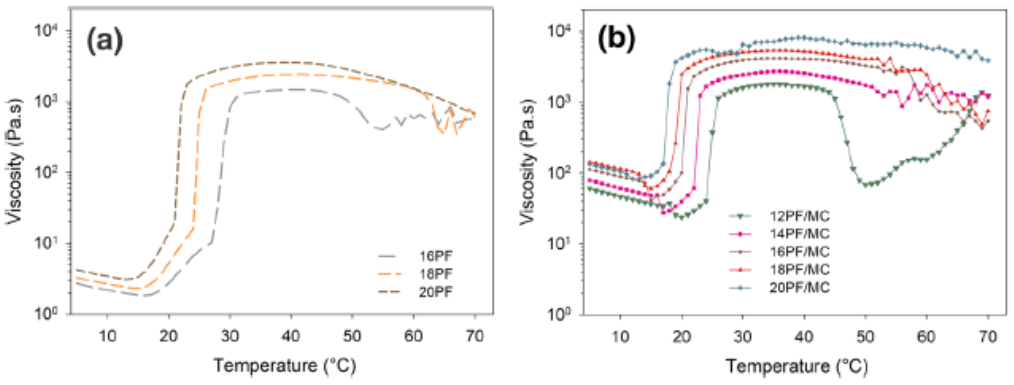

Fig. 6 Viscosity as a function of temperature upon heating at a rate of 1.0 °C/min of **a** 16PF, 18PF and 20PF and **b** the mixtures of 4%w/w of methylcellulose (MC) and various concentrations of PF

PF concentrations. The UT_{gel} of 20PF and 20PF/MC (high PF concentrations) was not observed because the temperature range of this study was not high enough to detect their UT_{gel}. The UTgel of 20PF was previously reported to be about 75 °C [42].

Viscosity of 4% w/w methylcellulose solution at low temperature was higher than that of 16PF, 18PF and 20PF solutions (Fig. S4). In addition, the viscosities of PF/MC co-solutions were much higher than those of their corresponding concentration of pure PF solutions (Fig. S4). Also, the viscosity of PF/MC gels was slightly higher than those of their corresponding concentration of pure PF. Furthermore, the sharp increase in the viscosity of PF/MC appeared at much lower temperature than that of the corresponding concentration of the pure PF (Fig. S4) and was consistent with the sol-to-gel transition temperatures from viscoelastic investigations in this study.

Mucoadhesive

Since 12PF/MC and 14PF/MC mixtures are sol near ambient temperature (about 24 °C), both mixtures were investigated as injectable implant matrices. Mucoadhesive behavior of both mixtures was investigated and compared to that of 12PF, 14PF and MC. The value of $\Delta G'_{relative}$ is considered to be an indicative parameter of the mucoadhesive strength of different polymeric platforms [14, 45]. The $\Delta G'_{relative}$ values of MC, 12PF, 14PF, 12PF/MC and 14PF/MC are shown in Fig. 7. Based on the $\Delta G'_{relative}$ values, MC demonstrated considerable mucoadhesive behavior, while the mucoadhesive property of 12PF and 14PF was relatively poor. Meanwhile, the mucoadhesive characteristics of PF correlated well with their concentrations (14PF > 12PF). These results are in general agreement with the property of both polymers reported in studies [46, 47]. Methylcellulose has been recognized as a mucoadhesive polymer [46, 48]. In contrast, a major drawback of PF is its poor mucoadhesive strength [47]. The $\Delta G'_{relative}$ value of 14PF/MC is slightly higher than

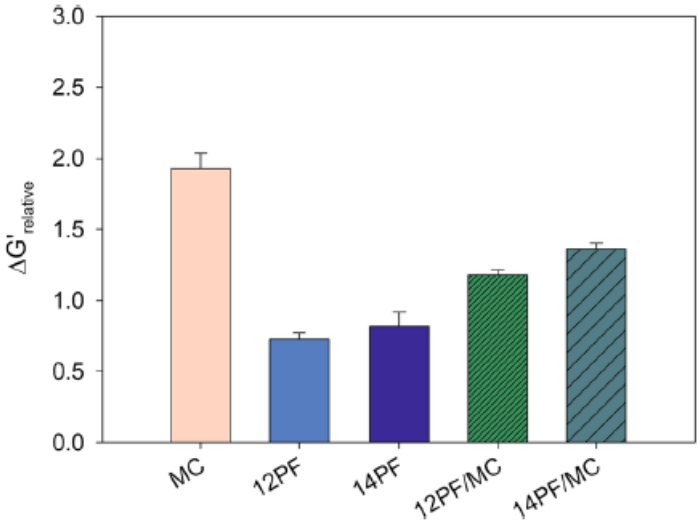

Fig. 7 Relative rheological synergism ($\Delta G'_{relative}$) at an angular frequency of 6.28 rad/s of 4% w/w MC (MC), 12PF, 14PF, 12PF/MC and 14PF/MC in 10% w/v mucin at 37 °C ($n = 3$)

12PF/MC. Both are significantly higher than their, respectively, concentration of the pure PF (12PF and 14PF) ($p < 0.005$). This may indicate that blending PF with MC improves the mucoadhesive property of PF-based thermosensitive gels.

Antimicrobial activity analysis

Some of the notable drugs typically used in the management of periodontitis include tetracycline, DX, metronidazole and macrolides [49]. The major causes of periodontitis are growth and accumulation of gram-negative anaerobes in the periodontal pockets including *P. gingivalis*, *A. actinomycetemcomitans* and *P. intermedia*. These anaerobic pathogens release toxins and enzymes which can stimulate inflammatory response causing the destruction of connective tissues around the teeth and alveolar bone [50]. In addition, these pathogens are the most predominant etiological agents for periodontitis associated with the chronic and aggressive form of the disease [51]. Therefore, these three pathogens were selected for investigating the activity of DX incorporated in 12PF/MC and 14PF/MC matrices compared to the pure drug.

The diameter of the zone of inhibition against the three microbes exposed to 0.25DX, 0.5DX, 12PF/MC/0.25DX, 14PF/MC/0.25DX, 12PF/MC/0.5DX and 14PF/MC/0.5DX is displayed in Fig. 8. The zone of inhibition diameter of 0.5DX

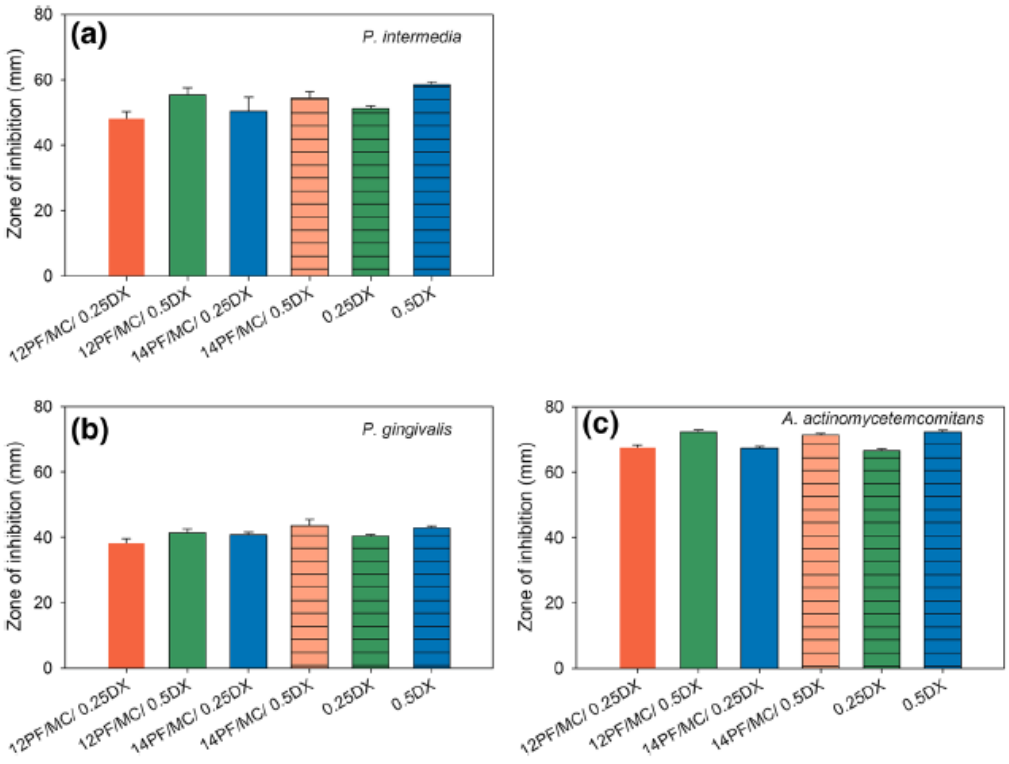

Fig. 8 Effect of 0.25DX and 0.5DX solutions as well as both DX concentrations in the 12PF/MC and 14PF/MC hydrogels on inhibition zone of **a** *P. Intermedia*, **b** *P. gingivalis* and **c** *A. actinomycetemcomitans* ($n = 3$)

was significantly greater than that of 0.25DX ($p < 0.05$) against all microbes. The microbial susceptibility was in the order of *A. actinomycetemcomitans* > *P. Intermedia* > *P. gingivalis*. The zone of inhibition diameters of the DX-loaded hydrogels was not significantly different from the corresponding concentration of pure DX. There were no significant differences among the inhibition zones of 0.25DX, 12PF/MC/0.25DX and 14PF/MC/0.25DX ($p > 0.05$) as well as those of 0.5DX, 12PF/MC/0.5DX and 14PF/MC/0.5DX ($p > 0.5$) against all microbes. These findings indicate that the polymeric matrices did not inhibit the biological activity of the drug.

In vitro drug release study

In vitro drug release of 0.25DX and 0.5DX from 12PF/MC and 14PF/MC was investigated using dialysis membrane in PBS (pH 7.4) at 37 °C. The in vitro release profile of 12PF/MC/0.25DX, 12PF/MC/0.5DX, 14PF/MC/0.25DX and 14PF/MC/0.5DX is shown in Fig. 9. The 12PF/MC and 14PF/MC prolonged the release of DX. Comparatively, the drug was released faster from 12PF/MC than from 14PF/MC. This may be due to the fact that the pore size of 12PF/MC was larger than that of 14PF/MC (Fig. 10). The higher amount of PF increased the compactness of the gel and slowed the release of DX. In addition, the viscosity at 37 °C of 12PF/MC was lower than that of 14PF/MC (Fig. 6B). The greater the viscosity of the gel layer, the more resistant the gel layer is to diffusion, and the drug release is prolonged as previously described [52]. This slow release in an extended period may have potential positive implications for the treatment of periodontitis.

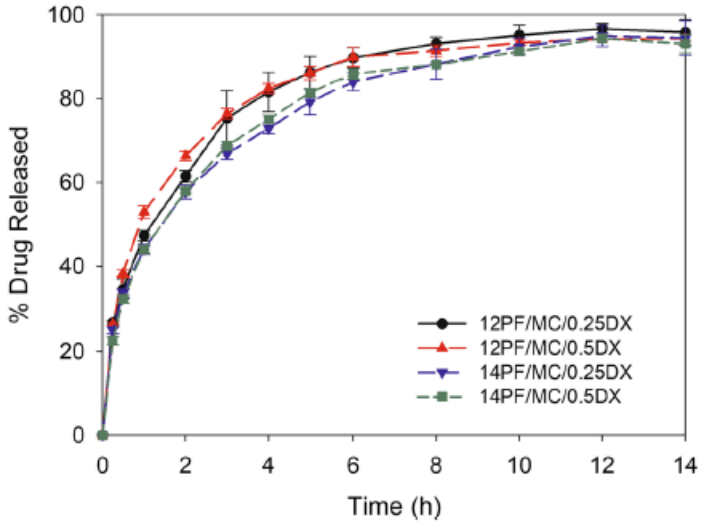

Fig. 9 In vitro release of DX at 37 °C from 12PF/MC and 14PF/MC hydrogels containing 0.25 and 0.5% DX (mean ± SD, $n = 3$)

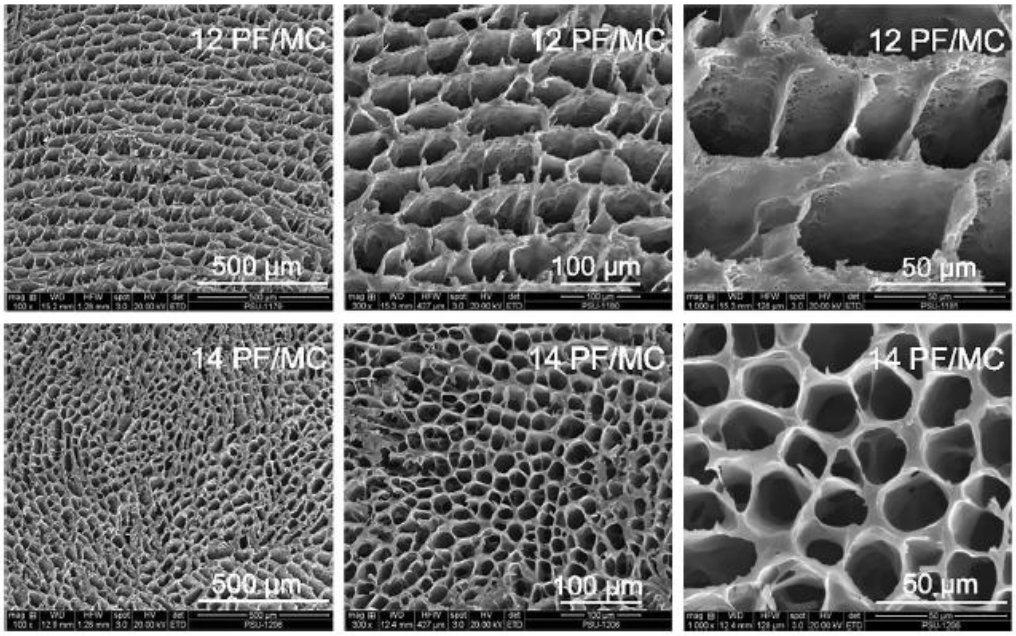

Fig. 10 SEM images of the freeze dried samples of MC, 12PF/MC and 14PF/MC hydrogels

Conclusion

In this study, TTM, turbidity, DSC and rheological analyses were systematically performed to determine the temperature-induced micellization and gelation of PF/MC systems. The clouding phenomenon observed in the PF/MC blends may reflect the efficient dehydration of PEO moiety of the micelles by MC. The CMT and the enthalpy of micellization were reduced by including MC into PF. The sol-to-gel temperature can be modulated and decreased by increasing PF concentrations. The mixtures of 12PF/MC and 14PF/MC were in sol state near ambient temperature of 24 °C and developed in situ gels at body temperature (37 °C). These mixtures were found to be suitable as injectable implant matrices. In addition, 12PF/MC and 14PF/MC showed substantially better mucoadhesive property than pure 12PF and 14PF, respectively. Furthermore, the incorporation of DX in 12PF/MC and 14PF/MC blends displayed the same antibacterial activity as the pure drug solution. This indicated that both PF/MC matrices did not obstruct the antibacterial activity of the drug. The 12PF/MC and 14PF/MC exhibited slow release of DX. Taken together, these findings demonstrated that the appropriate mixtures of PF/MC are promising matrices for the development of efficient periodontal drug delivery system.

Supplementary Information The online version contains supplementary material available at https://doi.org/10.1007/s00289-021-03722-w.

Acknowledgements This work was supported by the Integrated Research and Development of Medicine Project (Grant No. PHA610372S) and PSU-PhD scholarship (Grant No PSU/020/2557). We gratefully acknowledge the use of rheometer and DSC in the Center for Scientific and Technological Equipment, Walailak University.

Declaration

Conflict of interest The authors declare that they have no conflict of interest.

References

1. Escobar-Chávez JJ, López-Cervantes M, Naïk A, Kalia YN, Quintanar-Guerrero D, Ganem-Quintanar A (2006) Applications of thermo-reversible pluronic F-127 gels in pharmaceutical formulations. J Pharm Pharm Sci 9(3):339–358
2. Sun K, Raghavan SR (2010) Thermogelling aqueous fluids containing low concentrations of pluronic F127 and laponite nanoparticles. Langmuir ACS J Surf Colloids 26:8015–8020. https://doi.org/10.1021/la904907b
3. Sangfai T, Tantishaiyakul V, Hirun N, Li L (2017) Microphase separation and gelation of methylcellulose in the presence of gallic acid and NaCl as an in situ gel-forming drug delivery system. AAPS PharmSciTech 18(3):605–616. https://doi.org/10.1208/s12249-016-0546-7
4. Li L, Liu E, Lim CH (2007) Micro-DSC and rheological studies of interactions between methylcellulose and surfactants. J Phys Chem B 111:6410–6416. https://doi.org/10.1021/jp0712957
5. Wang Q, Li L, Liu E, Xu Y, Liu J (2006) Effects of SDS on the sol–gel transition of methylcellulose in water. Polymer 47:1372–1378
6. Rangabhatla ASL, Tantishaiyakul V, Oungbho K, Boonrat O (2016) Fabrication of pluronic and methylcellulose for etidronate delivery and their application for osteogenesis. Int J Pharm 499(1–2):110–118. https://doi.org/10.1016/j.ijpharm.2015.12.070
7. Pragatheeswaran AM, Chen SB (2016) The influence of poly (acrylic acid) on micellization and gelation characteristics of aqueous pluronic F127 copolymer system. Colloid Polym Sci 294(1):107–117. https://doi.org/10.1007/s00396-015-3757-7
8. Boucenna I, Royon L, Colinart P (2009) Effect of laponite clay particles on thermal and rheological properties of pluronic triblock copolymer. J Therm Anal Calorim 98(1):119–123. https://doi.org/10.1007/s10973-009-0339-2
9. Liu S, Li L (2015) Multiple phase transition and scaling law for poly (ethylene oxide)–poly (propylene oxide)–poly (ethylene oxide) triblock copolymer in aqueous solution. ACS Appl Mater Interfaces 7(4):2688–2697. https://doi.org/10.1021/am507749w
10. Boonrat O, Tantishaiyakul V, Hirun N, Rugmai S, Soontaranon S (2021) Structural characterization using SAXS and rheological behaviors of pluronic F127 and methylcellulose blends. Polym Bull 78(3):1175–1187. https://doi.org/10.1007/s00289-020-03154-y
11. Behera B, Patil V, Sagiri SS, Pal K, Ray SS (2012) Span-60-based organogels as probable matrices for transdermal/topical delivery systems. J Appl Polym Sci 125(2):852–863. https://doi.org/10.1002/app.35674
12. Park MJ, Char K (2002) Two gel states of a PEO-PPO-PEO triblock copolymer formed by different mechanisms. Macromol Rapid Comm 23(12):688–692. https://doi.org/10.1002/1521-3927(20020801)23:12%3c688::aid-marc688%3e3.0.co;2-r
13. Zheng PJ, Li L, Hu X, Zhao XY (2004) Sol-gel transition of methylcellulose in phosphate buffer saline solutions. J Polym Sci Part B Polym Phys 42(10):1849–1860. https://doi.org/10.1002/polb.20070
14. Hirun N, Tantishaiyakul V, Sangfai T, Ouiyangkul P, Li L (2019) In situ mucoadhesive hydrogel based on methylcellulose/xyloglucan for periodontitis. J Sol Gel Sci Technol 89(2):531–542. https://doi.org/10.1007/s10971-018-4878-5
15. Liu L, Fishman ML, Hicks KB, Kende M (2005) Interaction of various pectin formulations with porcine colonic tissues. Biomaterials 26(29):5907–5916. https://doi.org/10.1016/j.biomaterials.2005.03.005
16. Madsen F, Eberth K, Smart JD (1998) A rheological examination of the mucoadhesive/mucus interaction: the effect of mucoadhesive type and concentration. J Control Release 50(1–3):167–178. https://doi.org/10.1016/s0168-3659(97)00138-7
17. Goy RC, Morais STB, Assis OBG (2016) Evaluation of the antimicrobial activity of chitosan and its quaternized derivative on *E. coli* and *S. aureus* growth. Rev Bras 26:122–127

18. Fine DH, Markowitz K, Furgang D, Velliyagounder K (2010) Aggregatibacter actinomycetemcomitans as an early colonizer of oral tissues: epithelium as a reservoir? J Clin Microbiol 48(12):4464–4473. https://doi.org/10.1128/jcm.00964-10
19. Nagaoka K, Yanagihara K, Morinaga Y, Nakamura S, Harada T, Hasegawa H, Izumikawa K, Ishimatsu Y, Kakeya H, Nishimura M, Kohno S (2014) Prevotella intermedia induces severe bacteremic pneumococcal pneumonia in mice with upregulated platelet-activating factor receptor expression. Infect Immun 82(2):587–593. https://doi.org/10.1128/iai.00943-13
20. Katz J, Sambandam V, Wu JH, Michalek SM, Balkovetz DF (2000) Characterization of *Porphyromonas gingivalis*-induced degradation of epithelial cell junctional complexes. Infect Immun 68(3):1441–1449. https://doi.org/10.1128/iai.68.3.1441-1449.2000
21. Ji QX, Zhao QS, Deng J, Lü R (2010) A novel injectable chlorhexidine thermosensitive hydrogel for periodontal application: preparation, antibacterial activity and toxicity evaluation. J Mater Sci Mater Med 21(8):2435–2442. https://doi.org/10.1007/s10856-010-4098-1
22. Maheshwari M, Miglani G, Mali A, Paradkar A, Yamamura S, Kadam S (2006) Development of tetracycline-serratiopeptidase-containing periodontal gel: formulation and preliminary clinical study. AAPS PharmSciTech 7(3):E162–E171. https://doi.org/10.1208/pt070376
23. Tamimi F, Torres J, Bettini R, Ruggera F, Rueda C, López-Ponce M, Lopez-Cabarcos E (2008) Doxycycline sustained release from brushite cements for the treatment of periodontal diseases. J Biomed Mater Res A 85(3):707–714. https://doi.org/10.1002/jbm.a.31610
24. Prud'homme RK, Wu G, Schneider DK (1996) Structure and rheology studies of poly (oxyethylene−oxypropylene−oxyethylene) aqueous solution. Langmuir ACS J Surf Colloids 12(20):4651–4659. https://doi.org/10.1021/la951506b
25. de Lima CM, Siqueira SMC, de Amorim AFV, Costa KBS, de Brito DHA, Ribeiro M, Ricardo N, Chaibunditc C, Yeates SG, Ricardo N (2015) Effects of polypropylene glycol 400 (PPG400) on the micellization and gelation of pluronic F127. Macromolecules 48(21):7978–7982. https://doi.org/10.1021/acs.macromol.5b01655
26. Akbaş H, Boz M, Batıgöç Ç (2010) Study on cloud points of Triton X-100-cationic gemini surfactants mixtures: a spectroscopic approach. Spectrochim Acta Part A Mol Biomol Spectrosc 75(2):671–677. https://doi.org/10.1016/j.saa.2009.11.038
27. Rao WW, Wang Y, Han J, Wang L, Chen T, Liu Y, Ni L (2015) Cloud point and liquid-liquid equilibrium behavior of thermosensitive polymer L61 and salt aqueous two-phase system. J Phys Chem B 119(25):8201–8208. https://doi.org/10.1021/acs.jpcb.5b03201
28. Silva RCd, Loh W (1998) Effect of additives on the cloud points of aqueous solutions of ethylene oxide–propylene oxide–ethylene oxide block copolymers. J Colloid Interface Sci 202(2):385–390. https://doi.org/10.1006/jcis.1998.5456
29. Sharma R, Bahadur P (2002) Effect of different additives on the cloud point of a polyethylene oxide-polypropylene oxide-polyethylene oxide block copolymer in aqueous solution. J Surfactants Deterg 5(3):263–268. https://doi.org/10.1007/s11743-002-0226-9
30. Gu T, Galera-Gómez PA (1995) Clouding of Triton X-114: the effect of added electrolytes on the cloud point of Triton X-114 in the presence of ionic surfactants. Colloids Surf A 104(2):307–312. https://doi.org/10.1016/0927-7757(95)03217-1
31. Park MJ, Char K, Kim HD, Lee CH, Seong BS, Han YS (2002) Phase behavior of a PEO-PPO-PEO triblock copolymer in aqueous solutions: two gelation mechanisms. Macromol Res 10(6):325–331. https://doi.org/10.1007/bf03218326
32. Chaibundit C, Sumanatrakool P, Chinchew S, Kanatharana P, Tattershall CE, Booth C, Yuan X-F (2005) Association properties of diblock copolymer of ethylene oxide and 1,2-butylene oxide: E17B12 in aqueous solution. J Colloid Interface Sci 283(2):544–554. https://doi.org/10.1016/j.jcis.2004.09.030
33. Liu SJ, Li L (2015) Molecular interactions between PEO-PPO-PEO and PPO-PEO-PPO triblock copolymers in aqueous solution. Colloid Surface A 484:485–497. https://doi.org/10.1016/j.colsurfa.2015.08.034
34. Trong LC, Djabourov M, Ponton A (2008) Mechanisms of micellization and rheology of PEO-PPO-PEO triblock copolymers with various architectures. J Colloid Interface Sci 328(2):278–287. https://doi.org/10.1016/j.jcis.2008.09.029
35. Oshiro A, da Silva DC, de Mello JC, de Moraes VW, Cavalcanti LP, Franco MK, Alkschbirs MI, Fraceto LF, Yokaichiya F, Rodrigues T, de Araujo DR (2014) Pluronics f-127/l-81 binary hydrogels as drug-delivery systems: influence of physicochemical aspects on release kinetics and cytotoxicity. Langmuir ACS J Surf Colloids 30(45):13689–13698. https://doi.org/10.1021/la503021c

36. Pothan LA, George CN, John MJ, Thomas S (2010) Dynamic mechanical and dielectric behavior of banana-glass hybrid fiber reinforced polyester composites. J Reinf Plast Compos 29:1131–1145
37. Akkari ACS, Papini JZB, Garcia GK, Franco M, Cavalcanti LP, Gasperini A, Alkschbirs MI, Yokaichyia F, de Paula E, Tófoli GR, de Araujo DR (2016) Poloxamer 407/188 binary thermosensitive hydrogels as delivery systems for infiltrative local anesthesia: physico-chemical characterization and pharmacological evaluation. Mater Sci Eng C Mater Biol Appl 68:299–307. https://doi.org/10.1016/j.msec.2016.05.088
38. Hirun N, Tantishaiyakul V, Sangfai T, Boonlai W, Soontaranon S, Rugmai S (2021) The effect of poly (acrylic acid) on temperature-dependent behaviors and structural evolution of poloxamer 407. Polym Int. https://doi.org/10.1002/pi.6197
39. Curnutt A, Smith K, Darrow E, Walters KB (2020) Chemical and microstructural characterization of pH and [Ca2+] dependent sol-gel transitions in mucin biopolymer. Sci Rep 10(1):8760. https://doi.org/10.1038/s41598-020-65392-4
40. Zhang J, Gassmann M, Chen X, Burger C, Rong L, Ying Q, Chu B (2007) Characterization of a reversible thermoresponsive gel and its application to oligonucleotide separation. Macromolecules 40:5537–5544. https://doi.org/10.1021/ma070554n
41. Wu C, Liu T, Chu B (1998) Viscosity-adjustable block copolymer for DNA separation by capillary electrophoresis. Electrophoresis 19(2):231–241. https://doi.org/10.1002/elps.1150190216
42. Li X, Hyun K (2018) Rheological study of the effect of polyethylene oxide (PEO) homopolymer on the gelation of PEO-PPO-PEO triblock copolymer in aqueous solution. Korea Aust Rheol J 30(2):109–125. https://doi.org/10.1007/s13367-018-0012-z
43. Bromberg L (1998) Temperature-sensitive star-branched poly (ethylene oxide)–b-poly (propylene oxide)–b-poly (ethylene oxide) networks. Polymer 39(23):5663–5669. https://doi.org/10.1016/S0032-3861(98)00007-X
44. Wang Y, Tan Y, Huang X, Xu G (2009) Gelation behavior of thermo-responsive poly (ethylene oxide) and poly (propylene oxide) multiblock polycarbonates. J Macromol Sci Part A 46(4):397–404. https://doi.org/10.1080/10601320902728553
45. Duggan S, Hughes H, Owens E, Duggan E, Cummins W, O'Donovan O (2016) Synthesis and characterisation of mucoadhesive thiolated polyallylamine. Int J Pharm 499(1):368–375. https://doi.org/10.1016/j.ijpharm.2016.01.009
46. Barakat NS (2009) In vitro and in vivo characteristics of a thermogelling rectal delivery system of etodolac. AAPS PharmSciTech 10(3):724. https://doi.org/10.1208/s12249-009-9261-y
47. Ci L, Huang Z, Liu Y, Liu Z, Wei G, Lu W (2017) Amino-functionalized poloxamer 407 with both mucoadhesive and thermosensitive properties: preparation, characterization and application in a vaginal drug delivery system. Acta Pharmaceutica Sinica B 7(5):593–602. https://doi.org/10.1016/j.apsb.2017.03.002
48. Roy S, Pal K, Anis A, Pramanik K, Prabhakar B (2009) Polymers in mucoadhesive drug-delivery systems: a brief note. Des Monomers Polym 12(6):483–495. https://doi.org/10.1163/138577209X12478283327236
49. Prakasam A, Elavarasu SS, Natarajan RK (2012) Antibiotics in the management of aggressive periodontitis. J Pharm Bioallied Sci 4(Suppl 2):S252-255. https://doi.org/10.4103/0975-7406.100226
50. Chen X, Wu G, Feng Z, Dong Y, Zhou W, Li B, Bai S, Zhao Y (2016) Advanced biomaterials and their potential applications in the treatment of periodontal disease. Crit Rev Biotechnol 36(4):760–775. https://doi.org/10.3109/07388551.2015.1035693
51. AlJehani YA (2014) Risk factors of periodontal disease: review of the literature. Int J Dent 2014:9. https://doi.org/10.1155/2014/182513
52. Cheong LWS, Heng PWS, Wong LF (1992) Relationship between polymer viscosity and drug release from a matrix system. Pharm Res 9(11):1510–1514. https://doi.org/10.1023/A:1015883501871

VITAE

Name Miss Onpreeya Boonrat
Student ID 6310730006
Educational Attainment

Degree	Name of Institution	Year of Graduation
Bachelor of Science (Chemistry)	Prince of Songkla University	2006
Master of Science (Cosmetic Sciences)	Prince of Songkla University	2012

Scholarship Awards during Enrolment

1. PSU-Ph.D. Scholarship (Grant No. PSU/020/2557), Graduate School, Prince of Songkla University, 2014-2017.
2. Graduate School Dissertation Funding for Thesis, Graduate School, Prince of Songkla University, 2016-2018.
3. Research Grant for Thesis, Drug Delivery System Excellence Center (DDSEC), Faculty of Pharmaceutical Sciences, Prince of Songkla University, 2017-2018.
4. Scholarship (Support for Thesis), Faculty of Pharmaceutical Sciences, Prince of Songkla University, 2017-2018.
5. Conference Scholarship, Faculty of Pharmaceutical Sciences, Prince of Songkla University.

List of Publications

1. **Boonrat, O**., Tantishaiyakul, V., and Hirun, N. 2022. Micellization and gelation characteristics of different blends of pluronic F127/methylcellulose and their use as mucoadhesive in situ gel for periodontitis. Polymer Bulletin (79): 4515-4534. https://doi.org/10.1007/s00289-021-03722-w.
2. **Boonrat, O**., Tantishaiyakul, V., and Hirun, N. 2021. Structural characterization using SAXS and rheological behaviors of pluronic F127 and methylcellulose blends. Polymer Bulletin (78): 1175–1187. https://doi.org/10.1007/s00289-020-03154-y.
3. Sangfai, T., Dong, F., Tantishaiyakul, V., Jandt, K. D., Lüdecke, C., **Boonrat, O**., and Hirun, N. 2017. Layer-by-layer gelatin/chitosan polyelectrolyte coated nanoparticles on Ti implants for prevention of implant-associated infections. eXPRESS Polymer Letters 11 (1): 73-82. https://doi:10.3144/expresspolymlett.2017.8
4. Rangabhatla, Aparna Sai Laxmi., Tantishaiyakul, V., **Boonrat, O**., Hirun, N., Ouiyangkul, P. 2017. Novel in situ mucoadhesive gels based on Pluronic F127 and xyloglucan containing metronidazole for treatment of periodontal disease. Iranian Polymer Journal 26 (11): 851-859. https://doi:10.1007/s13726-017-0569-2.

5. Rangabhatla, Aparna Sai Laxmi., Tantishaiyakul, V., Oungbho. K., and **Boonrat, O**. 2015. Fabrication of pluronic and methylcellulose for etidronate delivery and their application for osteogenesis. International Journal of Pharmaceutics 499: 110-118. https://doi:10.1016/j.ijpharm.2015.12.070.

List of Proceedings

Oral presentation

1. **Boonrat, O**. and Tantishaiyakul, V. Effect of methylcellulose and xyloglucan on gelation temperature and cytotoxic enhancement of Pluronic-F127 injectable hydrogel for drug delivery system. The 11th IMT-GT UNINET Conference 2018 – *Bioscience for A Sustainable Future*, Hotel Jen, Penang, Malaysia, December 11-12, 2018. 142-148.

Poster presentation

1. **Boonrat, O**. and Tantishaiyakul, V. A Novel method to simulate organogel implantation using UV spectroscopy. The joint international conferences of the 5th Current Drug Development 2018 (CDD 2018) and the 3rd Herbal and Traditional Medicine 2018 (HTM2018). The 60th Anniversary of His Majesty the King's Accession to the Throne International Convention Center (PSU Conference Hall), Prince of Songkla University, Hat Yai, Songkhla, Thailand. May 23-25, 2018. 115-116.
2. **Boonrat, O**. and Hirun, N. The structural characteristic of polymer blend hydrogel for injectable in situ forming drug delivery system. THE 9th ANNUAL SLRI USER MEETING 2019: AUM2019. The Sukosol Hotel, Bangkok, Thailand. May 1st, 2019.